AD NUMBER

AD812441

LIMITATION CHANGES

TO:

Approved for public release; distribution is unlimited.

FROM:

**Distribution authorized to U.S. Gov't. agencies and their contractors;
Administrative/Operational Use; APR 1967. Other requests shall be referred to Arnold Engineering Development Center, Arnold AFB, TN.**

AUTHORITY

AEDC ltr 27 Jun 1973

BLOCK II AJ10-137 APOLLO SERVICE MODULE ENGINE TESTING AT SIMULATED HIGH ALTITUDE (REPORT II, PHASE IV DEVELOPMENT)

J. F. DeFord, M. W. McIlveen,
and A. L. Berg
ARO, Inc.

April 1967

ROCKET TEST FACILITY
ARNOLD ENGINEERING DEVELOPMENT CENTER
AIR FORCE SYSTEMS COMMAND
ARNOLD AIR FORCE STATION, TENNESSEE

NOTICES

When U. S. Government drawings specifications, or other data are used for any purpose other than a definitely related Government procurement operation, the Government thereby incurs no responsibility nor any obligation whatsoever, and the fact that the Government may have formulated, furnished, or in any way supplied the said drawings, specifications, or other data, is not to be regarded by implication or otherwise, or in any manner licensing the holder or any other person or corporation, or conveying any rights or permission to manufacture, use, or sell any patented invention that may in any way be related thereto.

Qualified users may obtain copies of this report from the Defense Documentation Center.

References to named commercial products in this report are not to be considered in any sense as an endorsement of the product by the United States Air Force or the Government.

BLOCK II AJ10-137 APOLLO SERVICE MODULE ENGINE TESTING AT SIMULATED HIGH ALTITUDE (REPORT II, PHASE IV DEVELOPMENT)

J. F. DeFord, M. W. McIlveen,
and A. L. Berg
ARO, Inc.

FOREWORD

The contents of this report are the results of an altitude development testing program on the Aerojet-General Corporation (AGC), AJ10-137, Block II, liquid-propellant rocket engine installed on the North American Aviation (NAA) F-3 propellant tankage fixture. This program was sponsored by the National Aeronautics and Space Administration - Manned Spacecraft Center (NASA-MSC). Technical liaison was provided by AGC which is a subcontractor of North American Aviation - Space and Information Division (NAA-S&ID) for the development of the Apollo Service Module (S/M) engine. North American Aviation is the prime contractor to NASA for the complete Apollo S/M vehicle. Quality control surveillance was provided by the U. S. Air Force, AGC, and ARO, Inc.

The test program was requested to support the Apollo project under Air Force Systems Command (AFSC) Program Area 921E/9158. Testing was conducted by ARO, Inc. (a subsidiary of Sverdrup & Parcel and Associates, Inc.), contract operator of the Arnold Engineering Development Center (AEDC), AFSC, Arnold Air Force Station, Tennessee. The results reported in this document were obtained in the Propulsion Engine Test Cell (J-3) of the Rocket Test Facility (RTF) during the period between August 4 and October 27, 1966, under ARO Project Number RM1607. The manuscript was submitted for publication on February 17, 1967.

Information in this report is embargoed under the Department of State International Traffic in Arms Regulations. This report may be released to foreign governments by departments or agencies of the U. S. Government subject to approval of the National Aeronautics and Space Administration - Manned Spacecraft Center, or higher authority. Private individuals or firms require a Department of State export license.

(U) The authors wish to acknowledge invaluable collaboration in the preparation of this report by their associates in the J-3 Projects Section: C. R. Bartlett, G. H. Schulz, C. E. Robinson, J. M. Pelton, and E. G. Grammer.

(U) This technical report has been reviewed and is approved.

Joseph R. Henry
Lt Col, USAF
AF Representative, RTF
Directorate of Test

Leonard T. Glaser
Colonel, USAF
Director of Test

ABSTRACT

Developmental testing was conducted on the Aerojet-General Corporation AJ10-137, Block II, Apollo Service Module Propulsion engine. The Block II engine was designed to improve performance and structural durability and was operated at nominal conditions of 97-psia chamber pressure and 1.6 mixture ratio with nitrogen tetroxide and Aerozine-50® propellants. Primary objectives of these tests were to determine engine ballistic performance and to verify durability of a new combustion chamber design. Performance and durability at off-design chamber pressures and mixture ratios were also documented. The test results presented indicate the trend in performance as a function of chamber pressure, propellant temperature, and mixture ratio. Erosion and blistering occurred in the ablative lining of the first two chambers tested. Altered construction of the last four chambers produced excellent durability. (AFR310-2, Statement 2)

CONTENTS

APPENDIXES

I. ILLUSTRATIONS

Figure

NOMENCLATURE

A_e	Nozzle exit area, in.^{2}
A_t	Throat area, in.^{2}
$A_{t_{calc}}$	Calculated throat area, in.^{2}
C_{F_v}	Vacuum thrust coefficient
C_{ij}	Calibration constants
c*	Characteristic velocity, ft/sec
c_i^*	Characteristic velocity calculated at the beginning of a test period for which a new combustion chamber was used, ft/sec
F_a	Axial thrust, lb_f
$F_{a_{cal}}$	Axial thrust calibrate, lb_f
$F_{a_{data}}$	Axial thrust data, lb_f
f_{corr}	Mixture ratio correction
$F_{fwt_{corr}}$	Fuel weigh tank corrected weight
$F_{owt_{corr}}$	Oxidizer weigh tank corrected weight
F_{P1cal}	Upper pitch force calibrate, lb_f
F_{P1data}	Upper pitch force data, lb_f
F_{P2cal}	Lower pitch force calibrate, lb_f
F_{P2data}	Lower pitch force data, lb_f
F_{PA}	Pitch actuator force, lb_f
$F_{R_{cal}}$	Roll force calibrate, lb_f
$F_{R_{data}}$	Roll force data, lb_f
FS-1	Engine start signal (fire switch one)
FS-2	Engine shutdown signal (fire switch two)
F_v	Vacuum thrust, lb_f
F_{Y1cal}	Upper yaw force calibrate, lb_f
F_{Y1data}	Upper yaw force data, lb_f
F_{Y2cal}	Lower yaw force calibrate, lb_f

$F_{Y_{2data}}$	Lower yaw force data, lb_f
F_{YA}	Yaw actuator force, lb_f
g	Dimensional constant, 32.174 lb_m-ft/lb_f-sec^2
I_{sp_v}	Vacuum specific impulse, lb_f-sec/lb_m
$\bar{K}$	Average flowmeter constant
K_{fm}	Flowmeter constant, lb_m-H_2O/cycle
K_{ji}	Balance constants
L_j	Applied load, lb_f
MR	Mixture ratio, oxidizer-to-fuel
P_a	Test cell pressure, psia
P_c	Combustion chamber pressure, psia
P_{fl}	Fuel line pressure, psia
P_{f_t}	Fuel tank pressure, psia
$P_{f_{t_{ca}}}$	Fuel interface pressure, psia
P_{o_t}	Oxidizer tank pressure, psia
$P_{o_{t_{ca}}}$	Oxidizer interface pressure, psia
R_i	Data load cell output, lb_f
T_c	Temperature - thrust chamber, °F
T_f	Temperature - fuel, °F
T_j	Temperature - injector, °F
T_N	Temperature - nozzle extension, °F
T_o	Temperature - oxidizer, °F
T_p	Average propellant temperature, °F
$\dot{W}_f$	Fuel weight flow, lb_m/sec
$\dot{W}_o$	Oxidizer weight flow, lb_m/sec
$\dot{W}_t$	Total propellant weight flow, lb_m/sec
$\dot{W}_{t_m}$	Measured total propellant weight flow, lb_m/sec
X	Distance of the thrust vector from the balance centerline in the balance pitch plane and engine gimbal plane, in.

X_e	Location of point of thrust vector intersection with engine gimbal plane on pitch axis (six-component balance), in.
X_p	Location of point of thrust vector intersection with engine gimbal plane on pitch axis (stiff link load cell), in.
Y	Distance of the thrust vector from the balance centerline in the balance yaw plane and engine gimbal plane, in.
Y_e	Location of point of thrust vector intersection with engine gimbal plane on yaw axis (six-component balance), in.
Y_y	Location of point of thrust vector intersection with engine gimbal plane on yaw axis (stiff link/load cell), in.
θ	Pitch angle, deg
ϕ	Yaw angle, deg

SUBSCRIPTS

e	Excursion
f	Fuel
o	Oxidizer

SECTION I
INTRODUCTION

The Apollo lunar exploration spacecraft consists of three modules, the Command Module, the Service Module (SM), and the Lunar Module (LM)(Fig. 1, Appendix I). The SM houses the Service Propulsion System (SPS) rocket engine which provides midcourse guidance correction and energy for injection into the lunar parking orbit and ejection from the lunar orbit. Descent to and ascent from the lunar surface to the lunar orbit is to be accomplished by the LM. The Command Module is the crew cabin, spacecraft control center, and earth re-entry capsule.

The SPS utilizes a rocket engine of 20,000-lb_f rated thrust with an ablatively cooled combustion chamber and a 62.5:1 nominal area ratio radiation-cooled nozzle extension. The earth-storable hypergolic propellants are pressure fed to the engine from SM tankage.

Three phases of simulated altitude testing above 110,000 ft have been completed on the SPS Block I rocket engine. Phases I, II, and III (Refs. 1 through 9) were the development, prequalification, and qualification testing, respectively, of the Block I engine. Phases II and III were conducted using a boilerplate replica, of the SM vehicle tankage (NAA F-3 fixture). Phase IV was the developmental testing of the Block II engine with the boilerplate SM tankage. During Phase IV, nine engines were tested during nine test series; the first three test series were reported in Ref. 10, and the last six test series are reported herein. For this testing, a developmental Block II injector and combustion chamber design was used along with the NAA F-3 fixture. Prior to this report period, the NAA F-3 fixture was modified to the Block II propellant system configuration. This modification consisted of modifying the propellant lines and routing them in such a manner as to make the oxidizer and fuel tankage capacities volumetrically equal.

The primary test objectives were (1) to prove combustion chamber durability and (2) to determine rocket engine ballistic performance. The engine was operated at both design and off-design conditions; two of the test series were conducted with propellant and test cell capsule temperature conditioned to 110°F. During one test series, the nozzle flange and nozzle extension were cooled between -100 and -300°F prior to three firings to demonstrate the nozzle extension's ability to withstand thermal shock. Also, during another test series, stiff links instrumented with load cells were installed in place of the

gimbal actuators to determine the steady-state null force at the zero gimbal angle position. The results presented in this report were obtained with six engine assemblies during six test periods; 168 test firings were made with a total firing duration of 4538 sec.

SECTION II
APPARATUS

2.1 TEST ARTICLE

The AJ10-137 rocket engine and Apollo SM propellant system (plumbing and heavy-duty tankage, designated the F-3 fixture and supplied by NAA/S&ID) constituted the test article for these AEDC tests. Six different flight-type engine assemblies (S/N 21A, 21B, 21C, 21D, 21E, and 21F) were tested during this report period. The engine configuration included one assembly without gimbal actuators and the remainder with actuators. Engine S/N 21A with gimbal actuators but without the nozzle extension is shown in Fig. 2.

2.2 ENGINE

The Block II AJ10-137 engine tested was a pressure-fed, liquid-propellant rocket engine consisting of a thrust chamber assembly, a bipropellant thrust chamber valve (TCV) assembly, and a gimbal actuator-ring mount assembly. The overall height of the engine was approximately 13 ft, and the maximum diameter of the engine (at the nozzle exit) was approximately 8 ft.

The design vacuum performance of the engine was 20,000 lb of thrust at a propellant weight mixture ratio of 1.6 and a chamber pressure (measured at the injector face) of 97 psia. The engine was designed for a minimum of 50 starts over the design operating life of 750 sec. The liquid propellants were hypergolic and storable; the oxidizer was nitrogen tetroxide (N_2O_4), and the fuel was a 50-50 weight blend of hydrazine (N_2H_4) and unsymmetrical dimethylhydrazine (UDMH). The oxidizer had approximately 0.5-percent NO additive.

The thrust chamber assembly consisted of a propellant injector, an ablatively cooled combustion chamber, and a radiation-cooled nozzle extension. The TCV was mounted on top (forward) of the injector dome. The thrust chamber assembly was mounted in a ring mount assembly and was gimbaled in two orthogonal planes by two electrically operated gimbal actuators.

One of the six engines tested is shown without the nozzle extension in Fig. 2. The engine assembly components were:

Test Series	Engine S/N	Injector S/N	Bipropellant Valve S/N	Combustion Chamber S/N	Nozzle Extension S/N
DD	21A	110	102	293	27
DE	21B	110	102	299	27
DF	21C	093	102	303	41
DG	21D	093	102	305	41
DH	21E	105	102*	309	42
DI	21F	105	102*	310	42

*Linear Potentiometers Installed

2.2.1 Propellant Injectors

Three different injectors were used during this report period (Figs. 3 and 4). As listed in the above table, injectors S/N 110, 093, and 105 were used during test series DD-DF, DG-DH, and DH-DI, respectively. The major differences between these injectors were:

1. Chamber pressure tap location. Injector S/N 93 had the Block I chamber pressure tap (Figs. 4a and c), whereas injectors S/N 105 and 110 had the Block II location (Figs. 4b and c).
2. Baffle configuration. Two different baffle configurations were used (a) the 5-4-2 configuration (Fig. 3b), hereafter referred to as the short baffle, was used on injector S/N 110, and (b) the 5-4-4 configuration (Fig. 3b), hereafter referred to as the long baffle, was used on injectors S/N 93 and 105. The 5-4-2 configuration represents an injector with five baffles, with each baffle having 4-in. chords at the central hub and 2-in. chords at the termination of the baffle. The 5-4-4 configuration represents a similar baffle configuration except that the chords are approximately 4 in. constant length.
3. Counterbored orifices. Injector S/N 105 had counterbored oxidizer orifices and selected counterbored fuel orifices (Fig. 3c). These counterbored orifices were incorporated to minimize combustion anomalies such as the spontaneous pops observed during testing using injectors without counterboring. Injectors S/N 93 and 110 had no counterbored orifices.

The injectors used during these tests had doublet orifice impingement in a concentric-ring pattern and were baffled for improved combustion stability. The injector baffles were regeneratively cooled with fuel, which was routed through the baffles and back to the injection ring passages. Fuel coolant was not discharged directly from the baffles. Film cooling of the combustion chamber was provided by fuel flow from orifices in the outer fuel ring passage of the injector, adjacent to the injector mounting flange. Approximately 5 percent of the engine fuel flow was injected for film cooling.

A pulse charge (Fig. 5) was placed in the combustion chamber for the first test firing of each engine series to prove the capability of the engine combustion mechanism to recover from induced combustion instability. The pulse charge consisted of 9.24 gm of C-4 explosive compound equivalent to 165 grains of tetryl held in a Teflon® holder which was screwed into the center of the injector face. The pulse charge was located on the centerline of the combustion chamber about 6 in. downstream of the injector face. Pulse charge detonation was by combustion heat.

2.2.2 Combustion Chamber

The combustion chamber was constructed with an ablative liner, an asbestos insulating layer, and an external structural wrap. The ablative material consisted of a silica-glass fabric tape oriented in conical "shingle" layers and impregnated with a phenolic resin compound. The maximum ablative thickness was located at the throat section. Several layers of resin-impregnated fiber glass wrap (glass fabric and glass filament) were bonded over the asbestos and constituted the chamber structural material. Mounting flanges for the injector and nozzle extension were attached to the chamber by bonding and wedging the flange lips in the layers of structural wrap. The exit cone of the chamber extended to the 6:1 area ratio station.

The combustion chambers used for this testing were designated the A-1 design. An asbestos overwrap was substituted for the flatwrap asbestos phenolic tape insulating layer used on previously tested chambers; and a mechanical lock was incorporated between the overwrap and liner to provide liner support for axial shear loading. For comparison the chamber design used for the first three tests of Phase IV (design A) (Ref. 10) and the A-1 design used for this testing are presented in Fig. 6.

2.2.3 Exhaust Nozzle Extension

The radiation-cooled nozzle extension was bolted to the ablative chamber at the 6:1 area ratio and extended to the 62.5:1 area ratio.

The nozzle extension design used during these tests was the same design developed for the Block I engine and is shown in Fig. 7.

The nozzle extension was fabricated with columbium to the 40:1 area ratio and titanium alloy from the 40:1 to the 62.5:1 area ratio (Fig. 7). The columbium section thickness was 0.030 in. to area ratio 20 and was 0.022 in. from area ratio 20 to the columbium-titanium joint. The titanium portion was fabricated from 0.025-in.-thick titanium alloy (5 Al and 2.5 Sn). The columbium section was coated to improve oxidation, and the titanium section was coated to improve emissivity for surface temperature reduction.

2.2.4 Thrust Chamber Propellant Valve

The thrust chamber propellant valve (TCV) consisted of a system of eight ball valves; two each in two parallel fuel passages and two each in two parallel oxidizer passages, as shown in Fig. 8. The valves were actuated by engine-stored gaseous nitrogen (GN_2) and were opened and closed by electrical commands to solenoid valves. Each of the TCV actuators operated one fuel and one oxidizer ball valve; opening force was effected by GN_2 pressure, and closing was effected by mechanical spring force when GN_2 pressure was released. Each actuator was provided with a solenoid pilot valve for GN_2 control. The pilot valves were electrically operated in pairs such that an electrical command operated two actuators to control one bank of propellant valves (one fuel passage and one oxidizer passage). Control room switches permitted engine firing and shutdown using either bank separately or together.

Orifices were provided at the TCV inlets to balance the parallel passages, so that engine operation using either valve bank would produce the same engine ballistic performance for given propellant interface pressures.

2.2.5 Gimbal Actuators/Stiff Links

The two actuators (pitch and yaw) were electrically powered and were components of a null-balance servo-loop gimbal subsystem designed for operation with the SM autopilot system. Gimbal actuators were used during all tests except test series DH, when stiff-link rods with load cells (Fig. 9) were used in place of gimbal actuators to measure the steady-state null force experienced by the gimbal actuator at the zero gimbal angle position.

2.3 NAA F-3 FIXTURE

Prior to this testing, the NAA F-3 fixture was modified to the Block II spacecraft configuration. The major part of this modification consisted of changing the fuel line size from 2-1/2 to 3 in. and connecting the propellant tanks so that the oxidizer and fuel capacities were volumetrically equal (2360 gal each). Figure 10 is a schematic diagram comparison of the F-3 fixture before and after the modification.

The F-3 fixture was designed to reproduce the propellant system hydrodynamics of the SM spacecraft with necessary modifications incorporated to facilitate ground test operations. The fixture structural frame, tanks, and plumbing had overall dimensions of about 100 by 153 in. laterally and 15 ft high. The fixture weighed approximately 27,500 lb.

2.3.1 Propellant System

The propellant tanks were of spacecraft size, shape, and volume, consisting of one 1050 gal and one 1310 gal tank for the fuel side with the identical situation for the oxidizer side, giving a total capacity for each side of 2360 gal. These four tanks were designed and fabricated to meet the specification of the ASME pressure vessel code. As in the SM spacecraft, the two propellant tanks were series connected with propellant crossover lines, the engine propellant feed lines were connected to the sump tanks, and propellant force-feed pressurization was through the storage tanks. The tandem tanks and crossover line arrangement resulted in variations of propellant feed pressures with changes in propellant level although force feed pressurization was constant.

The fixture propellant feed lines were modified to accommodate AEDC flowmeters and bypass connections for flowmeter calibration. Duplication of spacecraft line pressure losses was retained by fixture line balance orifices.

The fixture propellant lines configuration, used during this testing, was the Block II SM configuration.

The pneumatic pressurization system of the F-3 fixture did not duplicate the spacecraft system. Because of the frequent testing at off-design mixture ratios and chamber pressures, force-feed pressurization was provided by AEDC facility automatic control valve regulators.

2.3.2 Heat Shield

A heat shield, fabricated at AEDC and used during previous testing, was a compromise design intended to approximate the contour of the NAA Block I flight-type shield and to protect the thrust system instrumentation, F-3 fixture, and installation plumbing from the thermal radiation of the nozzle extension. This shield consisted of two layers of corrosion-resistant steel sheets separated by high temperature silica insulation (Fig. 11a). The conical area facing the nozzle extension was covered with black carbon-impregnated Teflon to provide heat dissipation by sublimation.

For test series DG, DH, and DI, an NAA heat shield (Fig. 11b), constructed of stainless steel, was attached to the combustion chamber/nozzle extension attachment flange. This heat shield was used in addition to the AEDC heat shield previously described.

2.4 INSTALLATION

The Apollo SM propulsion system F-3 fixture and the AJ10-137 engine were installed in Propulsion Engine Test Cell (J-3), a vertical test cell for testing rocket engines at pressure altitudes in excess of 100,000 ft (Fig. 12 and Ref. 11). An aluminum test cell capsule, 18 ft in diameter and 40 ft high, was installed over the test article to form the pressure-sealed test chamber.

The engine was installed in a multicomponent force balance. This balance was mounted in the F-3 fixture by six flexure-mounted load cells for thrust vector measurement (Fig. 13). The six load cells were used to determine the six components generated by the thrust vector: three forces (axial, pitch, and yaw) and three thrust moments (pitch, yaw, and roll).

Pressure altitudes were maintained, before and after engine test firing, by a stream-driven ejector in the test cell exhaust duct in series with the facility exhaust compressors (Fig. 12b). Ejector steam was supplied by the AEDC stationary boilerplant and the J-3 steam accumulators. During the steady-state portion of test firings, test cell pressure altitude was maintained by an engine exhaust-driven supersonic diffuser. Propellant and test cell capsule temperature conditioning systems are available to maintain temperatures from 30 to 140°F.

Facility systems included ground-level propellant storage; helium for test article propellant tank pressurization; GN_2 for test

article pressure/leak checking, purging, and valve operation; F-3 fixture helium pressurization controls, operable from the J-3 control room; and electrical power in both 28v dc and 100v, 60 cps, ac. Equipment for test article operation, located in the J-3 control room, included the gimbal system checkout and controls consoles and the engine firing control and combustion stability monitor (CSM) console.

2.5 INSTRUMENTATION

Instrumentation was provided to measure engine thrust (including axial and side forces); chamber pressure; propellant system pressures, temperatures, and flow rates; nozzle extension and combustion chamber case temperatures; gimbal system electrical signals; and various vibrations and accelerations. Schematic diagrams of relative locations of the test article and test cell instrumentation are shown in Fig. 14.

2.5.1 Force Measuring System

2.5.1.1 Axial Force

Axial force (F_a) was measured with a dual-bridge, strain-gage-type load cell of 50,000-lb_f rated capacity. In-place calibration was accomplished with a hydraulic actuator axial loading system containing a calibration load cell (Fig. 12b and Ref. 11). The calibration load cell was laboratory calibrated, with traceability to the National Bureau of Standards (NBS).

2.5.1.2 Side and Roll Forces

Two yaw forces, two pitch forces, and one roll force were measured with strain-gage-type load cells of 500-lb_f rated capacity. These forces completed the six-component system for engine thrust vector determination. In-place loading calibration with NBS traceability was also provided for these load cells.

2.5.2 Pressures

2.5.2.1 Combustion Chamber Pressure

Chamber pressure was measured using two strain-gage-type pressure transducers connected to a pressure tap located on the injector face near the outer edge. One transducer was close-coupled to optimize response to pressure transients; the other transducer was

provided with the capability for in-place applied-pressure calibration (Fig. 15). The calibration transducer was a precision reluctance type, which was laboratory calibrated with NBS traceability.

2.5.2.2 Cell Pressure

Test cell pressure was measured with two capacitance-type precision pressure transducers located outside the cell capsule in a self-contained, controlled-temperature environment. These transducers were laboratory calibrated with a precision mercury manometer. In-place calibrations were made by electrical voltage substitutions only.

Test cell pressure was also measured with two auxiliary strain-gage-type transducers. These were situated in the test cell behind the F-3 fixture support structure to minimize exposure to thermal radiation.

2.5.2.3 Propellant Pressures

Propellant pressures in the F-3 fixture lines, engine lines, thrust chamber valve, and injector manifolds were measured with strain-gage-type pressure transducers.

2.5.3 Temperatures

2.5.3.1 Engine Assembly Temperatures

Exhaust nozzle extension, combustion chamber, and injector surface temperatures were measured with Chromel®-Alumel® thermocouples. Combustion chamber case temperature thermocouples were welded, peened, or bonded to the structure as appropriate for the base material.

2.5.3.2 Propellant Temperatures

Propellant temperatures in the F-3 fixture tanks and engine line inlets were measured with copper-constantan thermocouple immersion probes. Temperatures in the F-3 fixture propellant lines were measured with resistance temperature transducer (RTT) immersion probes.

2.5.3.3 Test Cell Wall Temperature

Cell wall interior surface temperatures were sensed with copper-constantan thermocouples welded to the cell capsule wall surface.

2.5.4 Propellant Flow Rates

Propellant flow rates were measured with one flowmeter in each F-3 fixture propellant feed line, upstream of the engine interface. The flowmeters were axial-flow, turbine-type, rotating permanent magnet, volumetric flow sensors with two induction coil signal generators.

2.5.5 Engine Vibration and Acceleration

Engine injector, combustion chamber, and mount structure vibrations were measured in three perpendicular planes with piezoelectric-type accelerometers. Any engine vibration caused by combustion instability was sensed by one of the accelerometers mounted on the engine injector. The accelerometer output signal was analyzed by the AGC CSM to initiate engine shutdown automatically in the event of rough combustion (defined as engine acceleration exceeding 180 g's peak-to-peak at a frequency above 600 cps for longer than 0.080 sec). An NAA flight-type CSM was also used during all test periods, but because of interaction with the test facility electrical systems, the data were not considered valid. This problem was not resolved in time for data presentation during this report period.

2.5.6 Gimbal System Electrical Signals

Electrical voltage and current signals from the gimbal control and actuation systems were monitored to indicate gimbal actuator position, actuator position change rate, drive motor voltage and current, and actuator clutch currents.

2.5.7 Data Conditioning and Recording

A continuous recording of analog data was made on magnetic tape from analog instrument signals by (1) analog-to-frequency converters and (2) frequency-modulated (FM) recording with a saturation-level pulse technique. Instrument signals produced in a proportionate frequency form were amplified for continuous FM recording on magnetic tape.

Magnetic tape recordings in digitized form from an analog signal were also used. Various instrument analog signals were (1) amplified and converted to a common range of analog base-level and amplitude, (2) commutated for sequential scanning, and (3) converted to the binary code for magnetic tape recordings.

Light-beam oscillographs were used for continuous graphic recordings of analog and proportionate frequency signals. Frequency signals of the propellant flowmeters were recorded on the oscillograph with a divided frequency to improve record readability.

Direct-inking, strip-chart recorders were used for immediate access, continuous, graphic recordings. Analog signals produced pen deflections with a null-balance potentiometer mechanism. Frequency signals were converted to analog strip-chart recording.

2.5.8 Visual Coverage

Two closed-circuit television systems permitted visual monitoring of the test article during testing operations. Permanent visual documentation of engine test firings was provided by 16- and 70-mm motion-picture cameras located in the test cell. An oscilloscope enabled visual observation of the CSM accelerometer signals during testing operations. Various engine and F-3 fixture parameters were recorded on strip-chart recorders with visual indicators in addition to the direct-inking feature to provide control room indications of test article operation, performance, and environment during testing.

SECTION III
PROCEDURE

3.1 PRE-TEST OPERATIONS

3.1.1 Preparations at Ambient Atmospheric Pressure

Prior to each test period, the following functions were performed with the test cell environment at ambient atmospheric pressure:

1. The six-component thrust system was calibrated (with the engine propellant lines pressurized to 185 psia when side forces were measured).
2. Instrumentation, necessary for obtaining engine performance data, was checked.
3. Functional checks were performed on the firing sequences and the TCV.
4. The F-3 fixture was loaded with propellants.
5. In-place flowmeter check calibrations were conducted (using the flowmeter calibration system described in Appendix III).

6. The F-3 fixture was reloaded with propellants. Propellant samples were taken to determine the specific gravity, chemical analysis, and the particulate contamination, which were submitted for AGC approval.
7. The propellant tanks were pressurized, and axial thrust, chamber pressure, and test cell pressure measurement and devices were in-place calibrated.

3.1.2 Altitude Preparations

The test cell pressure was reduced to approximately 0.4 psia with the facility exhaust compressors in preparation for calibrations at pressure altitude. Instrumentation systems were calibrated; axial thrust, chamber pressure, and certain test cell pressure instruments were physically in-place calibrated; and a final, functional/sequence check of all instrumentation was performed.

3.1.3 Pre-Fire Final Preparation

Prior to each test firing, the following operations were performed:

1. Propellant tanks were pressurized to the required pressure.
2. The steam ejector was used to further reduce test cell pressure to less than 0.2 psia. Prior to engine firing, steam from the accumulators further reduced the test cell pressure to approximately 0.05 psia.
3. All pre-fire operations within 60 sec of firing were automatically sequenced (i.e., instrumentation and camera starts and engine firing). All immediate post-fire operations were also automatically sequenced (i.e., engine shutdown, instrumentation, and camera).
4. All firings were controlled with the AGC firing panel.
5. Immediately after engine shutdown, the J-3 accumulators were shut down, and lower simulated coast altitudes were maintained for the simulated coast using the facility exhaust compressors and the stationary boilerplant.

3.2 POST-TEST OPERATIONS

After the last firing of a test period, the following operations were performed:

1. The steam ejector was shut down, and test cell pressure was maintained at approximately 0.4 psia by the facility exhaust compressors.
2. Axial thrust, chamber pressure, and certain cell pressure measuring devices were physically in-place calibrated.
3. All transducers were resistance calibrated.
4. The F-3 fixture tanks were drained and depressurized.
5. The engine propellant valve was opened for propellant system aspiration for approximately one hour.
6. The TCV was then closed and the test cell pressure allowed to return to ambient atmospheric pressure.
7. Again all transducers were resistance calibrated.
8. Axial thrust, test cell pressure, and chamber pressure measuring devices were in-place calibrated.

3.3 PERFORMANCE DATA ACQUISITION AND REDUCTION

All engine operation parameters were recorded on magnetic tape in continuous modulated frequency form. Digital computers were used to recover data from the magnetic tape records, produce data printouts in engineering units, and calculate engine performance information, such as engine ballistic performance (vacuum thrust, thrust coefficient, characteristic velocity, and specific impulse), total impulse of ignition and shutdown transients, total impulse of minimum impulse bit operation, and thrust vector determination.

The equations used for determining engine performance were in accord with general industry practice, except for special adaptations which were incorporated to account for the area changes of the ablative nozzle throat. Performance calculations were based on combustion chamber pressure measured at the injector face. No corrections were made for the total pressure loss between the injector and the nozzle throat. Steady-state performance calculations were made from measured data which were averaged over 2-sec time intervals.

The estimated accuracies (one standard deviation) of the measured parameters required for engine performance are as follows:

Parameters	Accuracy, percent
F_a	0.15
P_c	0.25
$\dot{W}_f$	0.22
$\dot{W}_o$	0.21
P_a	1.85

The one standard deviation errors in calculated parameters are estimated to be:

Parameters	Accuracy, percent
$\dot{W}_t$	0.15
F_v	0.16
I_{sp_v}	0.22

3.3.1 Ballistic Performance

Because the effective nozzle throat area variations are nonuniform during a firing and cannot be physically measured between firings, the characteristic velocity and nozzle throat area were calculated during the firing series used the following assumptions:

1. Characteristic velocity, corrected to a mixture ratio of 1.6, is constant for a given injector and is independent of chamber geometry.
2. Characteristic velocity is a function of mixture ratio only, and
3. The slope of the c* versus MR curve conforms to previous experimental data.

The characteristic velocity (c_i^*) for a given injector was calculated using:

1. The engine data between 2 and 4 sec of the initial firing of a new chamber,
2. The pre-test measured nozzle throat area,

3. The relationship:

$$c_i^* = P_c A_t g/\dot{W}_t$$

The c* for a mixture ratio of 1.6 was derived from the AGC-supplied curve slope factor:

For test series DD-DF:

$$f_{corr} = 5714.51/[1069.699 + 8862.018\ (MR) - 6081.624\ (MR)^2 + 1795.943\ (MR)^3 - 201.6667\ (MR)^4]$$

For test series DG-DI:

$$f_{corr} = 5771.35/[5424.914 + 594.293\ (MR) - 236.080\ (MR)^2]$$

then:

$$c_i^*\ (MR = 1.6) = c_i^*\ f_{corr}$$

This c_i^* for MR = 1.6 was used as the standard for the given injector-chamber assembly for data reduction of subsequent firings. The c* for any other MR during subsequent firings was derived by reversing the process and applying the MR slope factor to the standard c_i^* at MR = 1.6.

The throat area of the nozzle for subsequent firings was calculated using the c* derived above, the measured chamber pressure, the measured propellant flow rates, and the relationship:

$$A_{t_{calc}} = c^*\ \dot{W}_t/gP_c$$

This calculated nozzle throat area was used with the axial thrust corrected to vacuum conditions and measured chamber pressure to determine the vacuum thrust coefficient (C_{F_V}). When the calculated throat area is used, the C_{F_V} becomes independent of the measured chamber pressure and is reduced to

$$C_{F_v} = F_v/(P_c A_t) = F_v/P_c\ (c^* \dot{W}_t/P_c g) = I_{sp_v} g/c^*$$

3.3.2 Total Impulse of Ignition and Shutdown Transients

The total impulse (lb_f-sec) of the ignition transient covered the time period from ignition (initial chamber pressure rise) to 100 percent of steady-state thrust. The impulse was integrated using thrust calculated from chamber pressure:

$$I_t = C_{F_v} \cdot A_{t_{calc}} \int_0^t P_c dt$$

The values of C_{F_V} and $A_{t_{calc}}$ (derived from steady-state operation nearest the transient of interest) were assumed to be constant throughout the transient. Intermediate levels of ignition impulse values were

also derived at intervals of percent of steady-state thrust level. The total impulse of the shutdown transient covered the time period from 100 to 0 percent of steady-state thrust. The 0-percent level was defined as the thrust level at which the exhaust flow in the nozzle throat became unchoked. The point of flow unchoking was taken to be when $P_c/P_a = 1.20$ (termed the critical ratio). The measured thrust could not be used to calculate transient vacuum thrust because force system dynamics invalidate the thrust data during the transients.

Measured combustion chamber pressure was reduced at 0.005-sec intervals (200 intervals/sec) during ignition and at 0.020-sec intervals (50 intervals/sec) during shutdown from the continuous magnetic tape recording of the close-coupled transducer data.

3.3.3 Total Impulse of Impulse Bit Operation

The method used to calculate the total impulse (lb_f-sec) of the impulse bit firings (< 1 sec) was identical to the method used for the ignition and shutdown transients. However, for the impulse bit firings, the impulse was totalized for the entire firing from ignition through thrust decay to the critical P_c/P_a ratio. Since the impulse bit firings were too short to establish steady-state engine performance levels, the C_{F_V} and the A_t used were obtained from the nearest previous engine firing which produced steady state at the same operating conditions. Again, C_{F_V} and A_t were assumed to be constant throughout the impulse bit firings.

3.3.4 Thrust Vector Determination

The multicomponent thrust vector measurement system is shown schematically in Fig. 13. The depicted load cells measured the six forces required to describe the six components of thrust; forward and aft pitch, forward and aft yaw, roll, and axial forces. To convert these forces into thrust vector components, it was assumed that the mechanical interactions were linear and repeatable for a given force application. That is, for a given load (L), the reaction force (R), measured in any load cell, could be obtained from the relationship

$$R_i = c_{ij}L_j$$

where C_{ij} represented the calibration constants based on the slope of the interaction. Because there were six data load cells (i) and six calibrate load cells (j), both varied from 1 to 6 and thus, constituted a 6-by-6 matrix.

To obtain true forces from the thrust system, equations of the form

$$L_j = K_{ji}\ R_i$$

were used, where K_{ji} represented the balance constants (inverse of the calibration constant matrix C_{ij}). A complete explanation of the force system and the method of determining the balance constants is given in Ref. 12. After determining the forces at the six load cells, equations of static equilibrium were used to resolve these forces into a thrust vector. This thrust vector was described with angles from the thrust cage centerline and deflection of the thrust vector/gimbal plane intersection from the thrust cage centerline in the pitch and yaw planes.

SECTION IV
RESULTS AND DISCUSSION

The primary objectives of this Phase IV developmental test program were to prove combustion chamber durability using a revised Block II chamber design (A-1) and to determine ballistic performance of the Apollo SM engine using three different propellant injectors at pressure conditions simulating altitudes above 110,000 ft. During one test series, the nozzle extension and nozzle flange were cooled with cold gaseous nitrogen prior to three firings to demonstrate the ability of the nozzle extension to withstand thermal shock. During another test series, stiff links instrumented with load cells were installed in place of the gimbal actuators to determine the steady-state null force at the zero gimbal angle. The engine was operated at both design (P_c = 97 psia and MR = 1.6) and off-design conditions, and two of the six test series were conducted with propellants and the test cell capsule temperature conditioned to approximately 110°F.

One hundred sixty-eight test firings with an accumulated firing time of 4538 sec were conducted using six different engine assemblies during six test series. Of these 168 tests, 39 were performance tests of 10 sec or greater in duration, and all other tests were for determination of transient characteristics. A brief description of the individual test series is presented in Appendix IV and a summary of test number, dates, objectives, and firing durations is listed in Table I (Appendix II).

4.1 ENGINE BALLISTIC PERFORMANCE

The ballistic performance of the Block II Apollo SM engine was determined for the six engine assemblies by conducting 39 test firings over a chamber pressure range from 76 to 118 psia, a mixture ratio range from 1.40 to 1.90, and with propellants temperature conditioned over a range from 70 to 110°F. Nominal operating conditions of the Block II SM engine are 97 psia chamber pressure and 1.6 mixture ratio.

Two basic parameters were used to describe engine performance: (1) specific impulse corrected to vacuum conditions (I_{sp_V}) was used to define overall engine performance and (2) characteristic velocity (c*), computed using injector face pressure (P_c), indicated the injector-combustion chamber performance. Because the calculation of I_{sp_V} used measured data only and the calculation of c* incorporates certain assumptions as described in Section 3.3.1, I_{sp_V} is considered the more accurate indication of performance.

An indication of nozzle performance was obtained with the thrust coefficient (C_{F_V}) calculated using the assumptions described in Section 3.3.1. The C_{F_V} thus derived is dependent on I_{sp_V} and the relative c* and is, therefore, not a true indication of nozzle performance. For this reason C_{F_V} is not discussed in this section, although tabulated values of C_{F_V} are presented in Table II.

4.1.1 Overall Engine Ballistic Performance

The vacuum specific impulse (I_{sp_V}) data obtained during steady-state engine operation are presented in Table II. The data used for this analysis were obtained between 7 and 40 sec of the test firings to ensure steady-state data and the absence of any thermal effects on the force measuring system.

For presentation purposes, the performance of the six engine assemblies is arranged into three groups corresponding to the three injectors used. Each of the three injectors was used in two engine assemblies. Each of the six engine assemblies employed new ablative chambers, and each used the same design nozzle extension. The hardware components used for each engine are tabulated in Section 2.2, and the injectors are described in Section 2.2.1. The major features of each injector are tabulated below:

	Test Series					
	DD	DE	DF	DG	DH	DI
Engine S/N	21A	21B	21C	21D	21E	21F
Injector S/N	110		93		105	
Baffle Configuration (See Section 2.2.1)	Short		Long		Long	
Orifice Pattern (See Section 2.2.1)	Impinging Doublet		Impinging Doublet		Impinging Doublet with Counterbored Oxidizer Orifices and Selected Counterbored Fuel Orifices	
P_c Tap Location (See Section 2.2.1)	Block II		Block I		Block II	

The short baffled injector (S/N 110) was tested at both design (97 psia) and high (110 psia) chamber pressures, at various mixture ratios (MR), and at an average propellant temperature (T_p) of 77°F. Average propellant temperature is the arithmetic average of the oxidizer and fuel temperature measured at the flowmeters. The trend of I_{sp_v} with MR shown in Fig. 16 was the same as that determined during previous testing of similar injectors (Ref. 10). The I_{sp_v} at MR = 1.6 and P_c = 97 psia was 314.7 lb_f-sec/lb_m and increased to 315.6 by raising P_c to 110 psia at the same MR.

The results, as shown in Fig. 17, from the first long baffled injector, S/N 93, tested at AEDC indicated that the engine performance using this injector was sensitive to the propellant temperature in addition to chamber pressure and mixture ratio. The cross-plotted data from Fig. 17 show in Fig. 18 that the I_{sp_v} (at MR = 1.6 and P_c of approximately 110 psia) varied from 315.6 lb_f-sec/lb_m to 314.4 lb_f-sec/lb_m as the average propellant temperature (T_p) increased from 78 to 112°F. The trend of I_{sp_v} versus MR for this injector was slightly different, as shown in Fig. 17, than for the previous injectors tested since the slope of the I_{sp_v} versus MR curve is positive at MR = 1.6. This was the only injector tested which had this trend with MR and the only injector tested which was significantly sensitive to propellant temperature.

The qualification prototype injector (S/N 105), which had long baffles and counterbored orifices, was tested with various chamber pressures in the range between 76 and 113 psia at nominal (74°F) and high (108°F) propellant temperatures. The data (Fig. 19) show that performance using this injector exhibited similar trends as a function of MR and P_c as similar injectors in a previous test (Ref. 10). The cross-plotted data from these tests (shown in Fig. 20) indicate, however, that the I_{sp_v} of the engine assemblies employing this long-baffled injector with counterbored orifices exhibits about 1.5 sec less I_{sp_v} than the engine assemblies employing the other two injectors and about 2 sec less I_{sp_v} than for previous tests (Ref. 10) at the Block II operating conditions. The I_{sp_v} at the nominal operating condition was 313.2 lb_f-sec/lb_m; raising P_c to 110 psia increased I_{sp_v} to 314.4 lb_f-sec/lb_m. Propellant temperatures had little effect on vacuum specific impulse.

The data obtained during testing at 110 psia P_c (test series DH) incurred scatter from mechanical binding in the thrust measurement system. The binding was not apparent in pre-test calibrations, and the resulting impairment of thrust measurement introduced uncertainties in I_{sp_v} of approximately ±1 lb_f-sec/lb_m. The data from this test series are, however, in good agreement with those obtained during test series DI using the same injector.

4.1.2 Combustion Chamber Performance

Characteristic velocity (c*), calculated by the method described in Section 3.3.1, is used as an indication of combustion efficiency. With this method of calculation, an intrinsic c* for an injector is established from the early portion of the first firing (2 to 4 sec) on a new chamber using the relation of $P_c/\dot{W}_t$ and the pre-fire measured nozzle throat area. The c* for subsequent times during the firing and for subsequent firings with the same injector was calculated by applying an MR slope factor (Section 3.3.1) to the initial c*.

The initial values of c*, corrected to a mixture ratio of 1.6, for the six engine assemblies tested appear in Fig. 21 and below:

	Test Series					
	DD	DE	DF	DG	DH	DI
Engine S/N	21A	21B	21C	21D	21E	21F
c* at MR = 1.6, ft/sec	5916	5901	5859	5852	5903	5899
Injector S/N	110		93		105	
Baffle Configuration (See Section 2.2.1)	Short		Long		Long	
Orifice Pattern (See Section 2.2.1)	Block II		Block I		Block II	

The difference (approximately 1 percent) between c* for injector S/N 93 and the other injectors tested is attributed to the difference in measured injector face chamber pressures because of the different tap locations shown in Fig. 4 and documented previously in Ref. 10.

It is apparent from these data on injectors 110 and 105 that c*, calculated using injector face pressure, is not a valid indicator of the relative vacuum performance for different injector designs. The characteristic velocity for injectors 105 and 110 is in agreement within 0.25 percent, whereas the vacuum specific impulse differs by 0.5 percent.

4.1.3 Effect of Propellant Tank Crossover on Engine Ballistic Performance

The F-3 propellant tanks were connected in series with a constant, regulated helium pressure supplied to the top of the storage tank (Fig. 10b).

The propellant flow rate, however, was a function of the pressure at the bottom of the sump tank, which varied with propellant level. When the propellant was depleted in the storage tank, the pressure in the sump tank increased suddenly because there was no propellant level difference between the tanks to overcome, and the connecting line flow loss became very small (defined as crossover). Because of the engine feed pressure variation, crossover had a pronounced effect on engine operation as shown in Fig. 22. The engine performance, however, does not change significantly as a result of the mixture ratio change during crossover because of the shallow slope of I_{sp} versus MR at the nominal mixture ratio. These feed pressure variations were partly a result of the gravitational effect (1 g in ground testing) and may be quite different in the actual space flight acceleration environment.

4.1.4 Engine Transient Characteristics

The total impulse (lb_f-sec) developed during engine ignition and shutdown transients was determined for each test firing greater than 1 sec duration during this testing phase by the method described in Section 3.3.2. A tabulation of the ignition impulse developed from FS-1 to 90 percent of the steady-state thrust during each test appears in Table III.

A correlation of ignition impulse with representative pre-fire temperatures of the TCV is shown in Fig. 23 and indicates that the impulse developed was markedly affected by the heat soak to the TCV. It is reasoned that high propellant temperature decreased the chamber pressure rise rate, which increased the ignition transient time and the total ignition impulse.

The data used for determination of the average ignition impulse were those obtained below 100°F, where heat soak appears to have little effect on the P_c rise rate. A typical ignition transient, and transient impulse developed, is shown in Fig. 24. The average ignition impulse (FS-1 to 90 percent steady-state thrust) using thrust chamber valve bank A was 471 lb_f-sec, with a one standard deviation of ±76 lb_f-sec. The average time required to develop the impulse was 0.53 sec with a one standard deviation of 0.004 sec. All data used in these calculations were obtained at 110 psia chamber pressure. There were no firings (duration > 1 sec) obtained with P_c of 97 psia or with TCV bank B where the TCV temperature was below 100°F. Because many of the test firings were conducted with the TCV temperature in the range in which impulse was affected, the average ignition impulse and the standard deviation would have been considerably different, as shown in Fig. 23, if the high TCV temperature ignitions were included in thrust calculations. During

test DI-12, the TCV temperature reached 207°F with a resultant transient impulse of 5348 lb_f-sec and a corresponding time to 90 percent of 0.831 sec.

A typical shutdown transient is shown in Fig. 25. A tabulation of the shutdown impulse (impulse from FS-2 to 1-percent steady-state thrust) developed during each firing is shown in Table IV and is summarized below:

Valve Bank	Steady-State P_c	Time from FS-2 to 1-percent Steady-State Thrust, sec	Impulse from FS-2 to 1-percent Steady-State Thrust, lb_f-sec
A	97	2.2018 ± 0.859	9710 ± 1175
A	110	2.7515 ± 0.590	10858 ± 789
B	97	2.323 ± 0.722	9322 ± 671
B	110	2.8075 ± 1.0668	10932 ± 1964

4.1.5 Impulse Bit Operation

The impulse data for impulse bit test firings (firings of duration less than 1 sec) were totalized from the time of ignition until the time that flow in the nozzle throat became unchoked after FS-2. The time for unchoked flow in the nozzle throat was defined as the time when the ratio P_c/P_a equals 1.20. These data are tabulated in Table V.

Figure 26 shows that the total impulse developed during the minimum impulse bit firings was almost a linear function of the firing duration and that the firing duration would have to be greater than 0.3 sec for any impulse to be developed. The total impulse developed using valve bank B was slightly lower than the impulse developed using valve bank A as shown in Fig. 26 and is attributed to the difference in the timing of the two valve banks.

4.2 THRUST VECTOR EXCURSION

Six-component force data were measured during 7 of the 11 firings during test series DH. The six-component force balance and thrust vector determination technique are described in Ref. 12. The

balance was also used in Apollo Block I engine prequalification, qualification, and development test phases (Refs. 7 through 10) to determine the change in thrust vector resulting from chamber ablation. During test series DH, stiff links were installed on the engine in place of the gimbal actuators.

The thrust vector excursion for firings of over 10 sec duration are presented in Fig. 27. The presentation is a time history for both the pitch and yaw planes of the angular excursion and the excursion of the point of intersection of the thrust vector with the gimbal plane. Data reduction techniques (Ref. 12) produce the vector referenced to the centerline of the force balance. The relationship between the engine geometric centerline and the balance centerline was not determined.

The maximum excursion of the point of intersection of the vector with the gimbal plane is tabulated below (dimensions are in inches):

DH-01		DH-02		DH-04	
x	y	x	y	x	y
-0.032	0	-0.045	-0.015	-0.055	+0.015

DH-05		DH-08		DH-09	
x	y	x	y	x	y
-0.022	-0.025	-0.075	-0.055	0	-0.020

The intersection position displayed a similar excursion trend during each firing. Progressive thermal and ablative effects on the centroid of the chamber throat are the probable reasons for the initial value not being the same for each firing. The initial values at the start of each firing differed from the initial value of DH-01 by a maximum of +0.06 and -0.065 in. in the pitch and yaw planes, respectively. The thrust vector data obtained during the 495-sec firing (DH-04) are not presented beyond the first 100 sec because temperature effects on the balance structure invalidated the vector position indication. The coast period after test DH-04 was of sufficient length to allow the balance structure to return to its original conditions and, therefore, produce valid vector data following DH-04.

Angular excursion for the first two tests (DH-01 and 02) was essentially zero in the pitch plane and -0.10 deg in the yaw plane. During test DH-03 (which was a set of eleven 3-sec firings), the nut at the top attachment point of the pitch stiff link loosened (discussed in Section 4.3.3) and resulted in a thrust vector angle change 0.1 deg in pitch plane and 1.08 deg in yaw plane as shown in Fig. 28. Thrust vector angle excursion data are not presented for tests subsequent to DH-04 because no confidence can be placed in the data with the loosened stiff link.

During this test series, stiff links equipped with strain-gage load cells were used in place of gimbal actuators to determine the steady-state null force at the zero gimbal angle position. No valid data were obtained after loosening of the pitch stiff link retaining nut during test DH-03 (described in Section 4.3.3). The forces measured during the first two tests (DH-01 and 02) are presented in Fig. 29 which shows that the maximum forces measured were 165 and 66.5 lb_f (tension) for the pitch and yaw stiff links, respectively.

4.3 ENGINE DURABILITY

4.3.1 Nozzle Extension

Three nozzle extensions were used for these tests. Each nozzle endured about 1500 sec of test time (two complete engine tests) without adverse effects. No difficulty was experienced when the nozzle extension and nozzle flange were cooled to between -100 and -300°F with cold GN_2 before four firings during test series DH.

4.3.2 Combustion Chamber

A new chamber was used for each of the six test periods. These chambers were of different design from those used during the first three tests of this testing phase as discussed in Section 2.2.2 and in Ref. 10. Figure 6 presents a comparison of the previous chamber design with that used for the testing reported herein (A-1 design). Post-test condition of the chamber used for test series DD exhibited one perforated blister in the ablative liner about midway between the injector flange and the chamber throat (Fig. 30). Post-test condition of the chamber used for the DE test series sustained extensive losses of material in the forward few inches of the ablative lining (Fig. 31); the remainder of the chamber endured well. For the remaining four chambers, which were used during test series DF, DG, DH, and DI, the post-test chamber condition was excellent. Although these four

chambers were of the same design as the ones used on the DD and DE test series, the resin curing cycle was changed.

4.3.3 Injector

Post-test inspection of the injector used on the DG series revealed several cracked welds at the juncture of the radial baffles and the central hub. This condition did not noticeably affect the performance or operation of the engine. This injector had been used on both the DF and DG test periods for a total of about 1500 sec firing duration.

After the test series DH, the injector pitch actuator bracket exhibited a small crack in the weld at the center attachment point to the injector. The pitch stiff link top attachment nut was found to be stripped and backed off several turns after the DH series. It was concluded that the loose attachment of the pitch stiff link caused unusual engine movement and impact loads which resulted in the crack of the pitch actuator bracket. The same injector was used for the following test series (DI) without difficulty or further progression of the crack.

Prior to each test period, a pulse charge of the type described in Section 2.2.1 was installed on the injector. The heat of combustion fired the pulse charge at about 1 sec after engine ignition. The resulting pulse in chamber pressure was used to determine the capability of the combustion mechanism to recover from induced instability. Combustion stability recovery was satisfactory for all tests during which the explosive charge was used.

No combustion anomalies (spontaneous pops), which were observed during tests using injectors 93 and 110, were observed with injector 105 (long baffled, counterbored-orifice injector).

4.3.4 NAA Flight-Type Combustion Stability Monitor

An NAA flight-type combustion stability monitor was used on all engines tested. However, because of the interactions between the test facility electrical systems, the data were not considered valid, and the problem was not resolved until completion of the tests reported herein.

4.4.1 Nozzle Extension Temperature

Because satisfactory nozzle extension durability had been adequately demonstrated and equilibrium temperatures had been

documented from previous testing at AEDC (Refs. 1 through 9), nozzle extension temperature measurements were minimized for this testing.

Three firings (DH-01, 02, and 04) were conducted during test series DH with the nozzle extension precooled with cold GN_2 to between -100 and -300°F. During these tests, the test cell wall was maintained at near 65°F. A comparison of two tests, one conducted with 85°F test cell environments (DF-04) and the other with the cold nozzle starting conditions and test cell wall of 65°F (DH-04), is presented in Fig. 32. This comparison shows that the initial nozzle temperature conditions had little or no effect on the final operating temperature of the nozzle extension.

4.4.2 Combustion Chamber and Injector Temperatures

Only gross conclusions can be drawn from the chamber surface temperature data because the temperatures experienced were greatly dependent on the thermal conductivity time lags associated with various lengths of firings and duration of coasts preceding a test. Also, outer surface thermocouples were relatively insensitive to internal chamber conditions. For example, Fig. 33 shows no significant difference in chamber temperature between tests (test series DD and DE) which culminated with ablative lining failures and a test (test series DG) in which chamber durability was satisfactory. The outer surface aft temperature shows the local effect of heat conduction from the nozzle extension mounting flange.

Chamber durability problems and successes, which were encountered in this testing, were more clearly reflected in the temperatures measured at the outer periphery of the injector and at the forward chamber/injector attachment flange. Figures 34 and 35 show both the injector periphery and the attachment flange to have a somewhat cooler trend and final peak temperatures between 60 and 100°F lower when chamber durability was satisfactory. This was so because the ablative lining failures of the earlier tests were mainly at the forward portion of the chamber, which disrupted the fuel film cooling and/or permitted hot gas access deeper into the chamber/injector joint.

4.5 GIMBAL SYSTEM OPERATION

Gimbaling operations were conducted during 49 of the 167 total firings of this testing. Gimbal operations were omitted for engine S/N 21E (series DH) on which the gimbal actuators were replaced with stiff links instrumented with load cells.

The gimbal amplitude was limited to ±1.5 deg during gimbaling to prevent spilling the nozzle exhaust over the inlet of the exhaust diffuser and into the test cell. The gimbal operations included ramp, step, and sine function command signals of various frequencies to document gimbal system mechanical and electrical dynamics. A description of these operations and examples of oscillograph data are given in Ref. 7. These gimbal operations of the engine, complete with nozzle extension at latitude pressure conditions, were performed to provide data for definition of the engine mount/gimbal system vibration characteristics (such as system spring rate, effective mass, and damping). Analysis of the gimbal data was done by AGC and NAA.

SECTION V
SUMMARY OF RESULTS

Significant results obtained during the last six Apollo Service Module Block II Development tests are:

1. The combustion chambers used for the first two tests exhibited inadequate durability of the ablative lining. However, with small changes in chamber design and manufacture, the durability of the remaining four chambers tested was excellent.
2. The engine ballistic performance in terms of vacuum specific impulse (I_{sp_v}) was found to be a function of the injection design and the operating conditions.
   a. The injector with short baffles (S/N 110) produced I_{sp_v} of 314.7 lb_f-sec/lb_m at design conditions (chamber pressure 97 psia, mixture ratio 1.6, propellant temperature near 70°F). The I_{sp_v} increased by 0.29 percent to 315.6 lb_f-sec/lb_m for operation at 110-psia chamber pressure and design mixture ratio.
   b. The injector with long baffles (S/N 93) was tested over a propellant temperature range from 78 to 112°F at 110-psia chamber pressure and design mixture ratio. The I_{sp_v} varied from 315.6 to 314.4 lb_f-sec/lb_m with the highest temperature producing the lowest impulse. This trend was not evident for short baffled injectors during previous testing.

c. The injector with long baffles, counterbored orifices, and selected counterbored fuel orifices (S/N 105) produced the lowest I_{sp_v} of the three injectors tested. The I_{sp_v} at nominal conditions was 313.2 lb_f-sec/lb_m, which was 1.5 sec less than that for injector 110 and approximately 2 sec lower than the values obtained during Block I Qualification testing at the same conditions. Raising chamber pressure to 110 psia increased I_{sp_v} to 314.4 lb_f-sec/lb_m.

3. No spontaneous pops were exhibited in chamber operational parameters during the two test series using the injector with the counterbored orifices (S/N 105).

4. The TCV valve bank selection had no effect on steady-state engine ballistic performance.

5. Nozzle extension durability was excellent; the three nozzles each endured testing equivalent to twice design life without adverse effects.

6. The nozzle extension's ability to withstand cold starts was demonstrated during three starts prior to which the nozzle extension and mounting flange were cooled to between -100 and -300°F.

7. The maximum steady-state null force at the zero gimbal angle position, measured with the pitch and yaw stiff-link load cells, were 165 and 66.5 lb_f (tension), respectively.

8. No difficulty was experienced with the NAA heat shield attached to the combustion chamber/nozzle extension attachment flange.

REFERENCES

1. DeFord, J. F. "Simulated Altitude Testing of the Aerojet-General Corporation AJ10-137 Rocket Engine (Report I, Phase I Development Test)." AEDC-TDR-64-81 (AD350408), May 1964.

2. McIlveen, M. W. "Simulated Altitude Testing of the Aerojet-General Corporation AJ10-137 Rocket Engine (Report II, Phase I Development Test)." AEDC-TDR-64-82 (AD350407), May 1964.

3. Vetter, N. R. and DeFord, J. F. "Simulated Altitude Testing of the Aerojet-General Corporation AJ10-137 Rocket Engine (Report III, Phase I Development Test)." AEDC-TDR-64-146 (AD352141), July 1964.

4. McIlveen, M. W. "Simulated Altitude Testing of the Aerojet-General Corporation AJ10-137 Rocket Engine (ReportIV, Phase I Development Test." AEDC-TDR-64-147 (AD352357), August 1964.

5. Vetter, N. R. and DeFord, J. F. "Simulated Altitude Testing of the Aerojet-General Corporation AJ10-137 Rocket Engine (Report V, Phase I Development Test)." AEDC-TDR-64-158 (AD352700), August 1964.

6. Vetter, N. R. and McIlveen, M. W. "Simulated Altitude Testing of the Aerojet-General Corporation AJ10-137 Rocket Engine (Report VI, Phase I Development Tests)." AEDC-TDR-64-171, September 1964.

7. Schulz, G. H. and DeFord, J. F. "Simulated Altitude Testing of the Apollo Service Module Propulsion System (Report I, Phase II Development Test)." AEDC-TR-65-233 (AD368743), January 1966.

8. Schulz, G. H. and DeFord, J. F. "Simulated Altitude Testing of the Apollo Service Module Propulsion System (Report II, Phase II Development Test)." AEDC-TR-66-17 (AD369807), February 1966.

9. Gall, E. S., McIlveen, M. W., and Berg, A. L. "Qualification Testing of the Block I Apollo AJ10-137 Service Module Engine." AEDC-TR-66-129, August 1966.

10. Pelton, J. M. and McIlveen, M. W. "Block II AJ10-137 Apollo Service Module Engine Testing at Simulated High Altitude (Report I, Phase IV Development)." AEDC-TR-66-169 (AD376952L), November 1966.

11. Test Facilities Handbook (6th Edition). "Rocket Test Facility, Vol. 2." Arnold Engineering Development Center, November 1966.

12. Robinson, C. E. and Runyan, R. B. "Thrust Vector Determination for the Apollo Service Propulsion Engine Using a Six-Component Force Balance." AEDC-TR-65-250 (AD475564), December 1965.

APPENDIXES

I. ILLUSTRATIONS
II. TABLES
III. PROPELLANT FLOWMETERS AND WEIGH SCALE CALIBRATIONS
IV. TEST SUMMARY

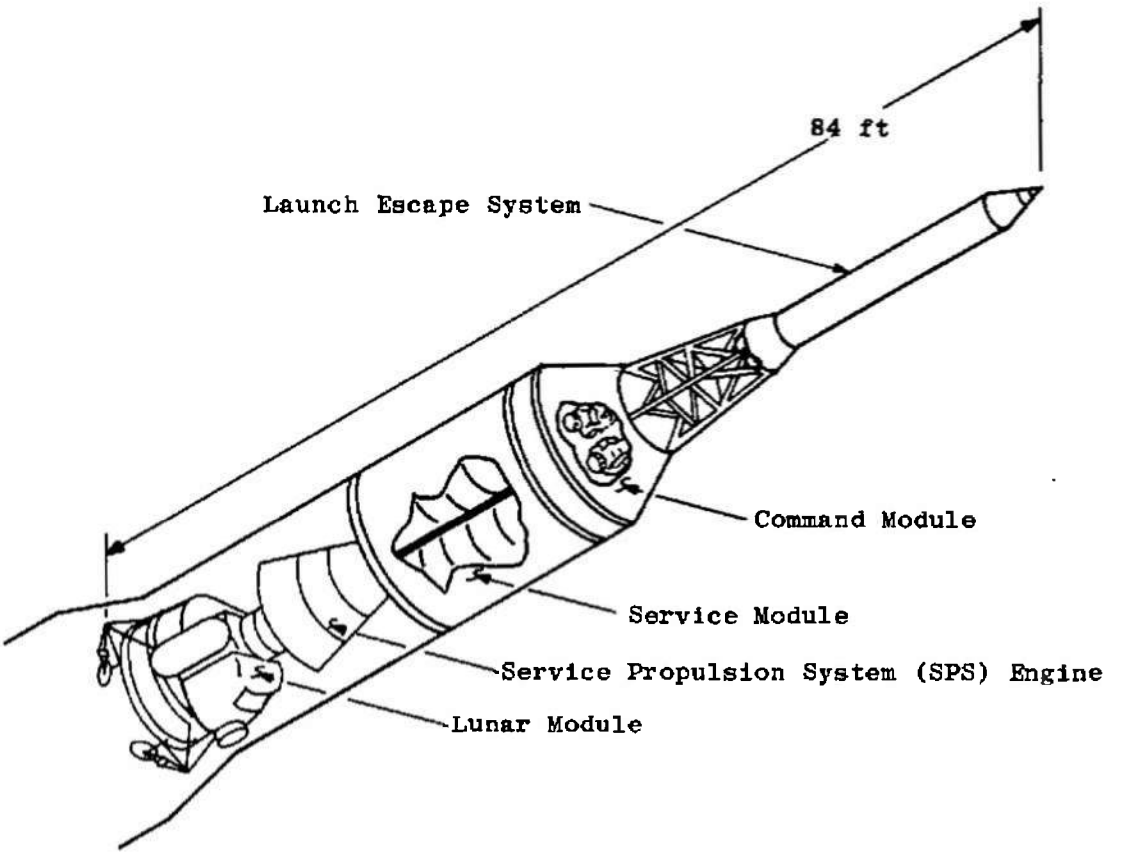

Fig. 1 Apollo Spacecraft

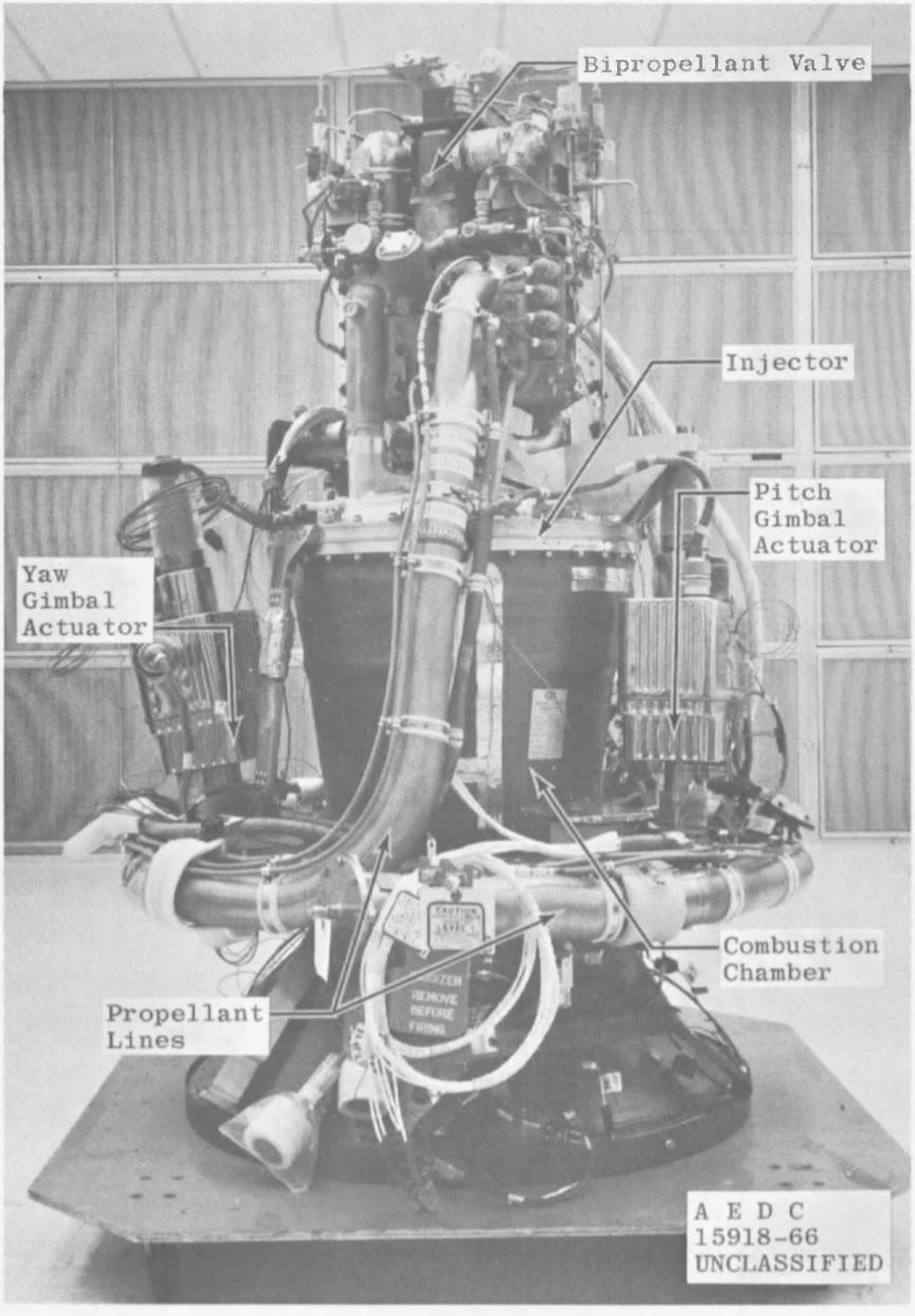

Fig. 2 AJ10-137 Rocket Engine S/N 21A (without Nozzle Extension)

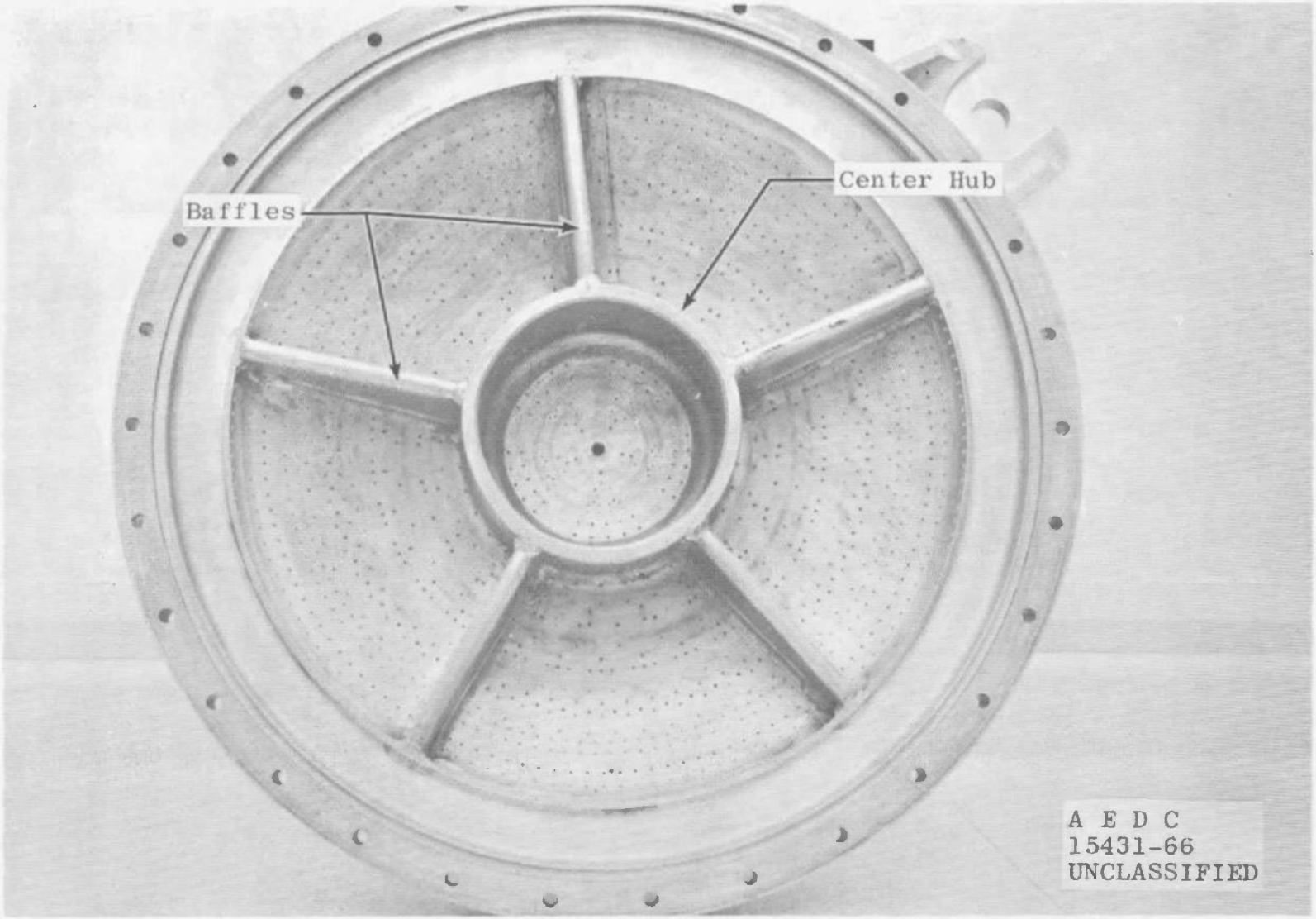

a. Injector Face

Fig. 3 Baffled Injector

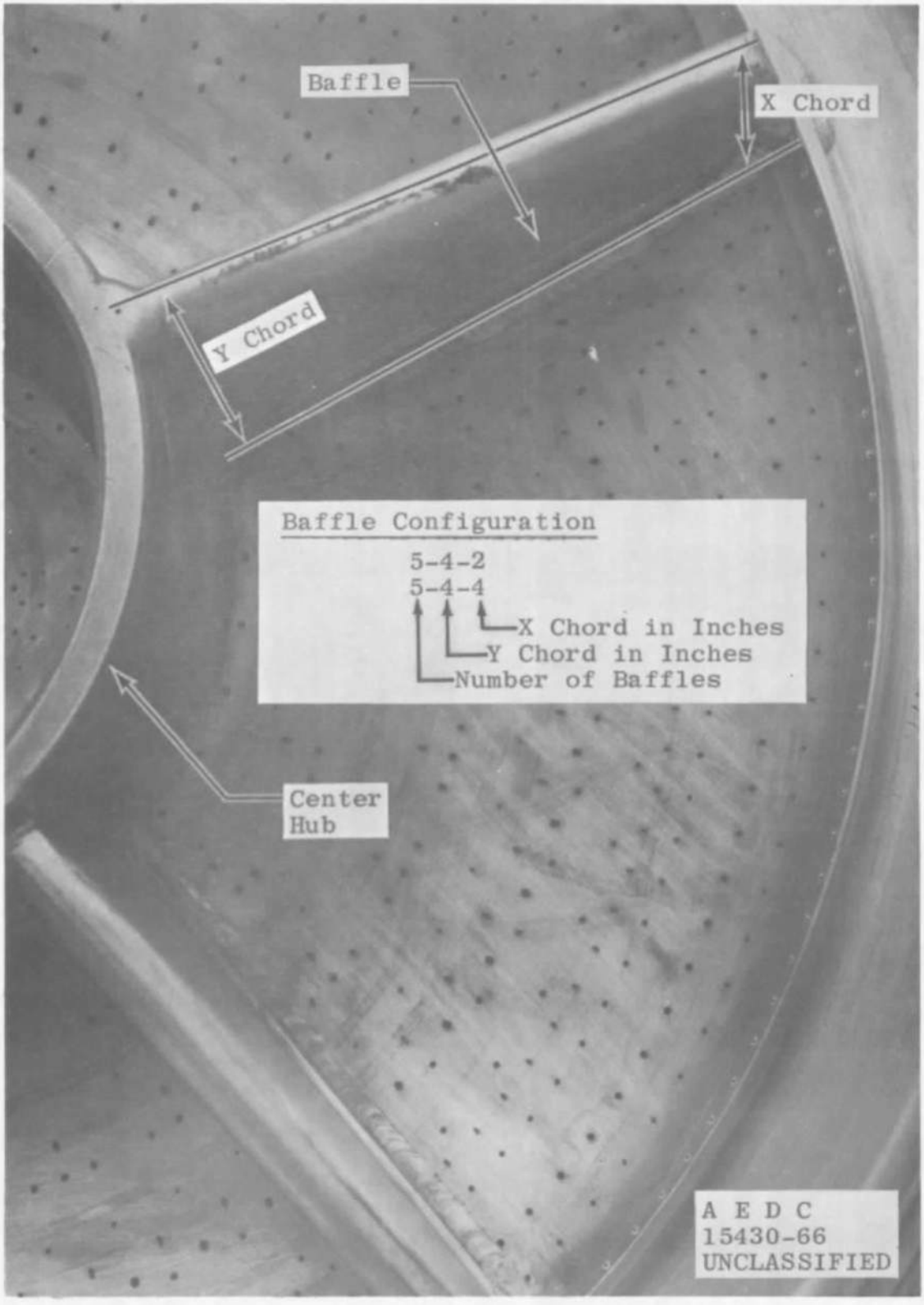

b. Baffle Configuration

Fig. 3 Continued

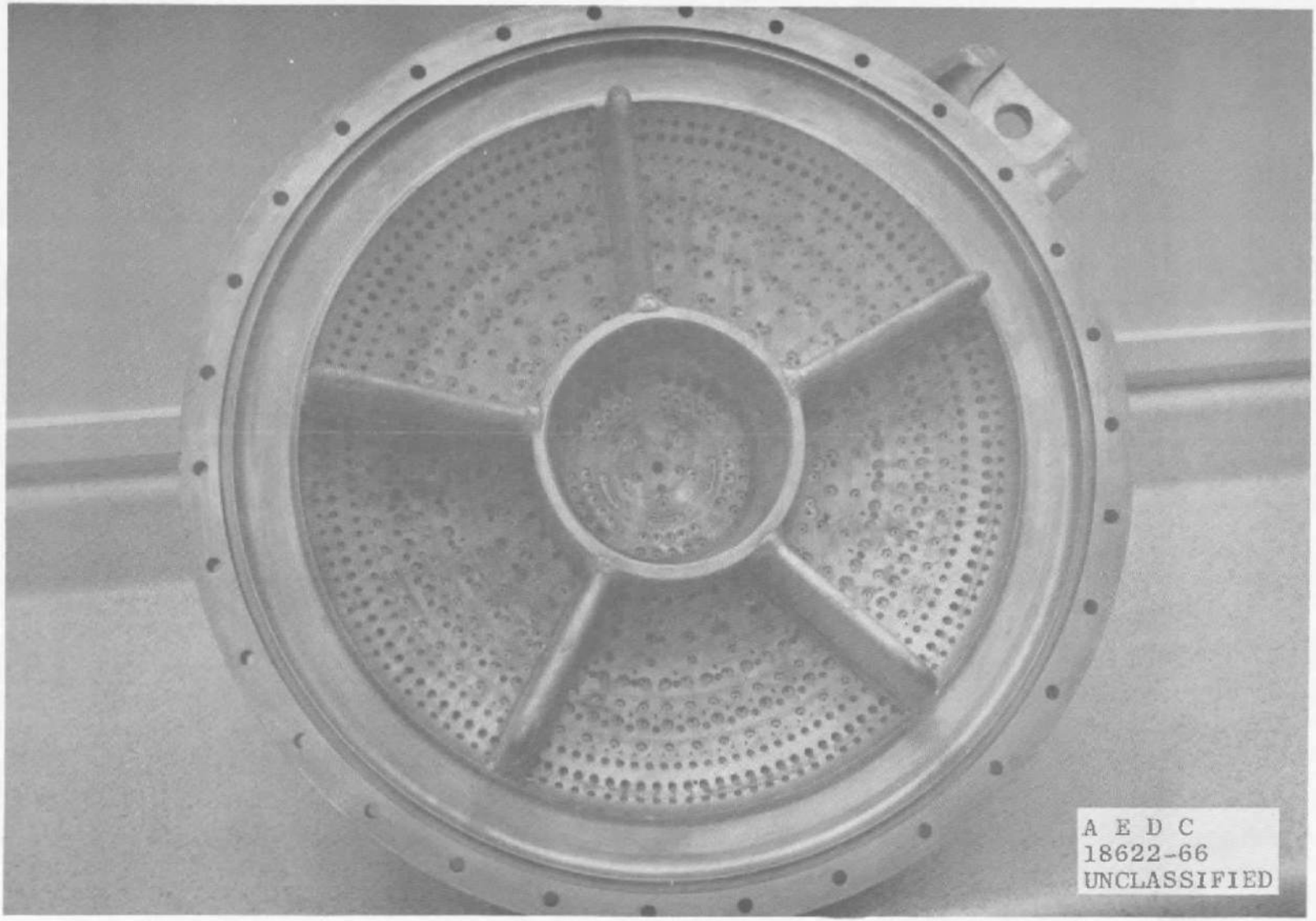

c. Counterbored Injector S/N 105

Fig. 3 Concluded

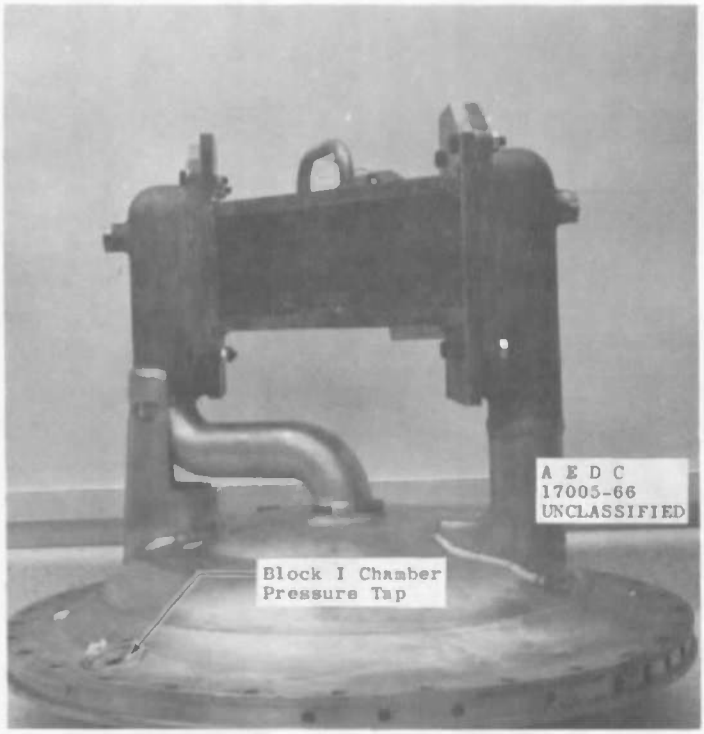

a. Block I Upstream Face

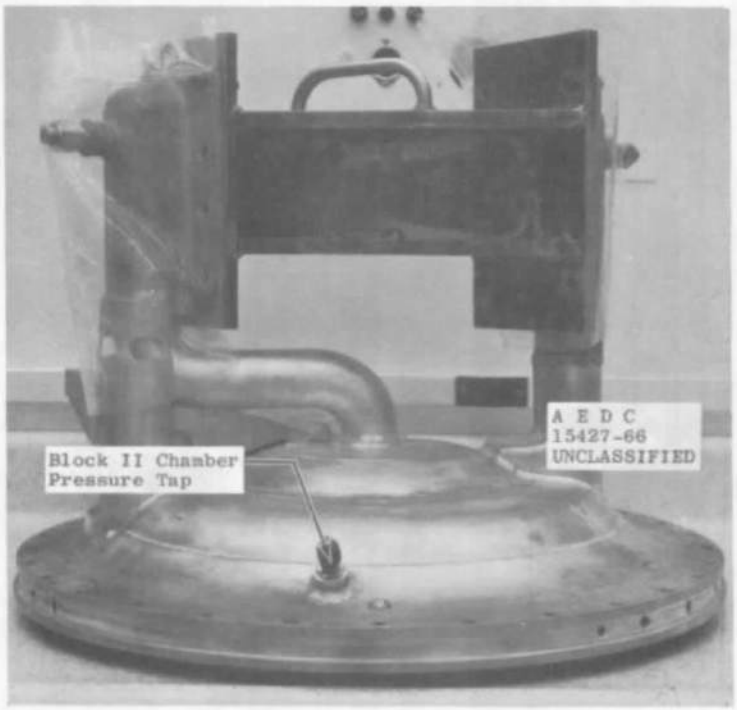

b. Block II Upstream Face

Fig. 4 Comparison of Block I and Block II Chamber Pressure Tap Location on the Injector

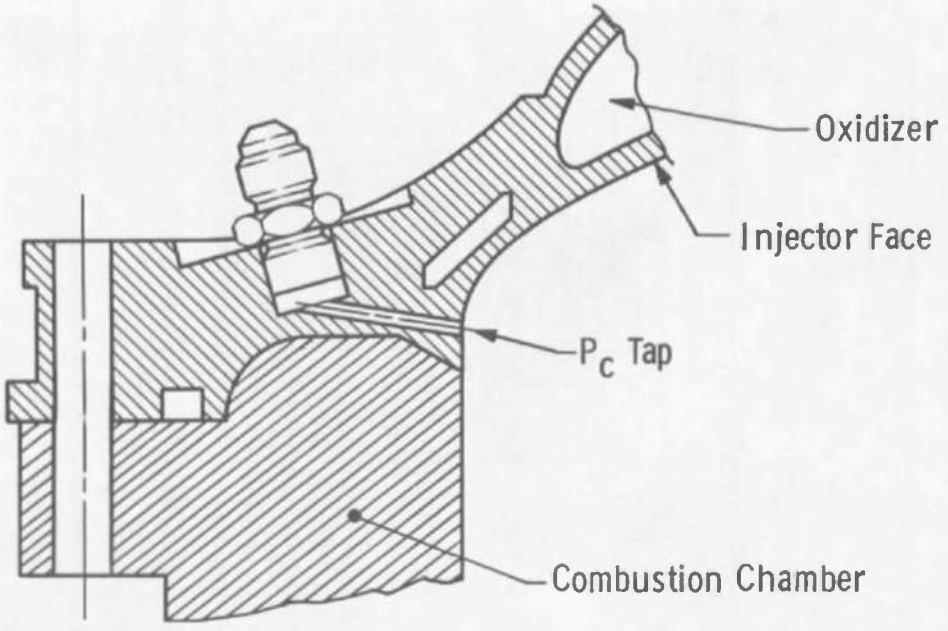

Block I

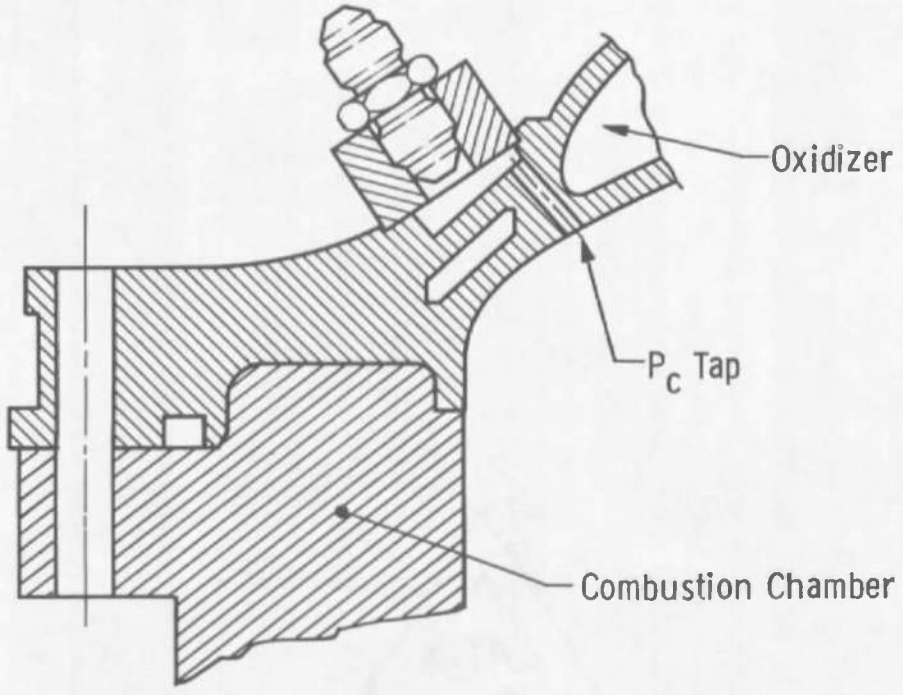

Block II

c. Cross Section Showing Block I and Block II Chamber Pressure Taps

Fig. 4 Concluded

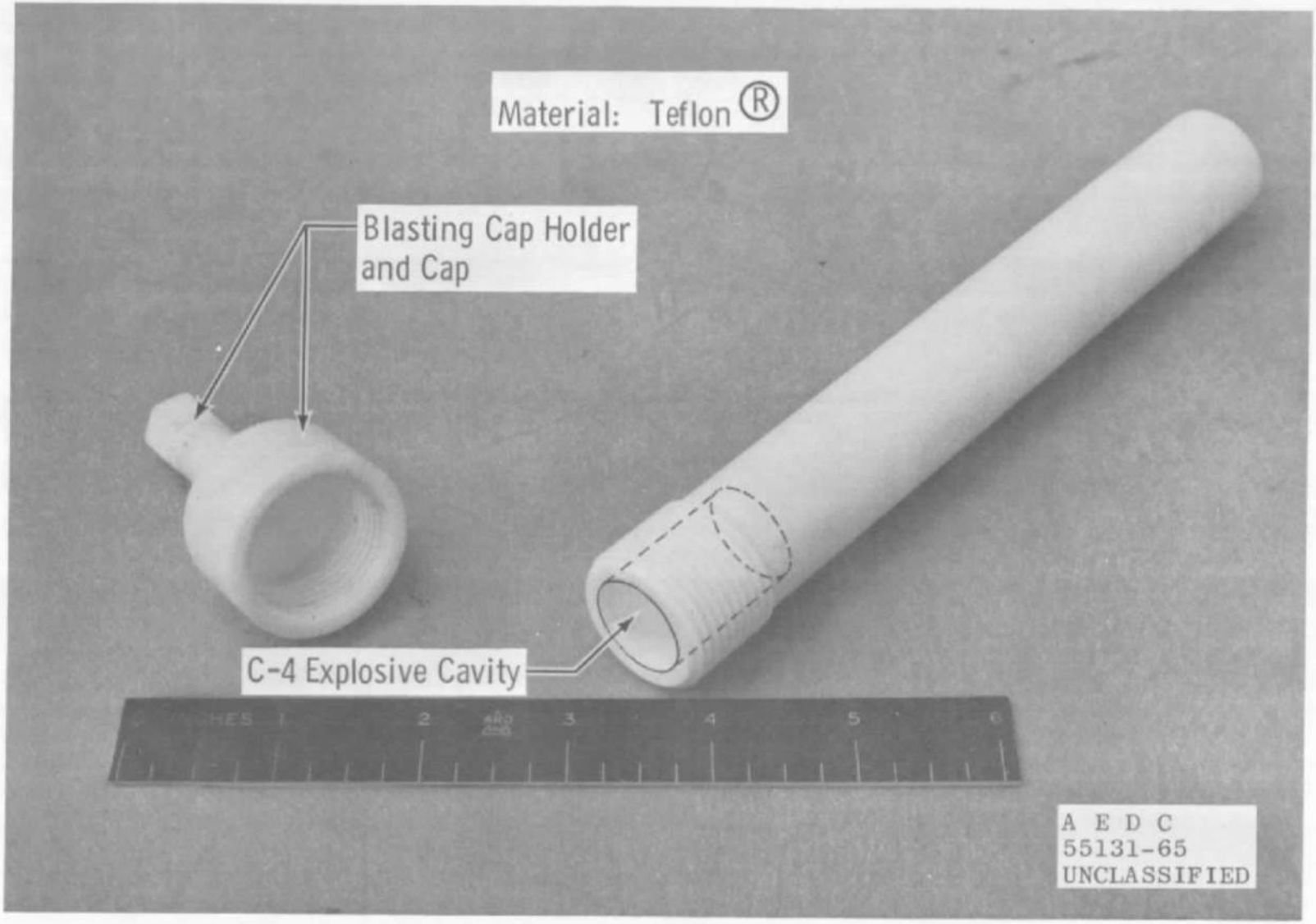

Fig. 5 Pulse Charge Container

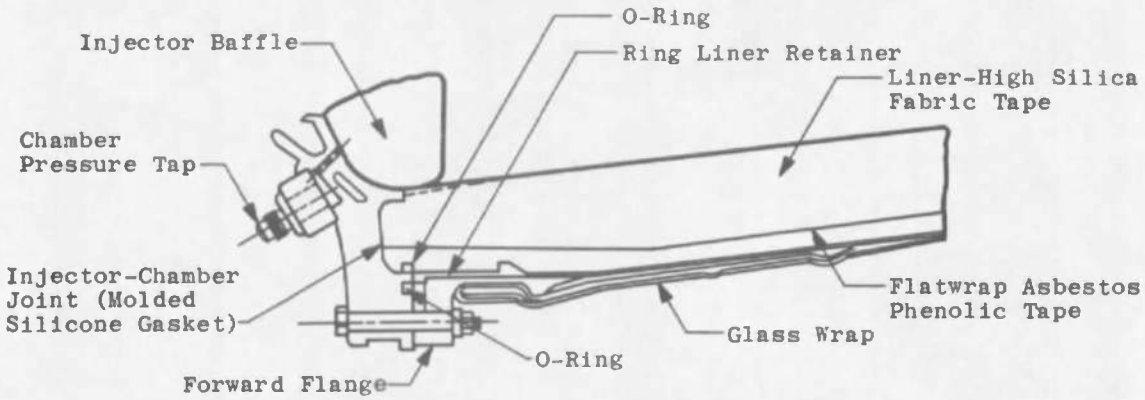

Chamber Design A

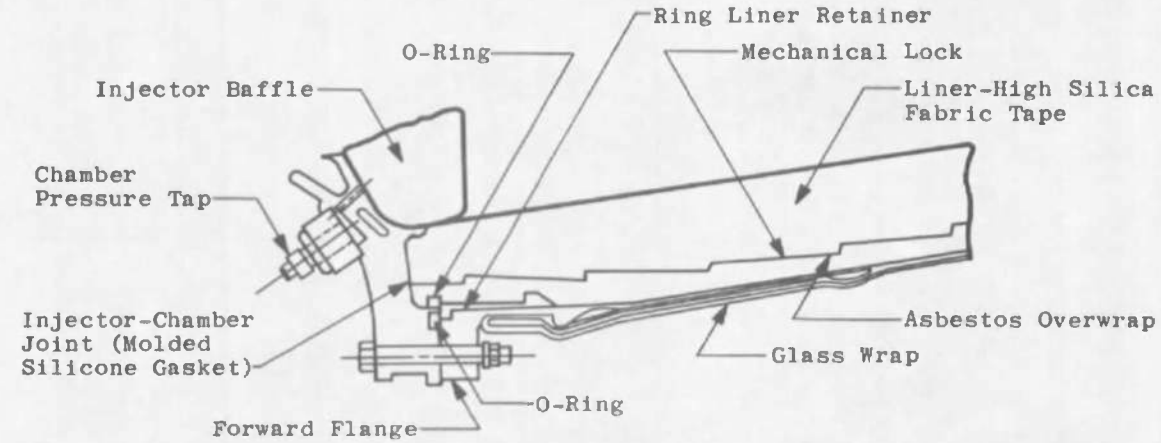

Chamber Design A-1

Fig. 6 Comparison of Combustion Chamber Designs Used during Phase IV Apollo Testing

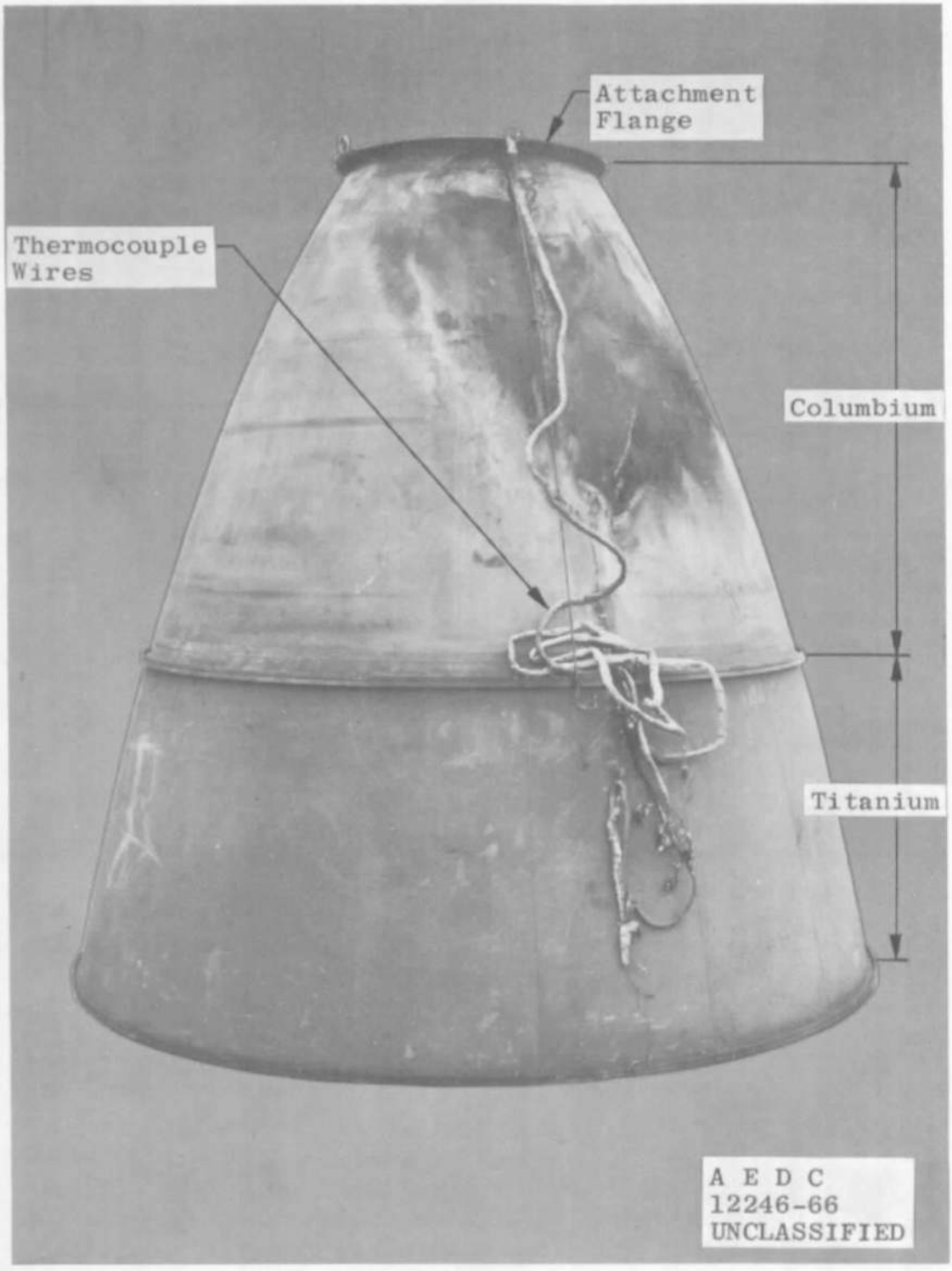

Fig. 7 Nozzle Extension

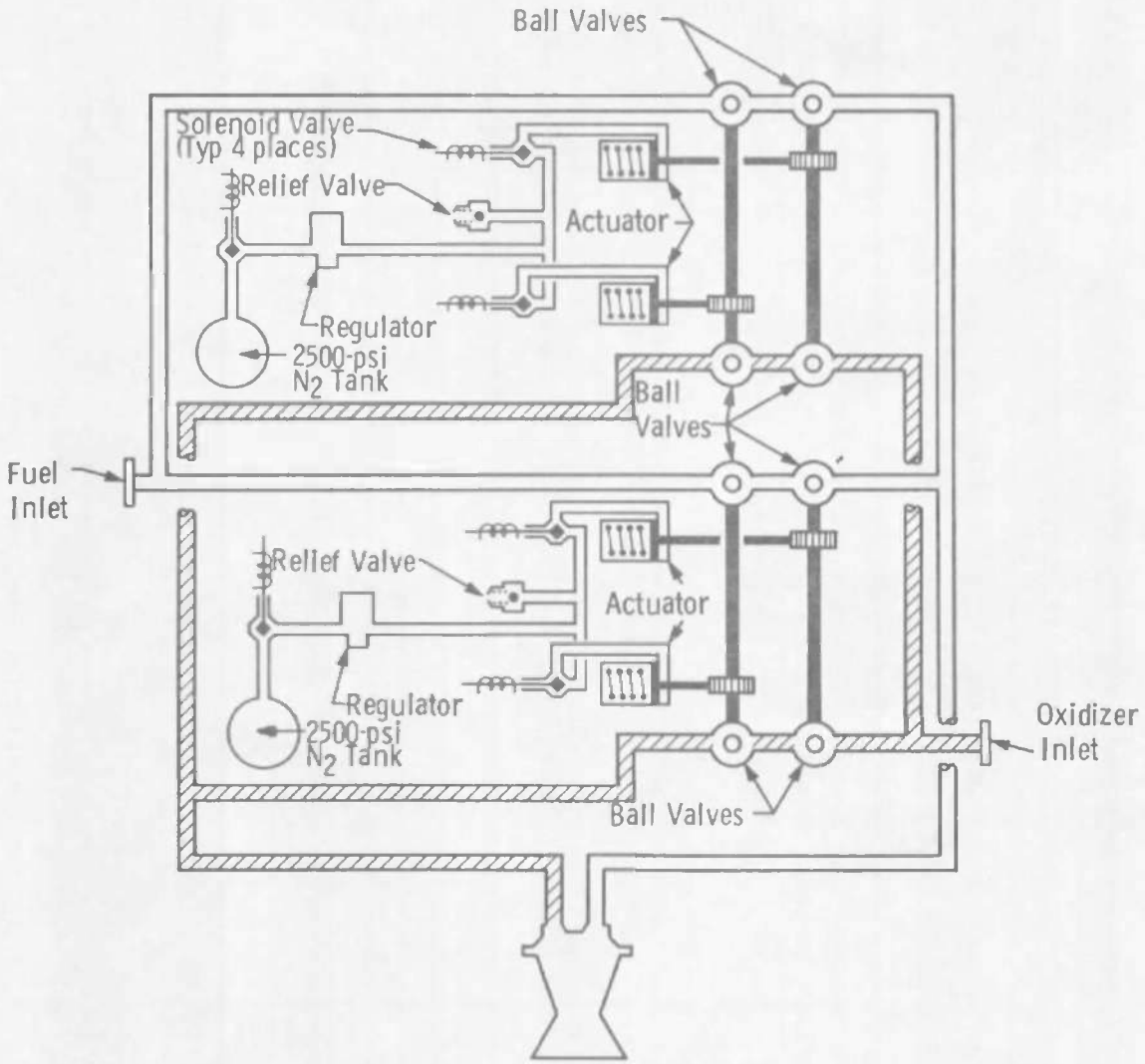

Fig. 8 Schematic of Thrust Chamber Valve

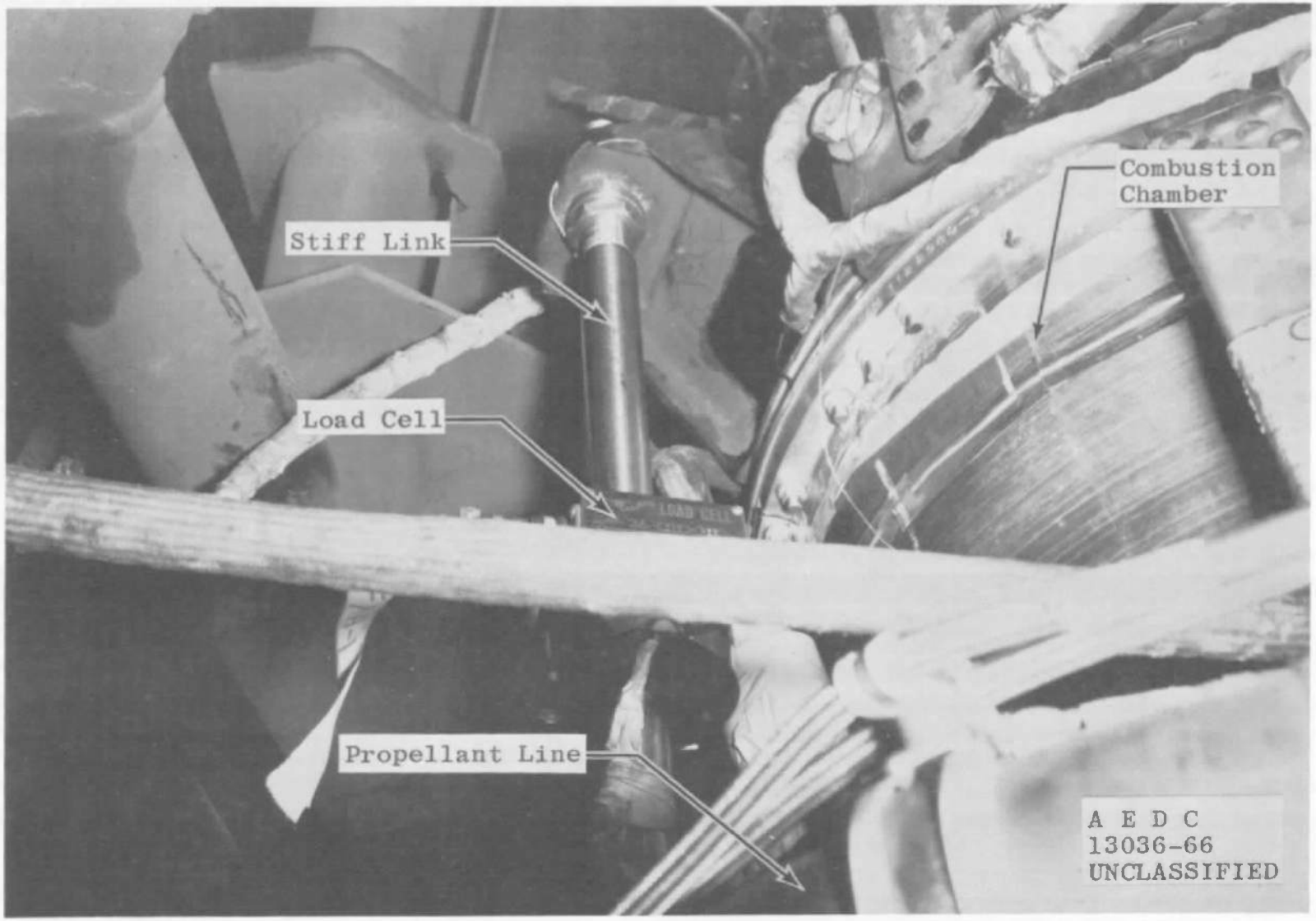

Fig. 9 Stiff Link/Load Cell as Mounted on Engine

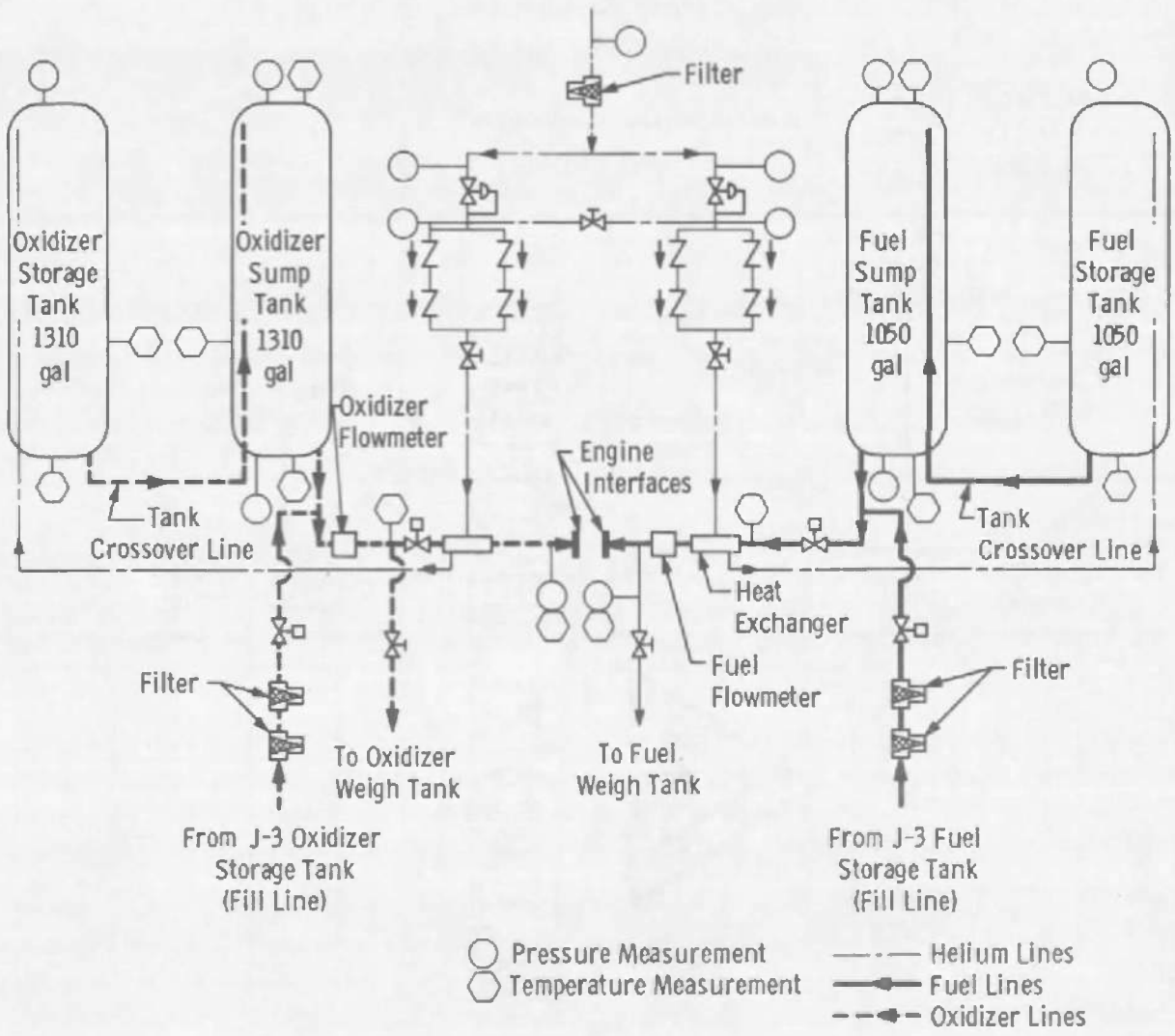

a. Before Modifications

Fig. 10 Schematic of F-3 Fixture

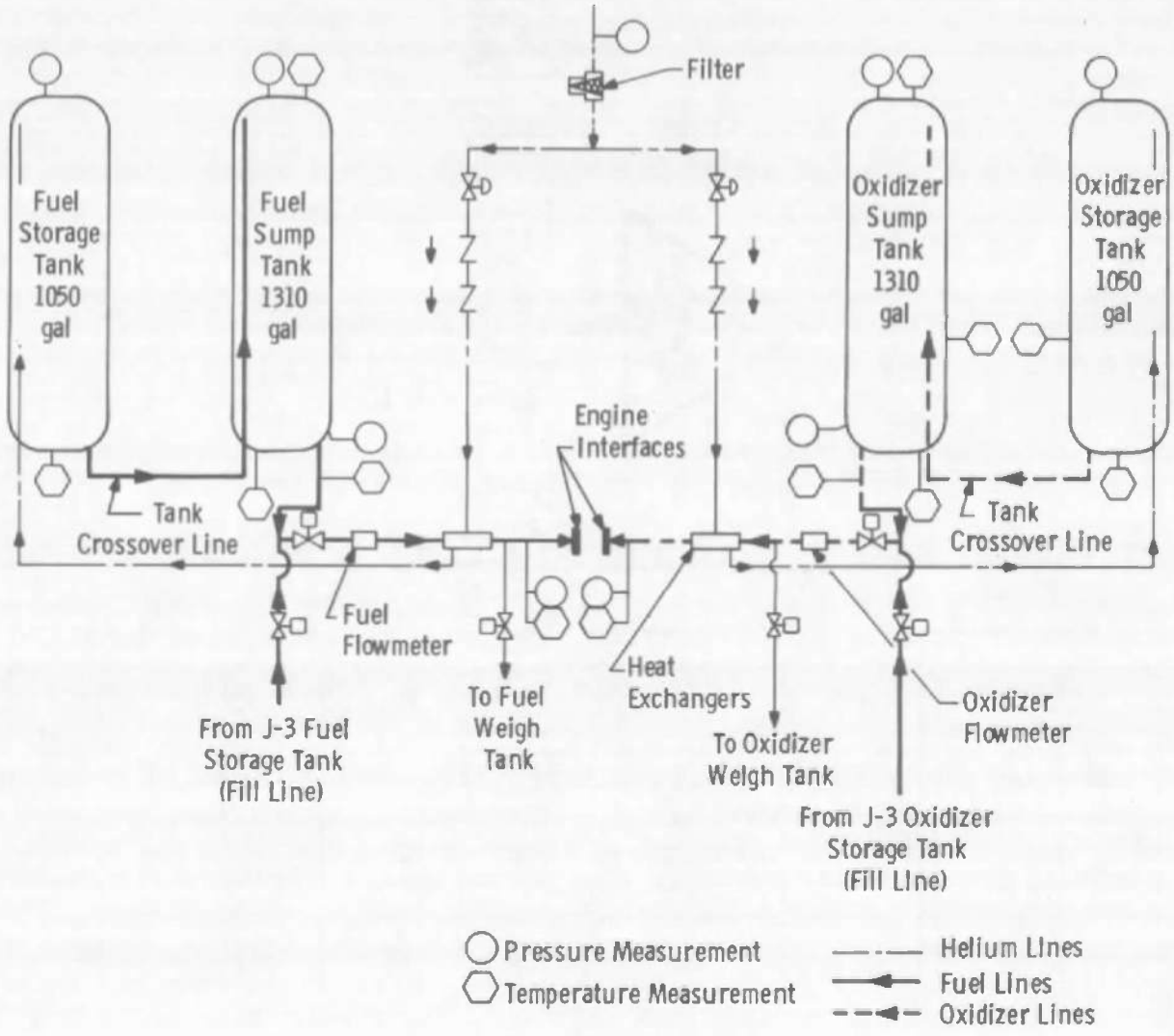

b. After Modifications

Fig. 10 Concluded

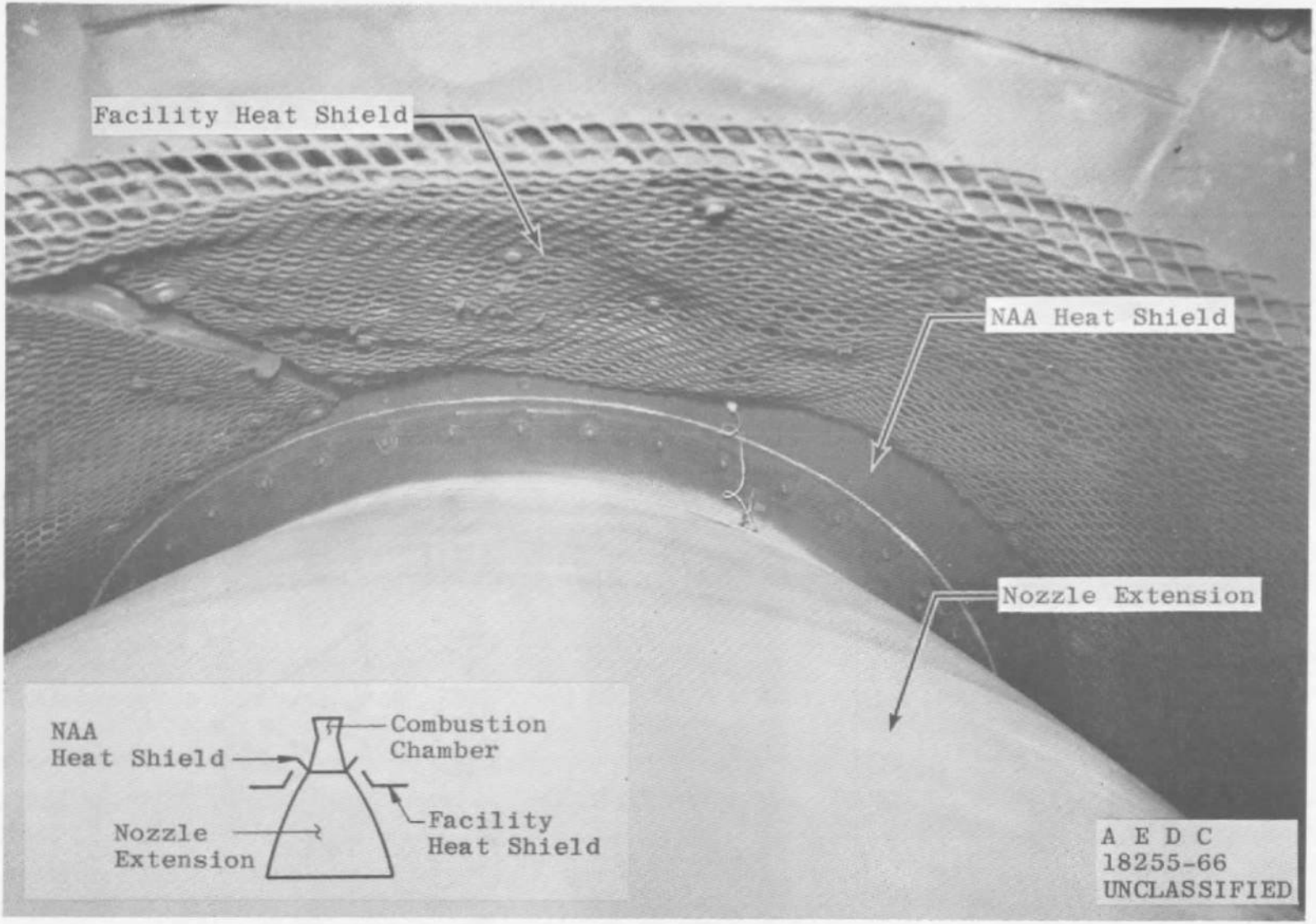

a. NAA and Facility Heat Shields Installed

Fig. 11 Radiation Heat Shield Configurations

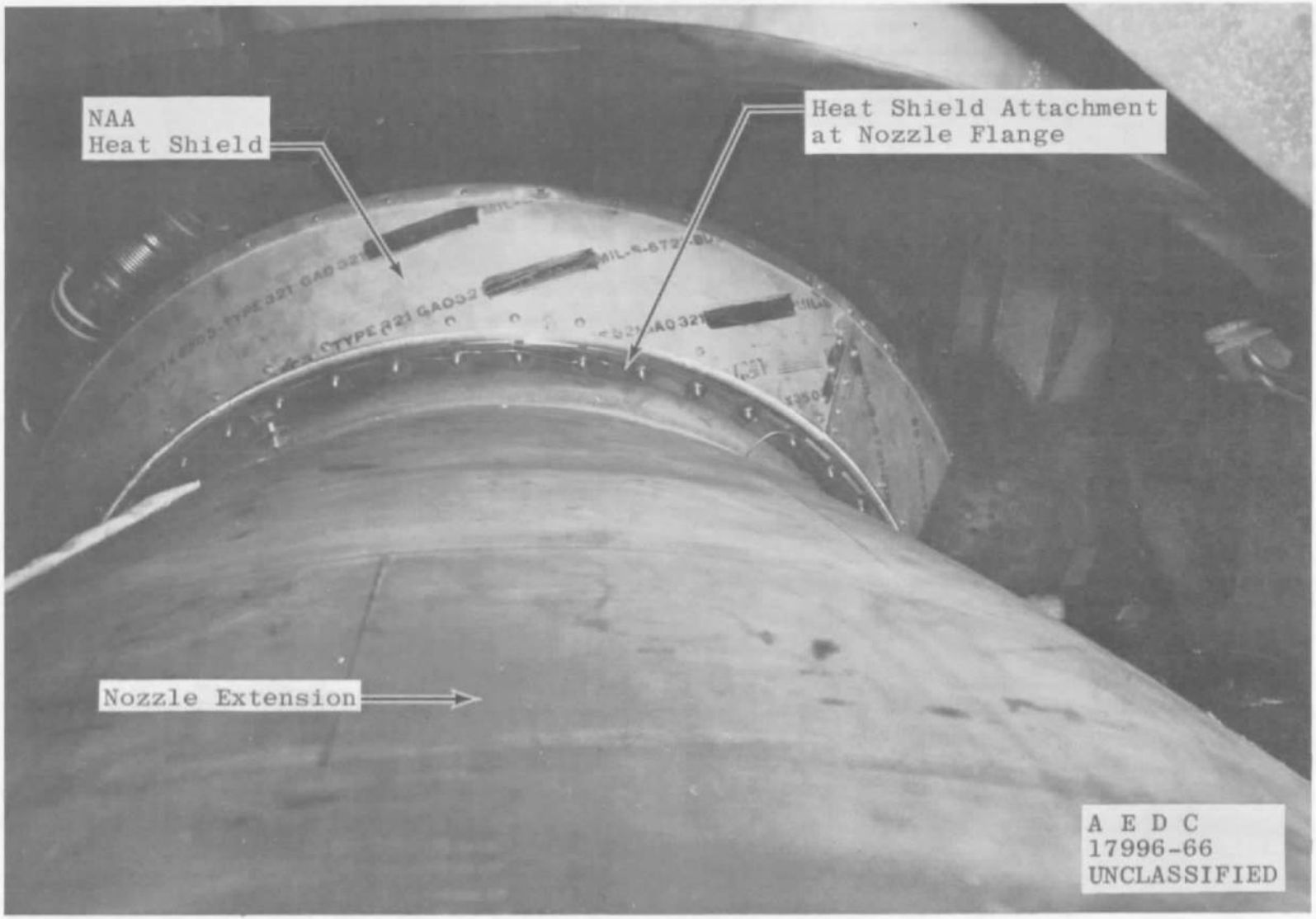

b. NAA Heat Shield Installed

Fig. 11 Concluded

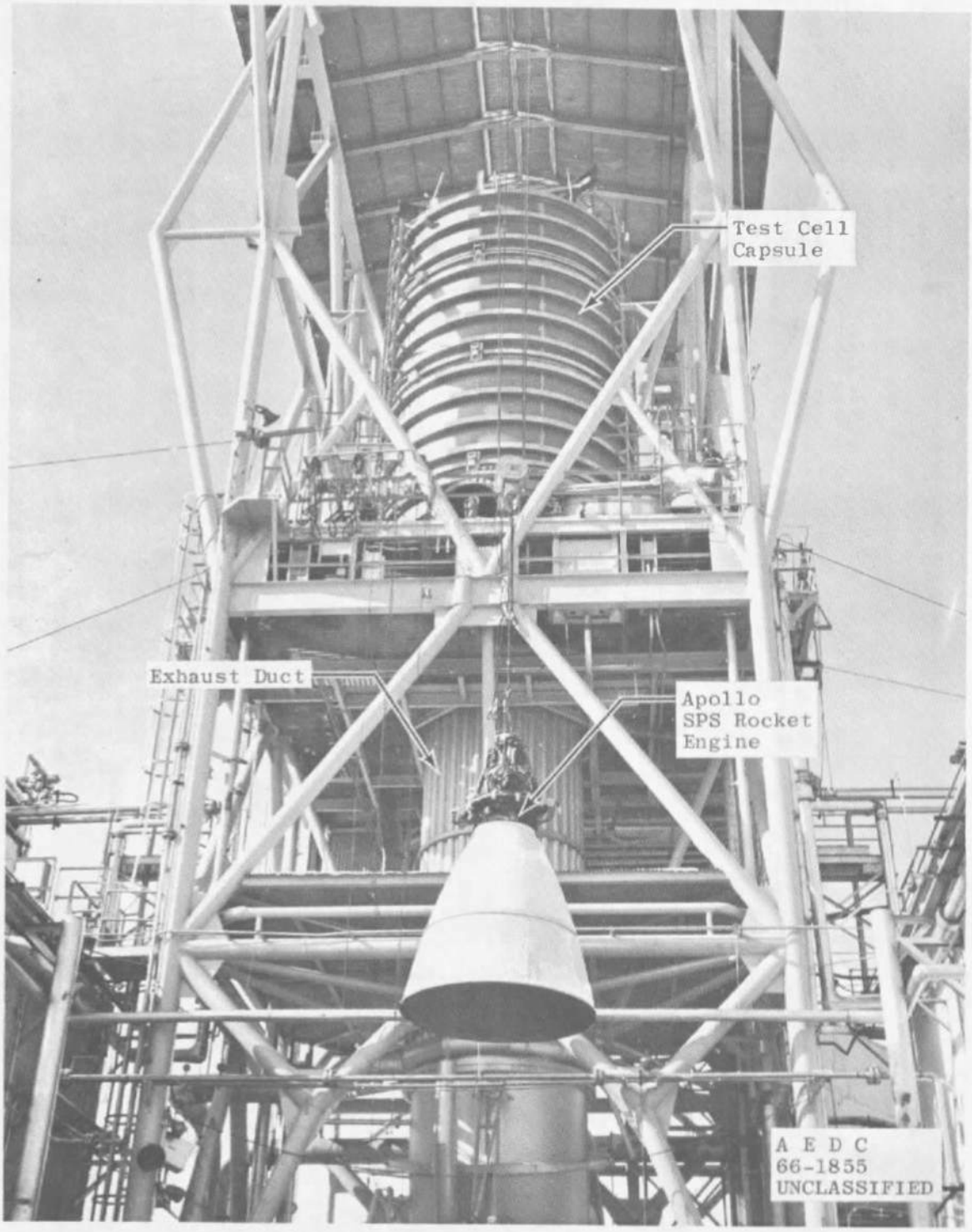

o. AJ10-137 Rocket Engine Installation

Fig. 12 Propulsion Engine Test Cell (J-3)

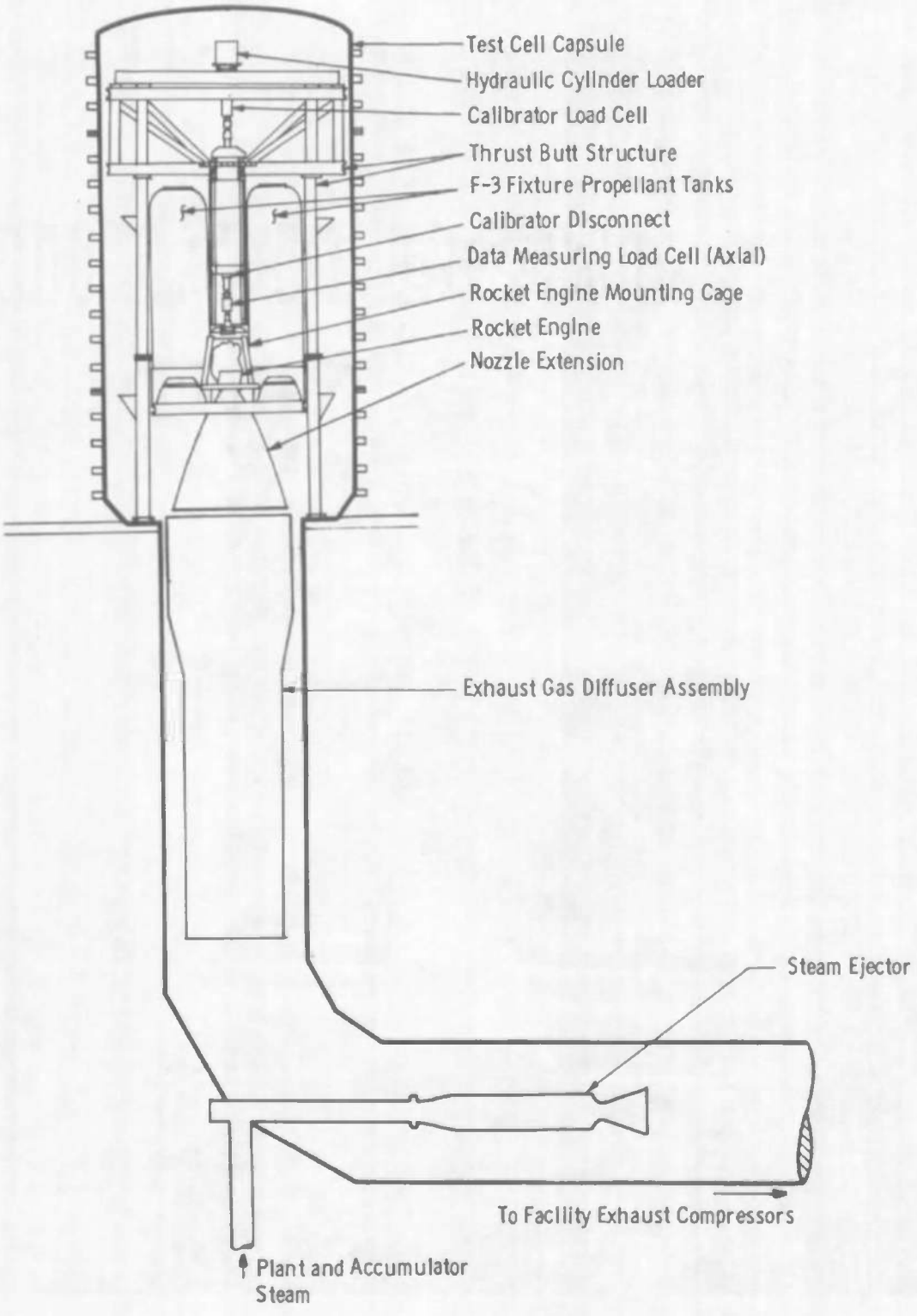

b. Test Cell Schematic

Fig. 12 Concluded

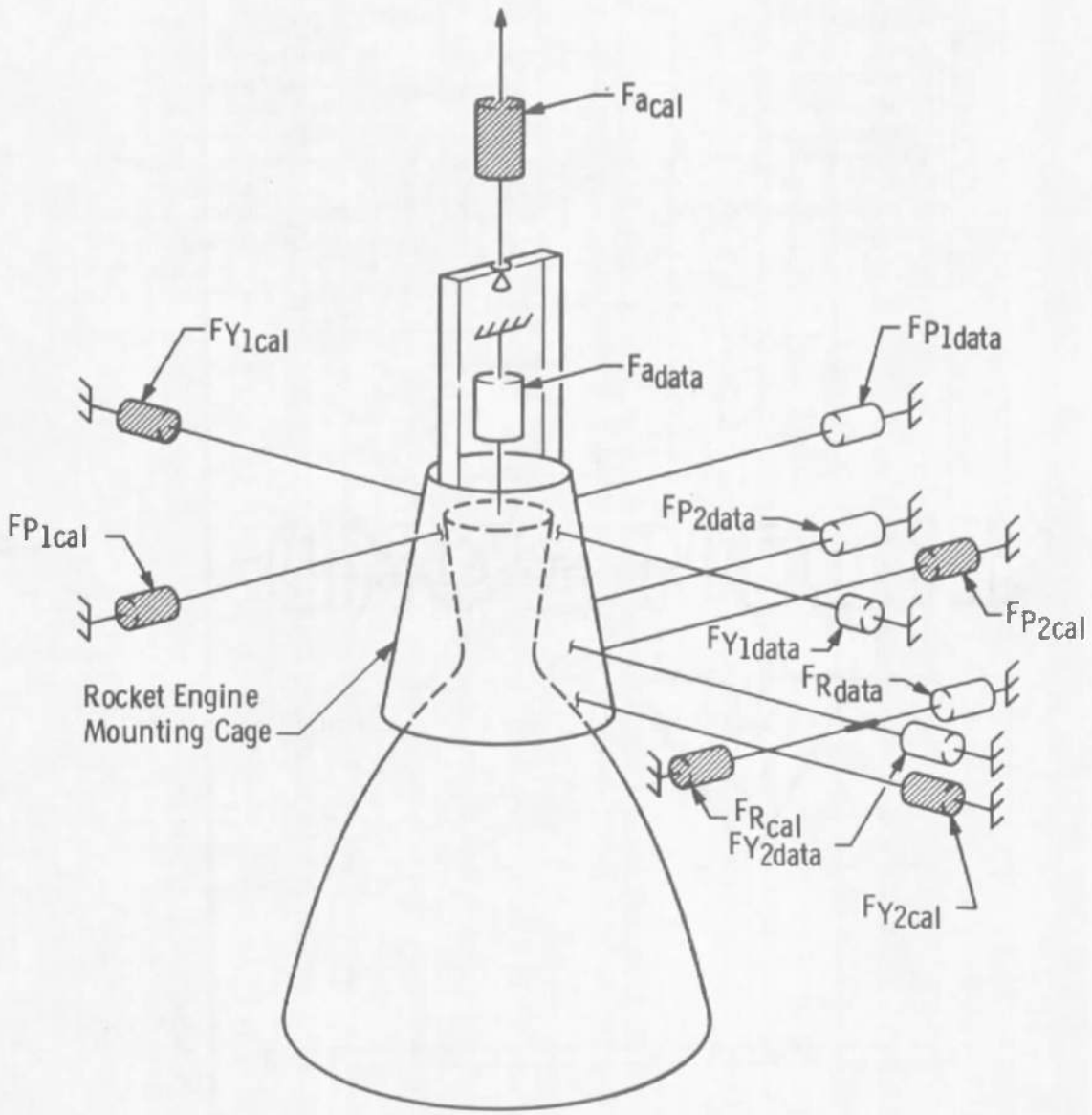

Fig. 13 Schematic of Six-Component Force System

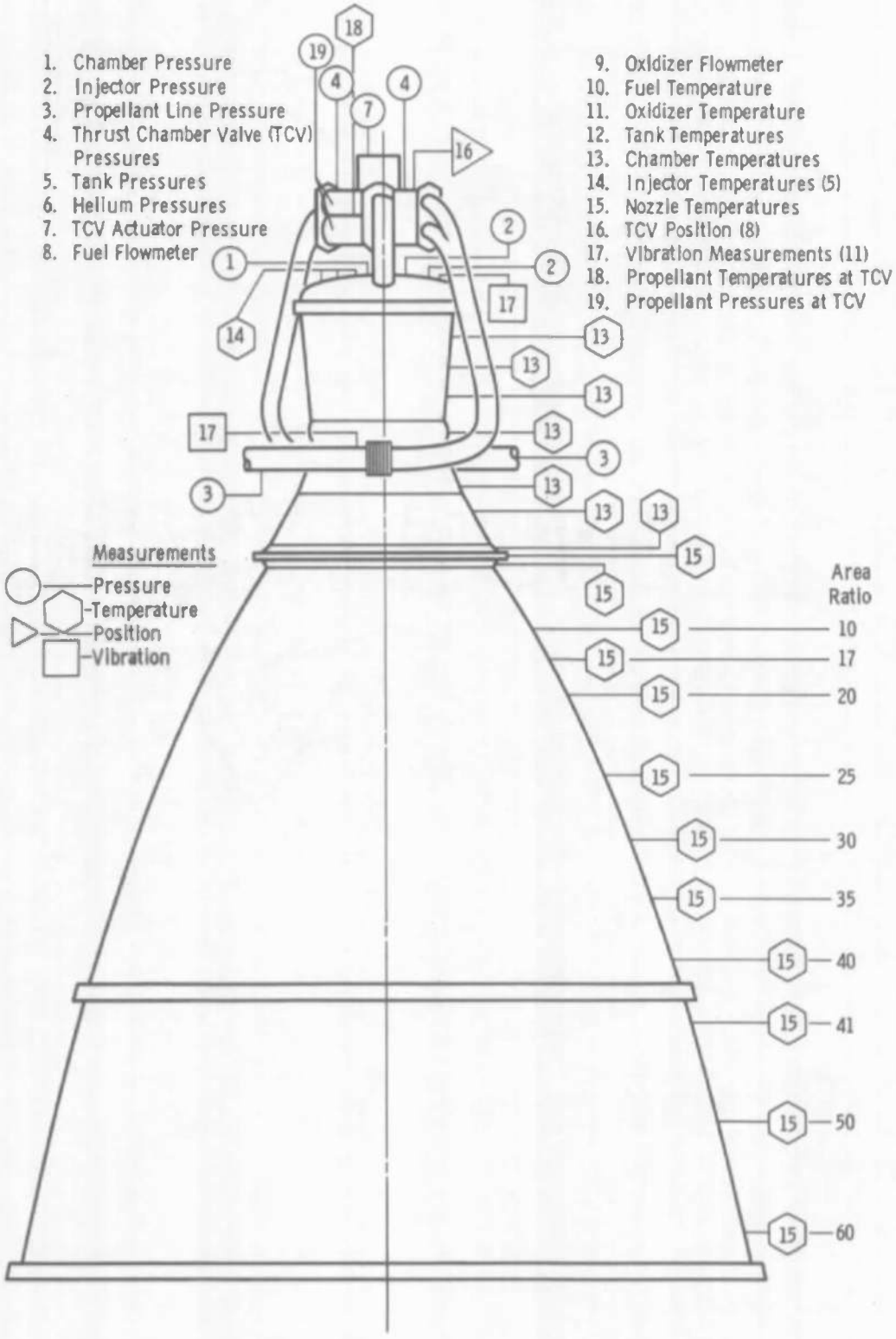

Fig. 14 Engine and Nozzle Extension Instrumentation Location

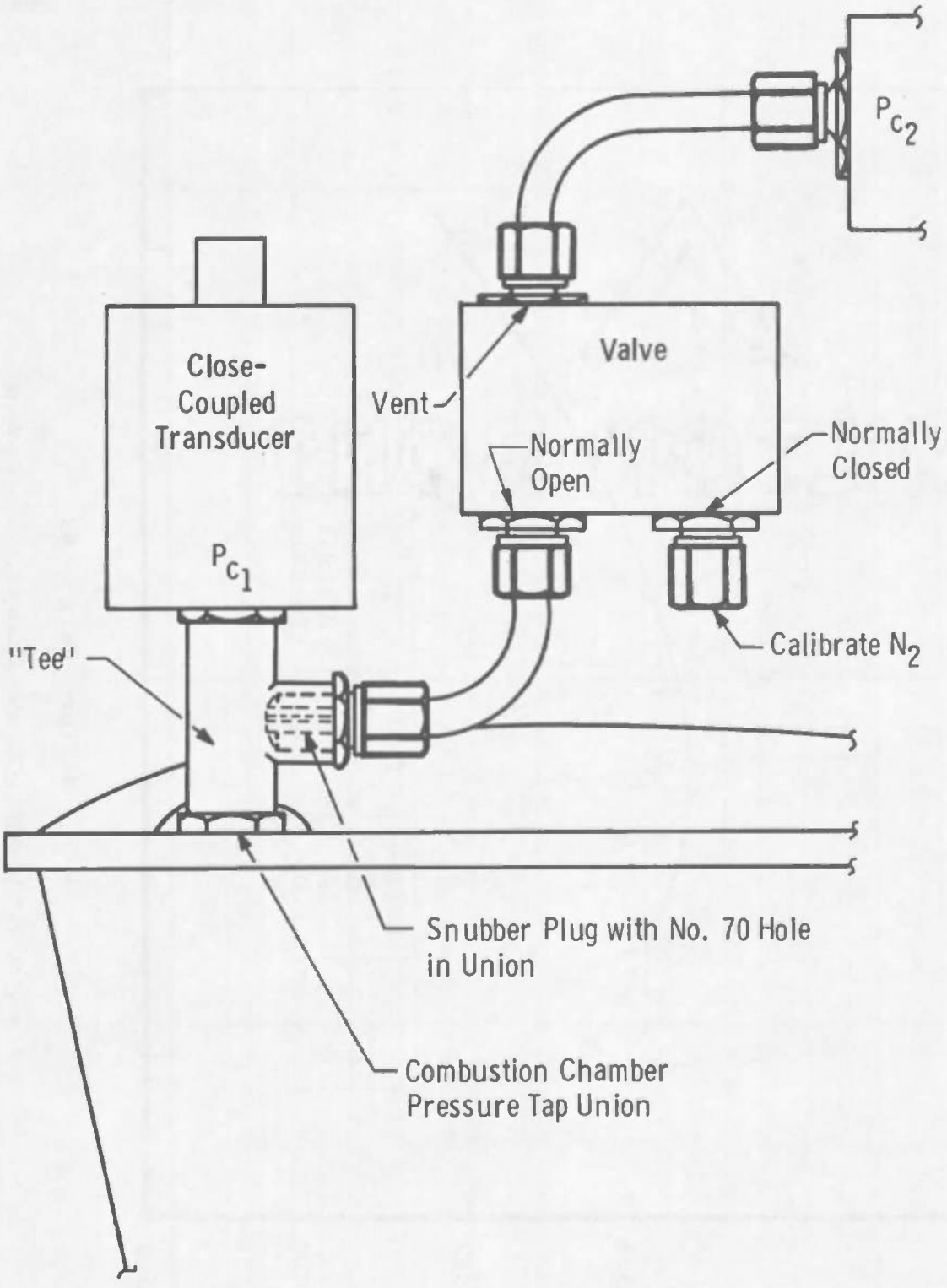

Fig. 15 Schematic of In-Place Chamber Pressure Calibration System

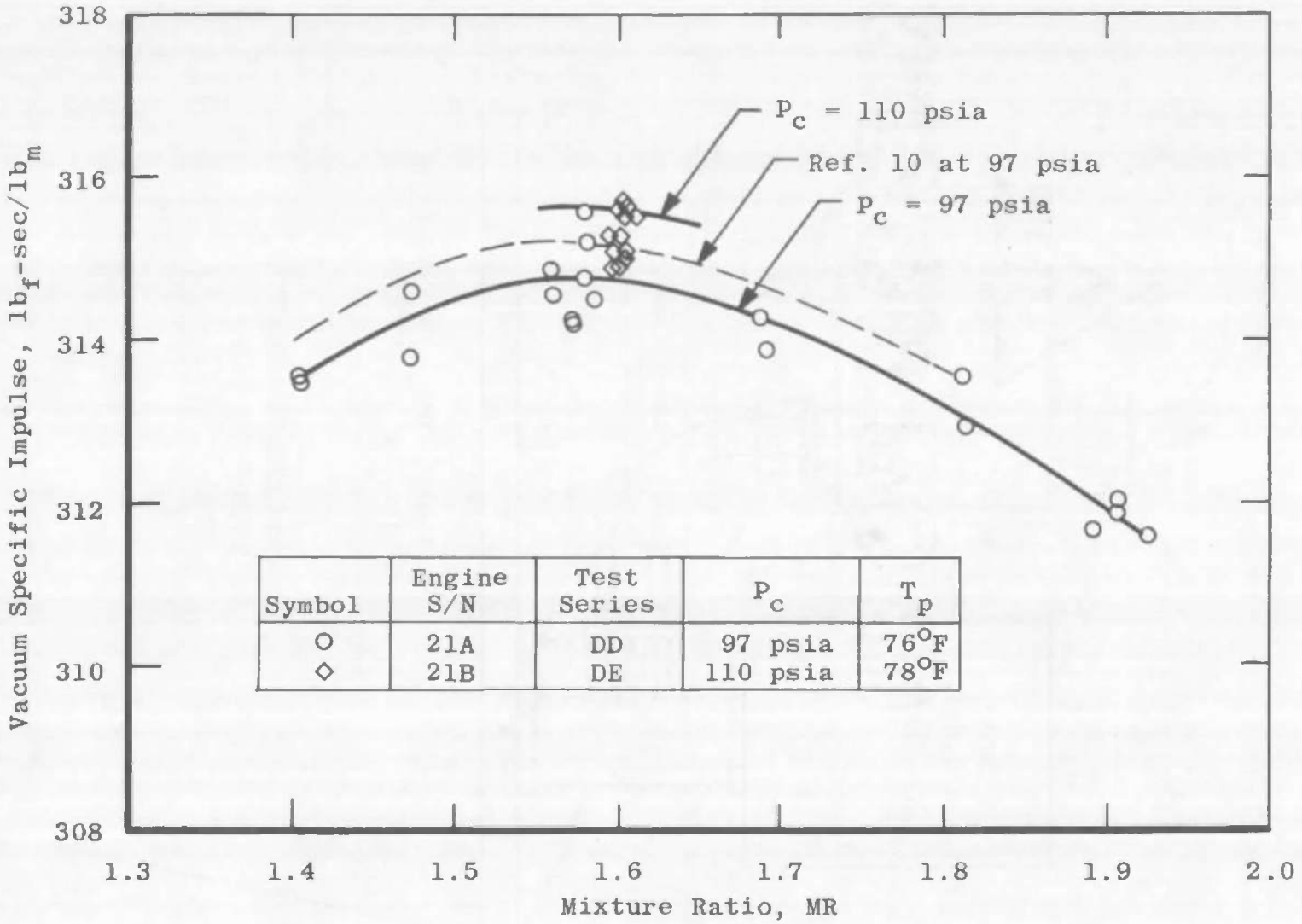

Fig. 16 Vacuum Performance with Short Baffled Injector S/N 110

Symbol	Engine S/N	Test Series	p_c	T_p
○	21C	DF	110 psia	78-96°F
◇	21D	DG	77-118 psia	112°F

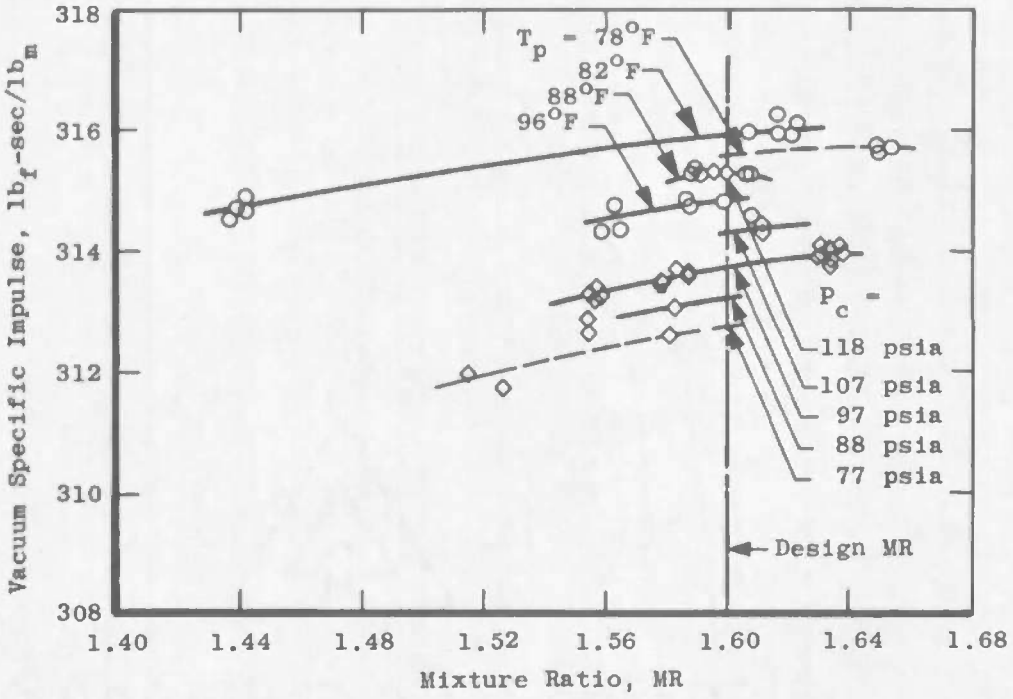

Fig. 17 Vacuum Performance with Long Baffled Injectar S/N 93

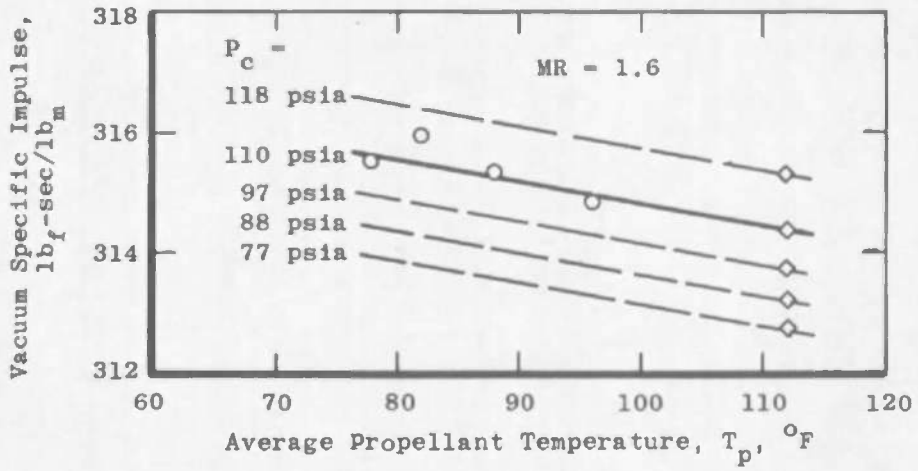

Fig. 18 Propellant Temperature Effect on Performance with the Long Baffled Injectar S/N 93

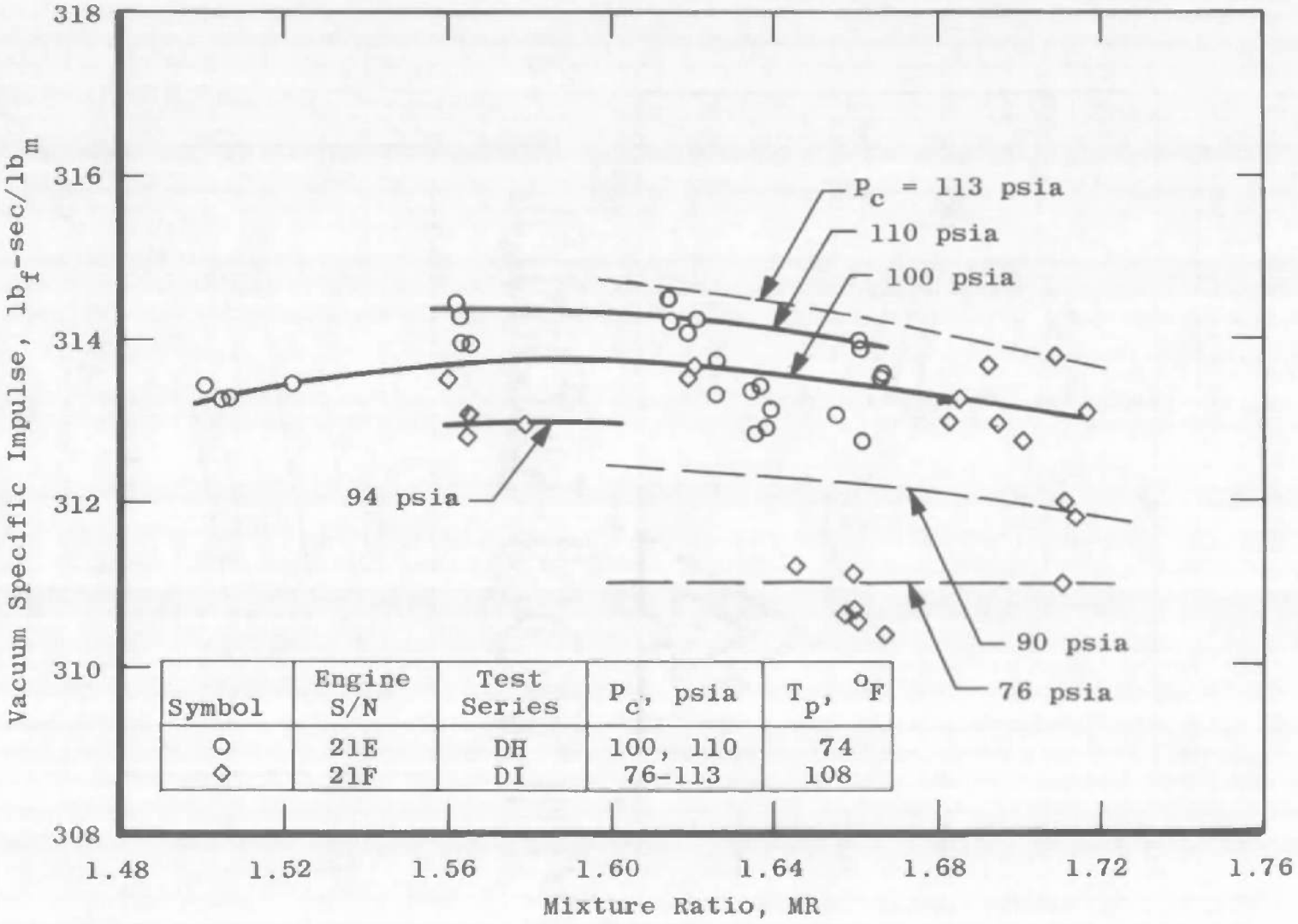

Fig. 19 Vacuum Performance with Long Baffled, Counterbored-Orifices Injector S/N 105

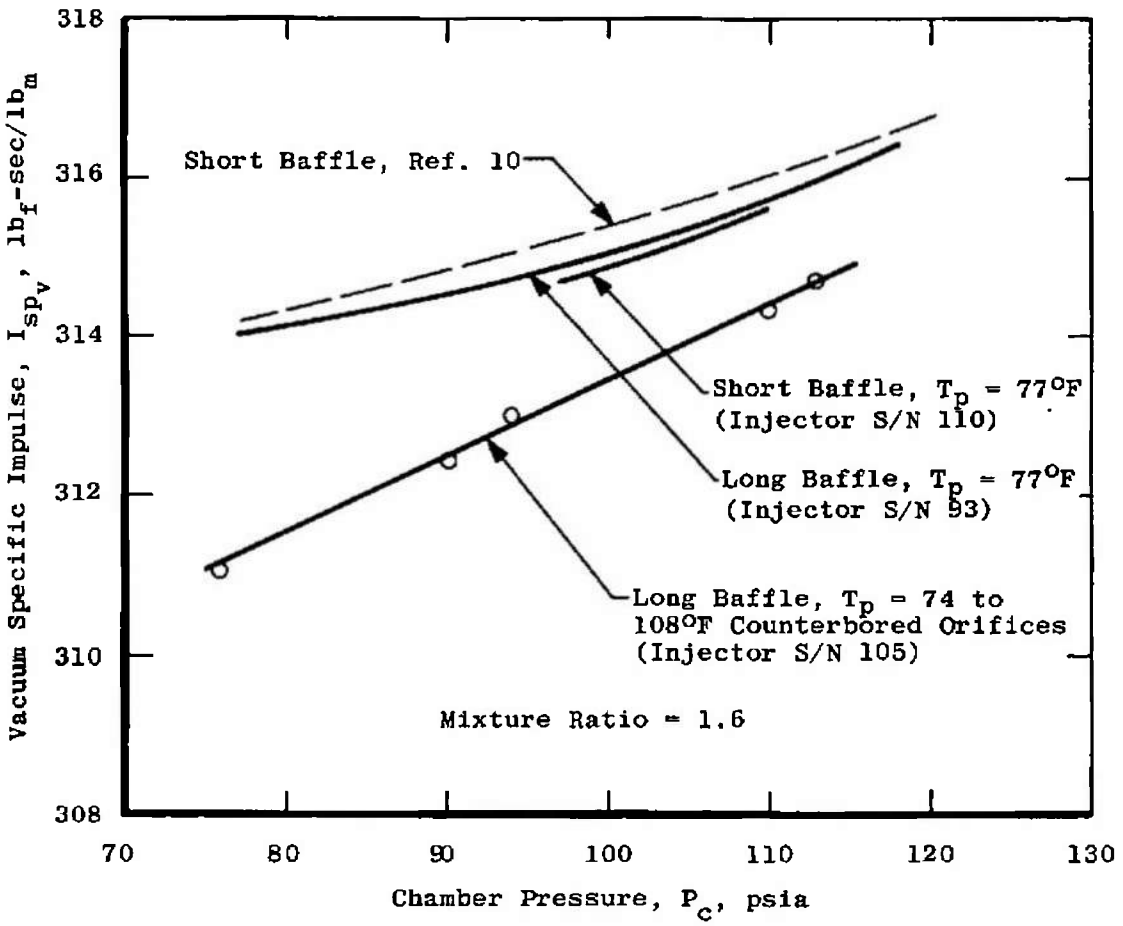

Fig. 20 Chamber Pressure Effect on Performance

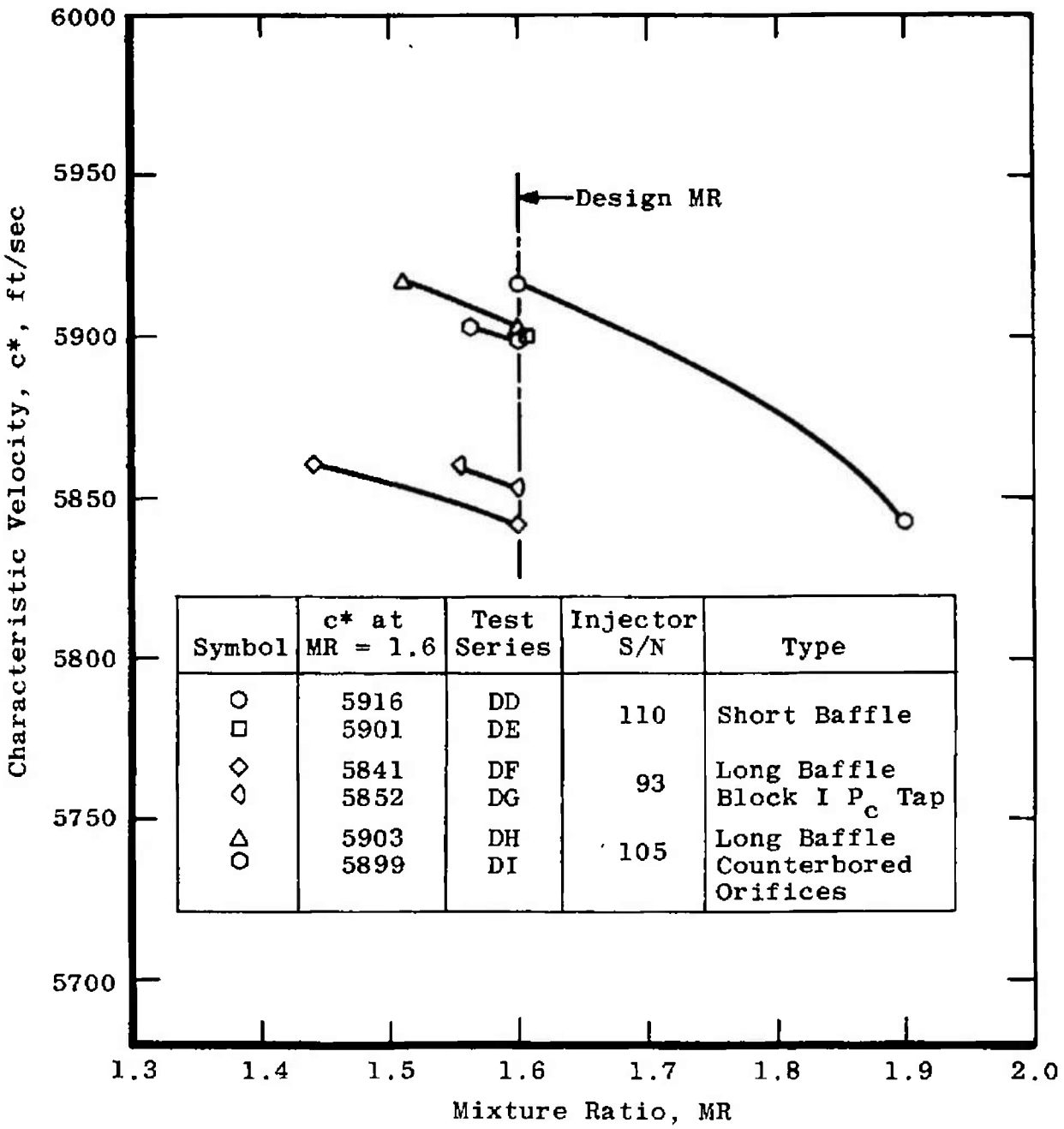

Fig. 21 Characteristic Velocity as a Function of Mixture Ratio

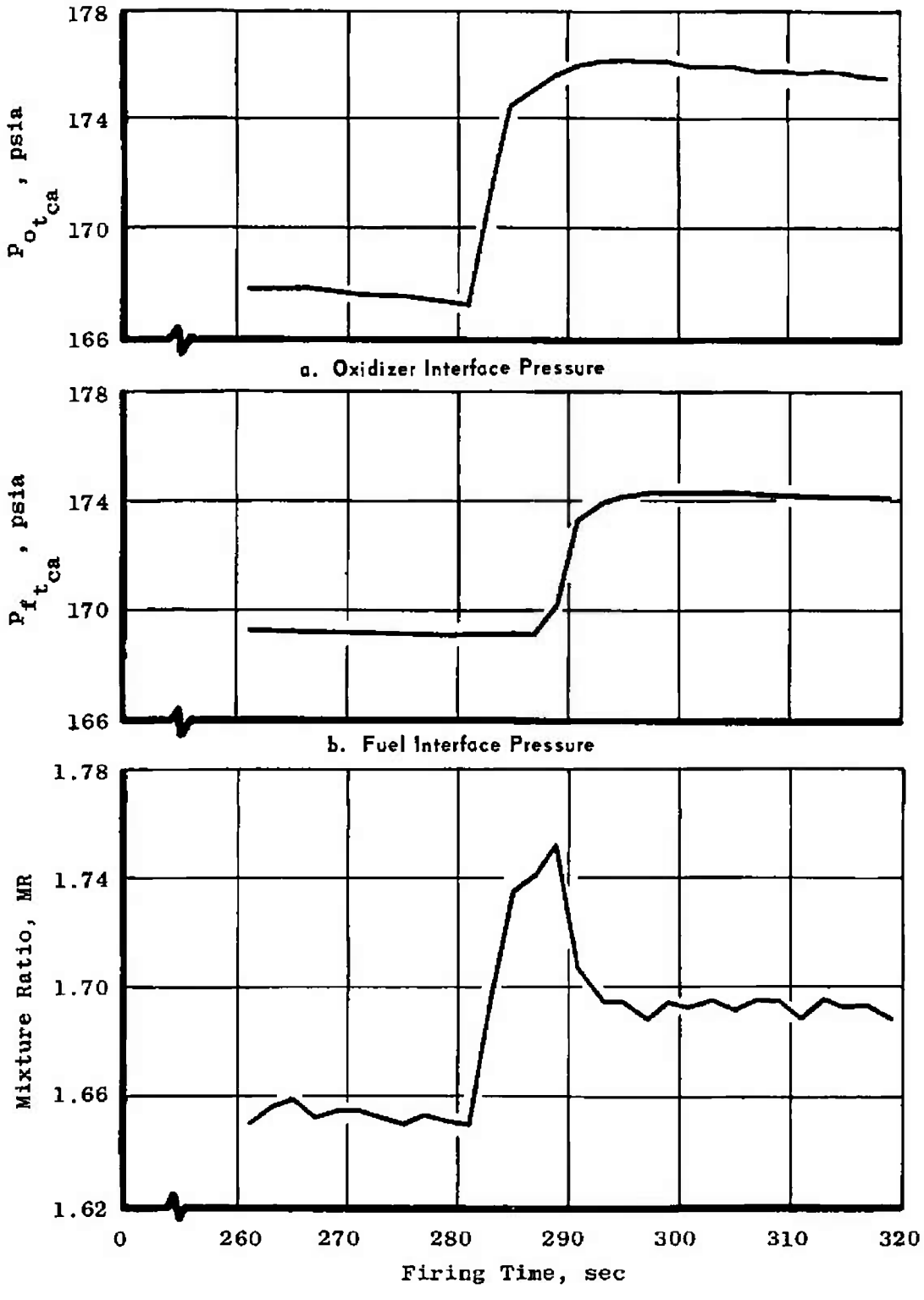

Fig. 22 Effect of Propellant Tank Crossover on Engine Operation (Test DI-06)

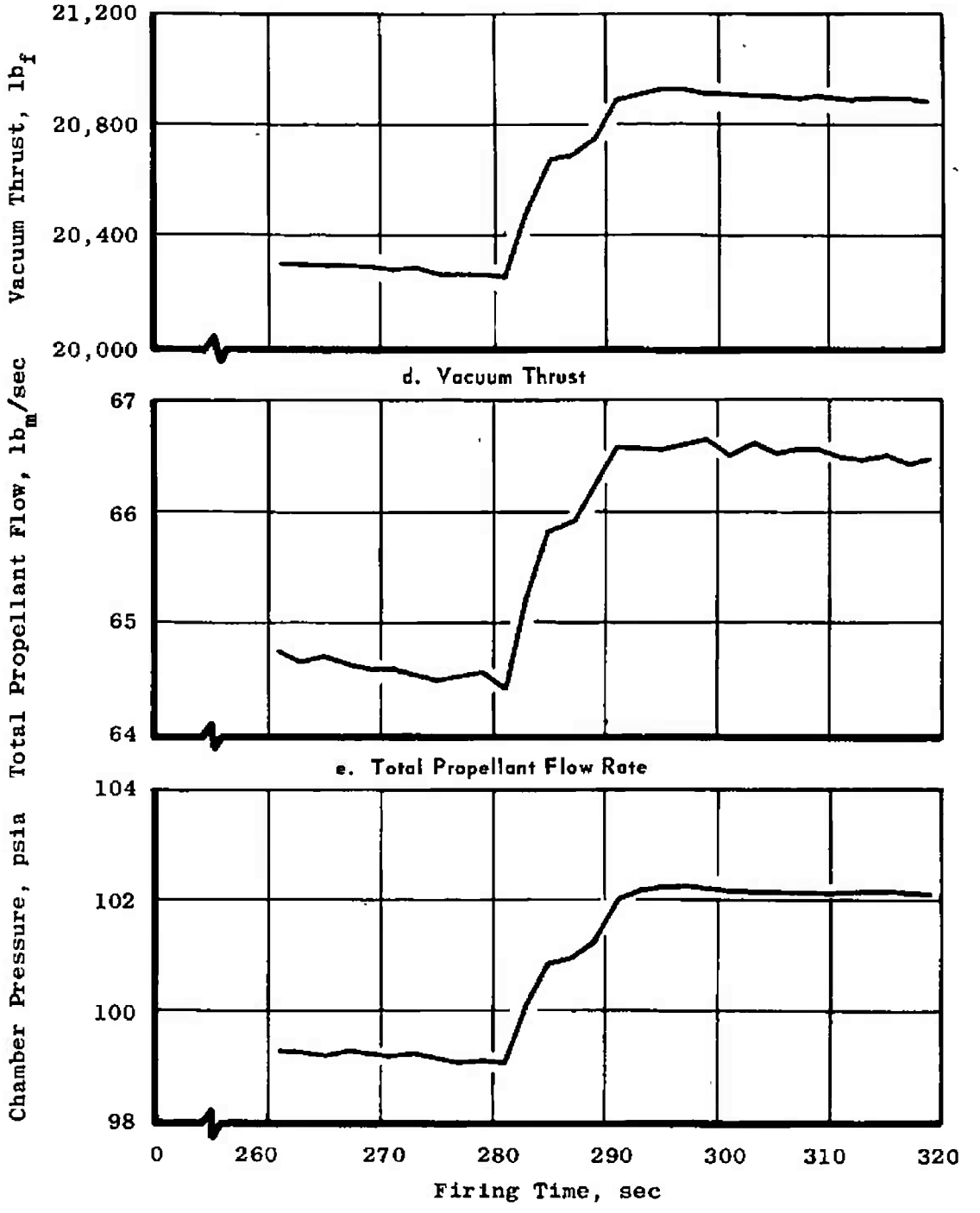

Fig. 22 Concluded

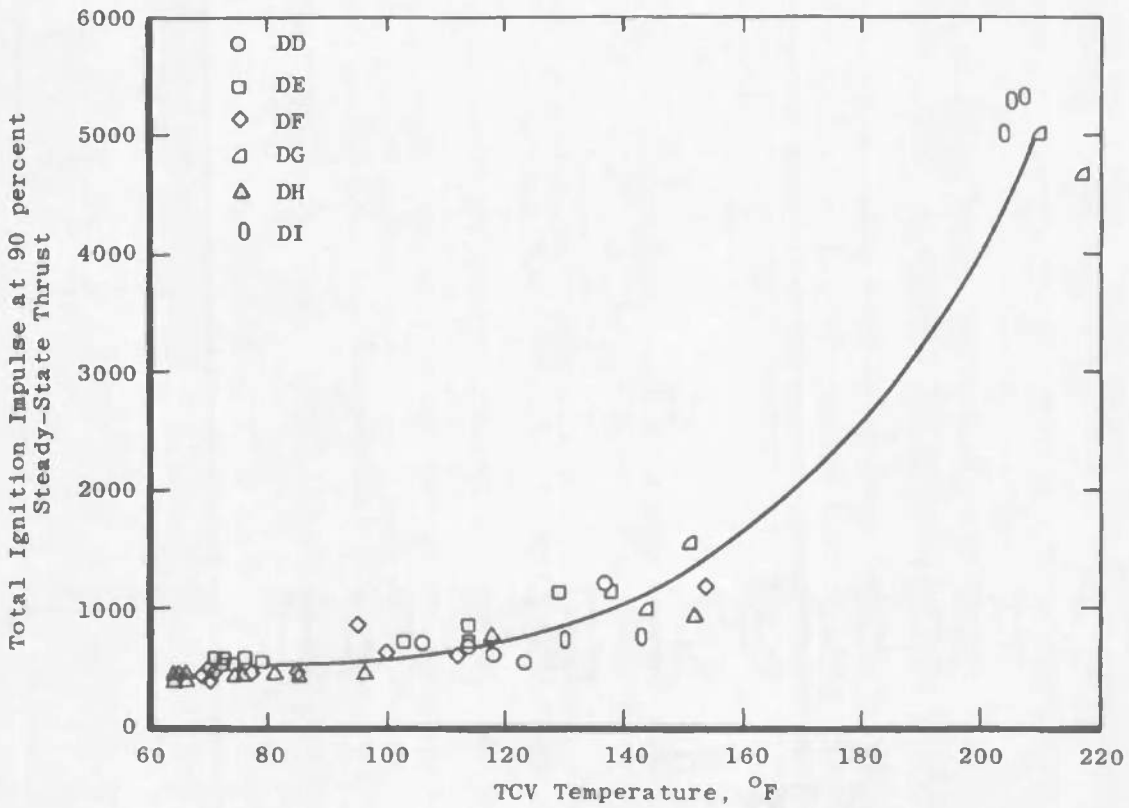

Fig. 23 Effect of TCV Temperature on Ignition Impulse

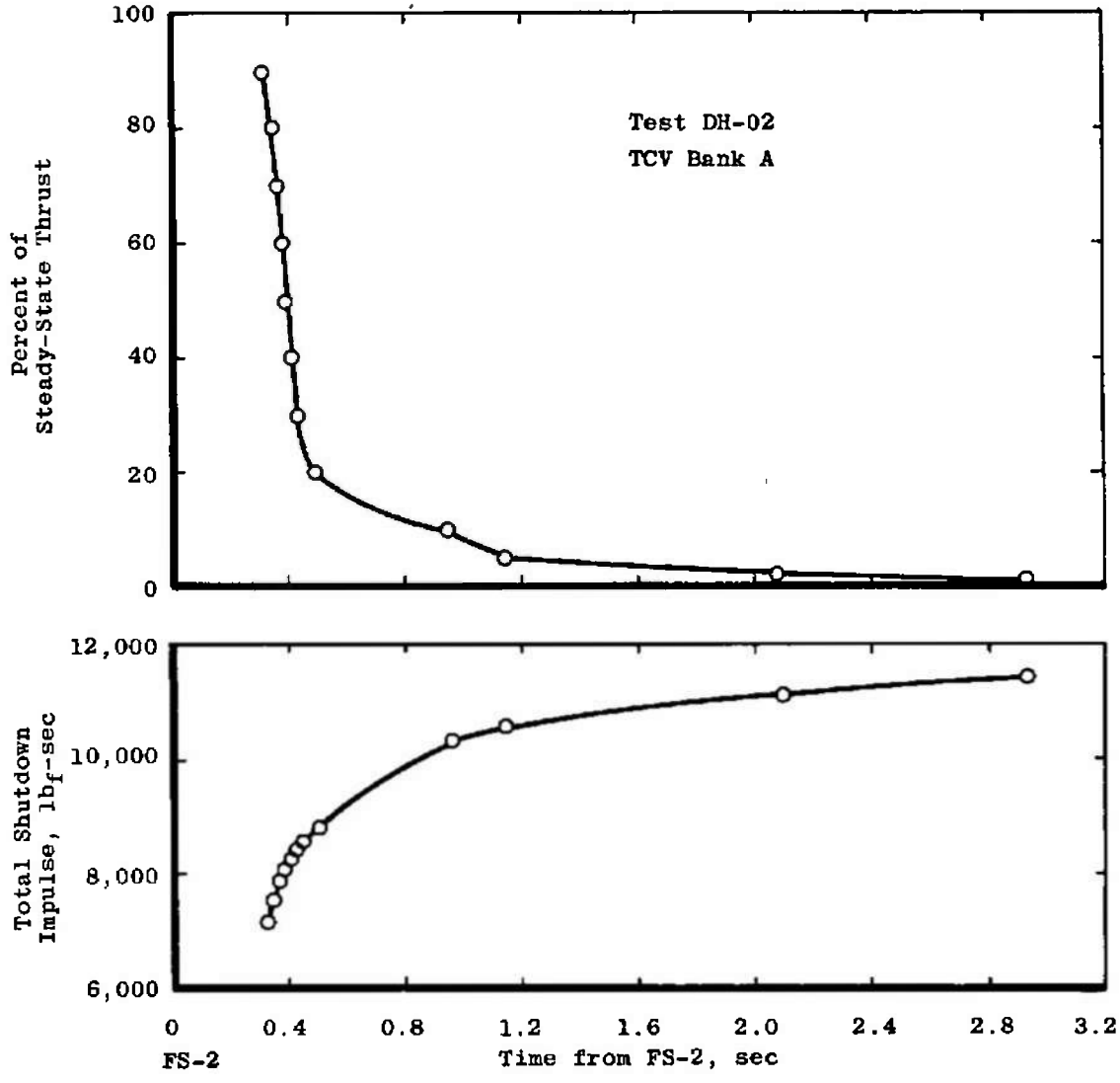

Fig. 25 Typical Shutdown Transient

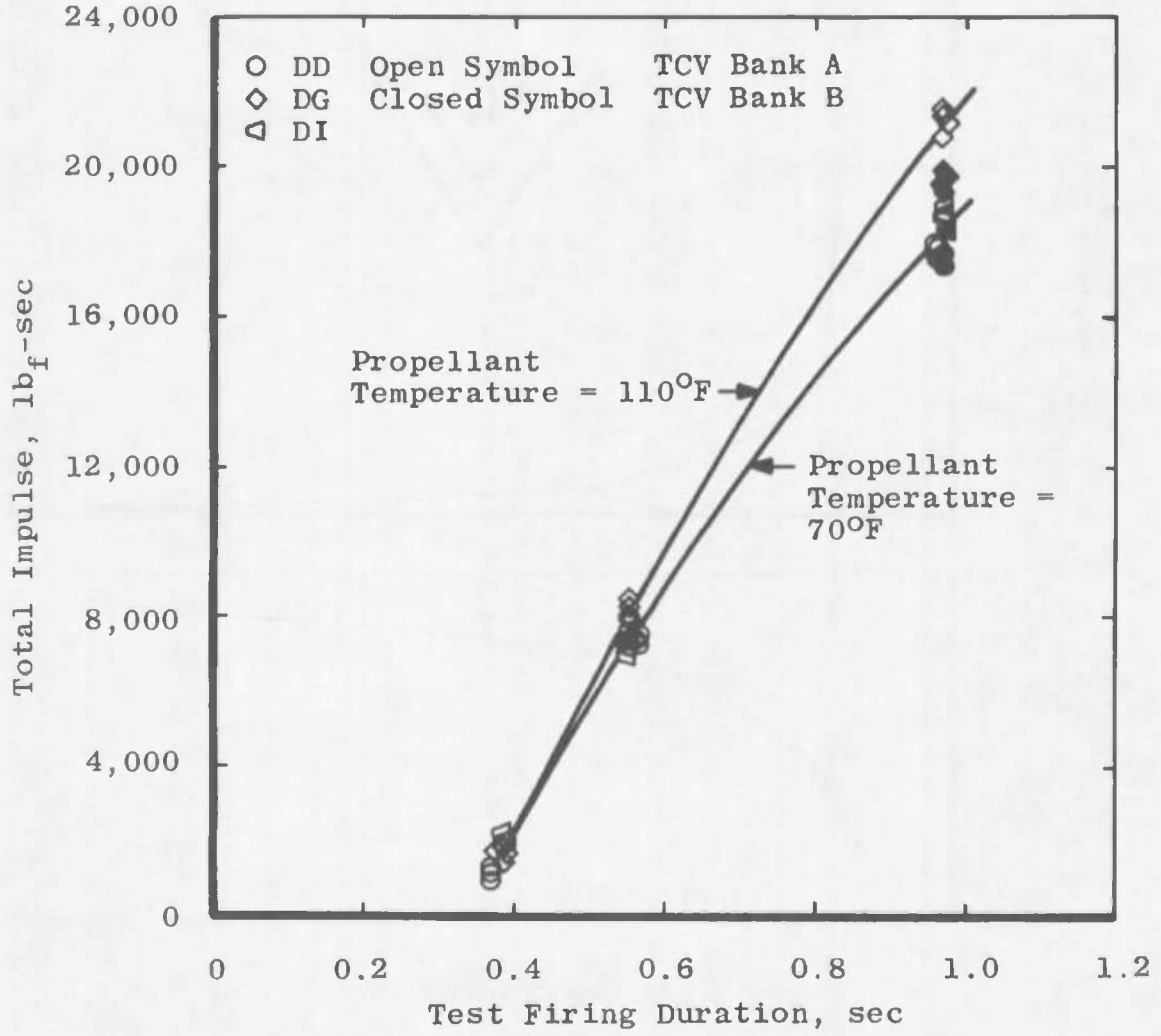

Fig. 26 Total Impulse Developed during Impulse Bit Firings

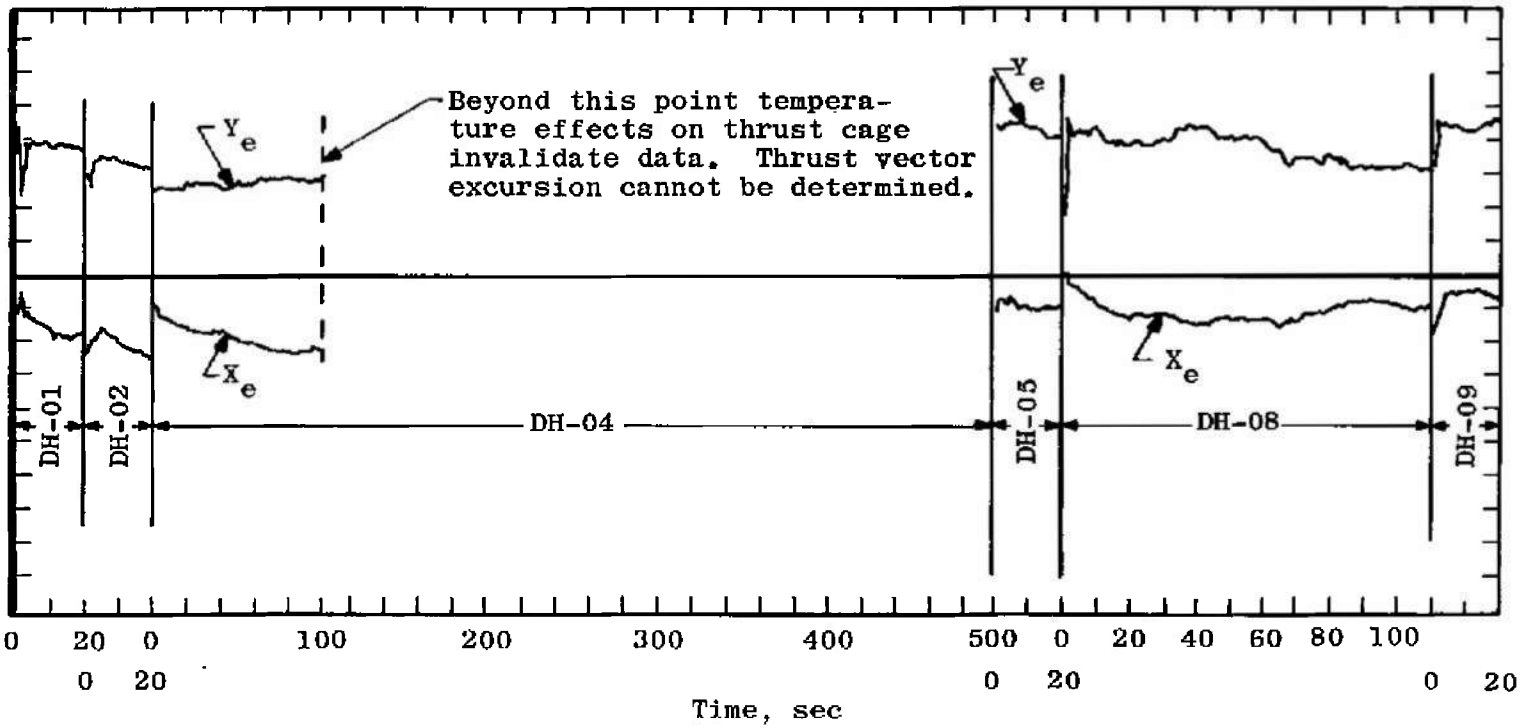

Fig. 27 Variation of Thrust Vector Intercept Components in the Chamber Throat Plane of Engine S/N 21E

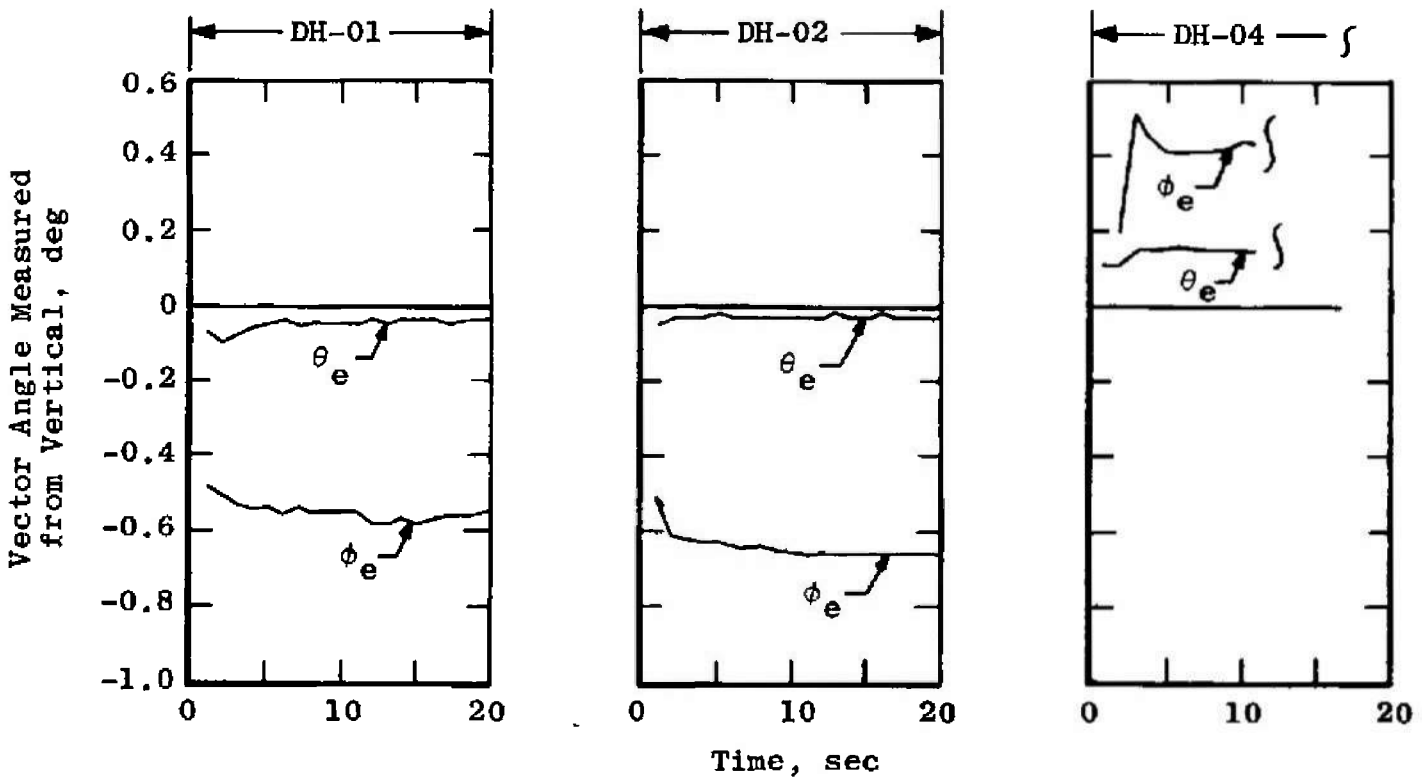

Fig. 28 Angular Variation of Thrust Vector Components of Engine S/N 21E

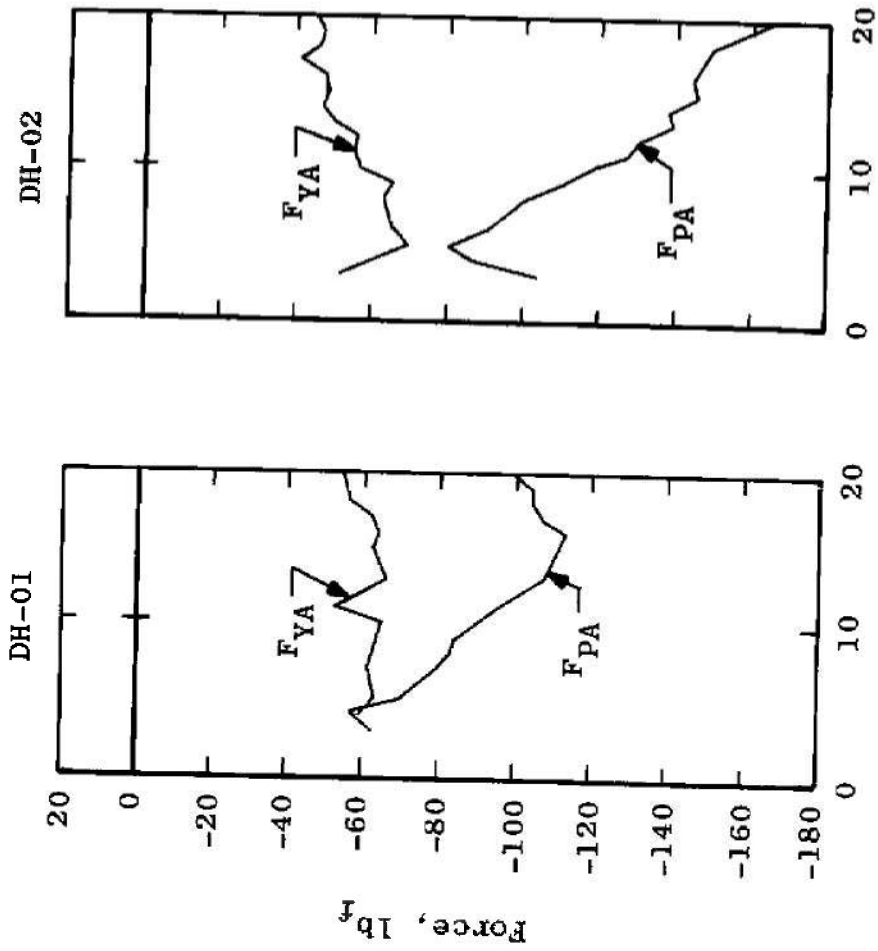

Fig. 29 Stiff Link Forces

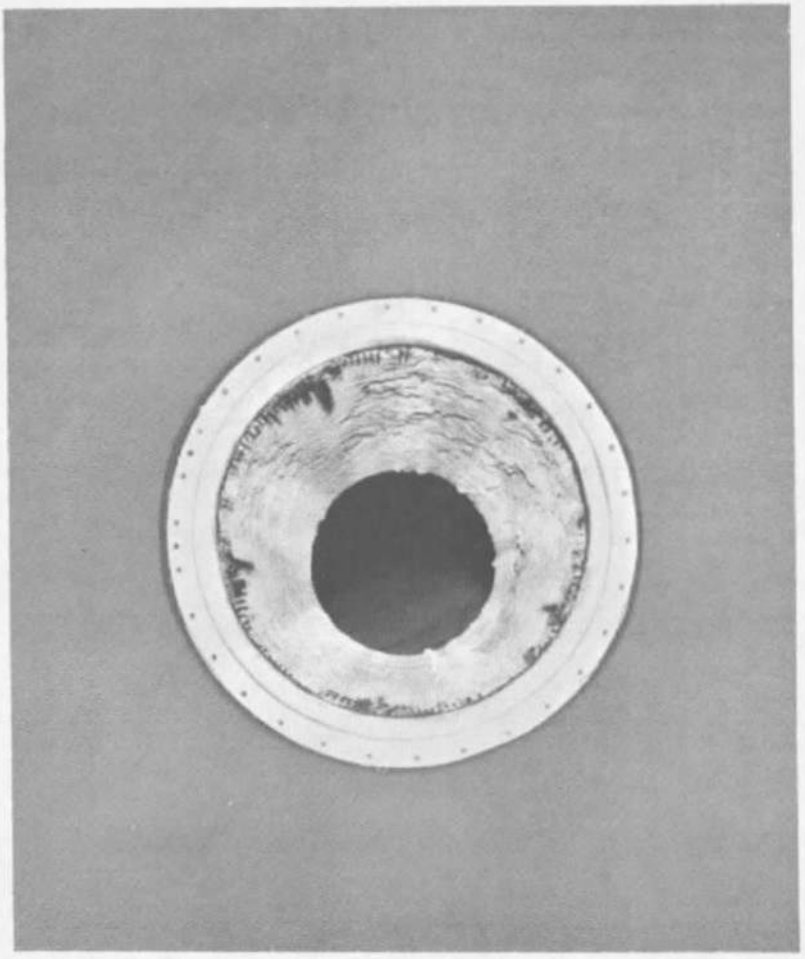

Fig. 30 DD Series Post-Test Combustion Chamber

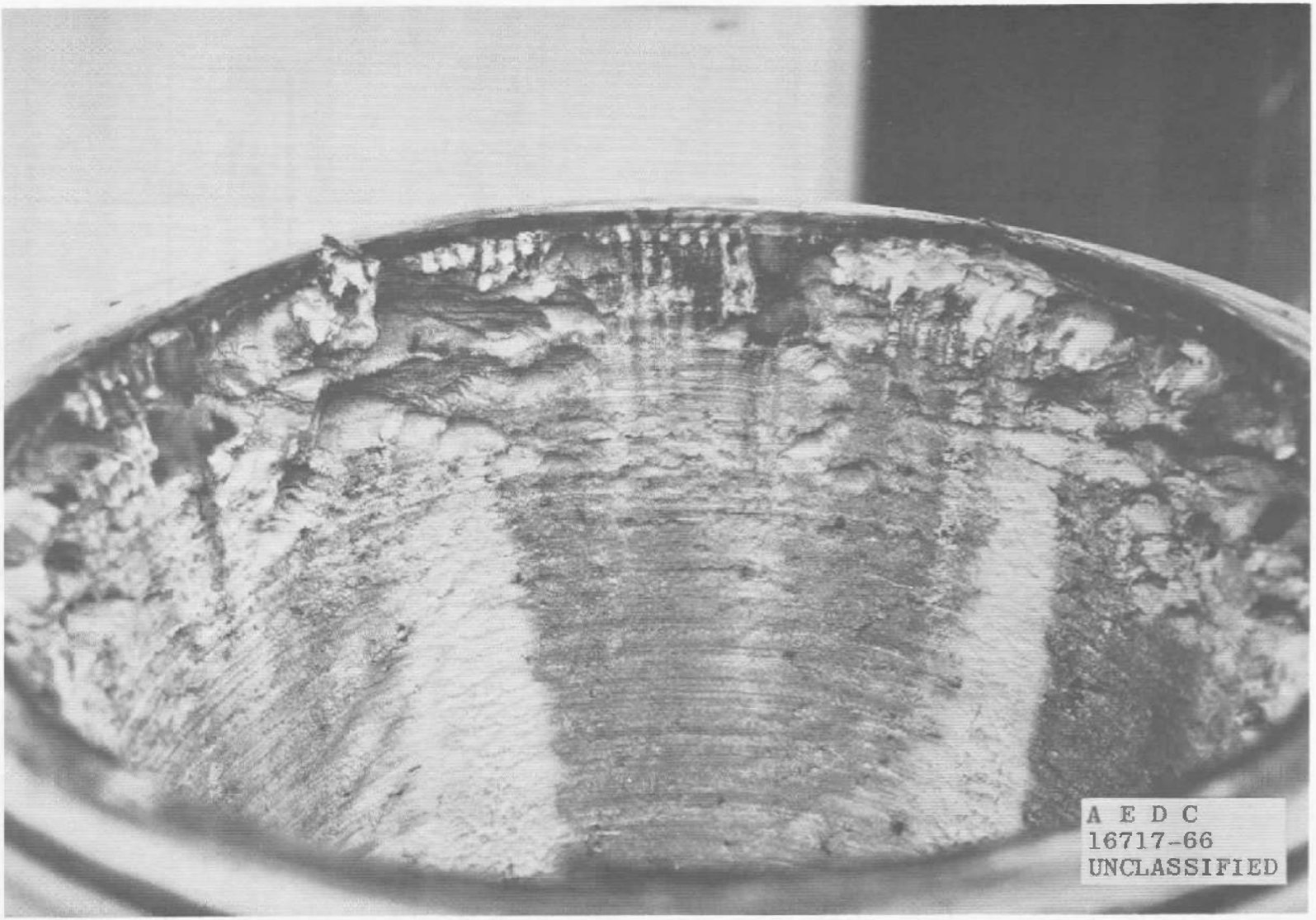

Fig. 31 DE Series Post-Test Combustion Chamber

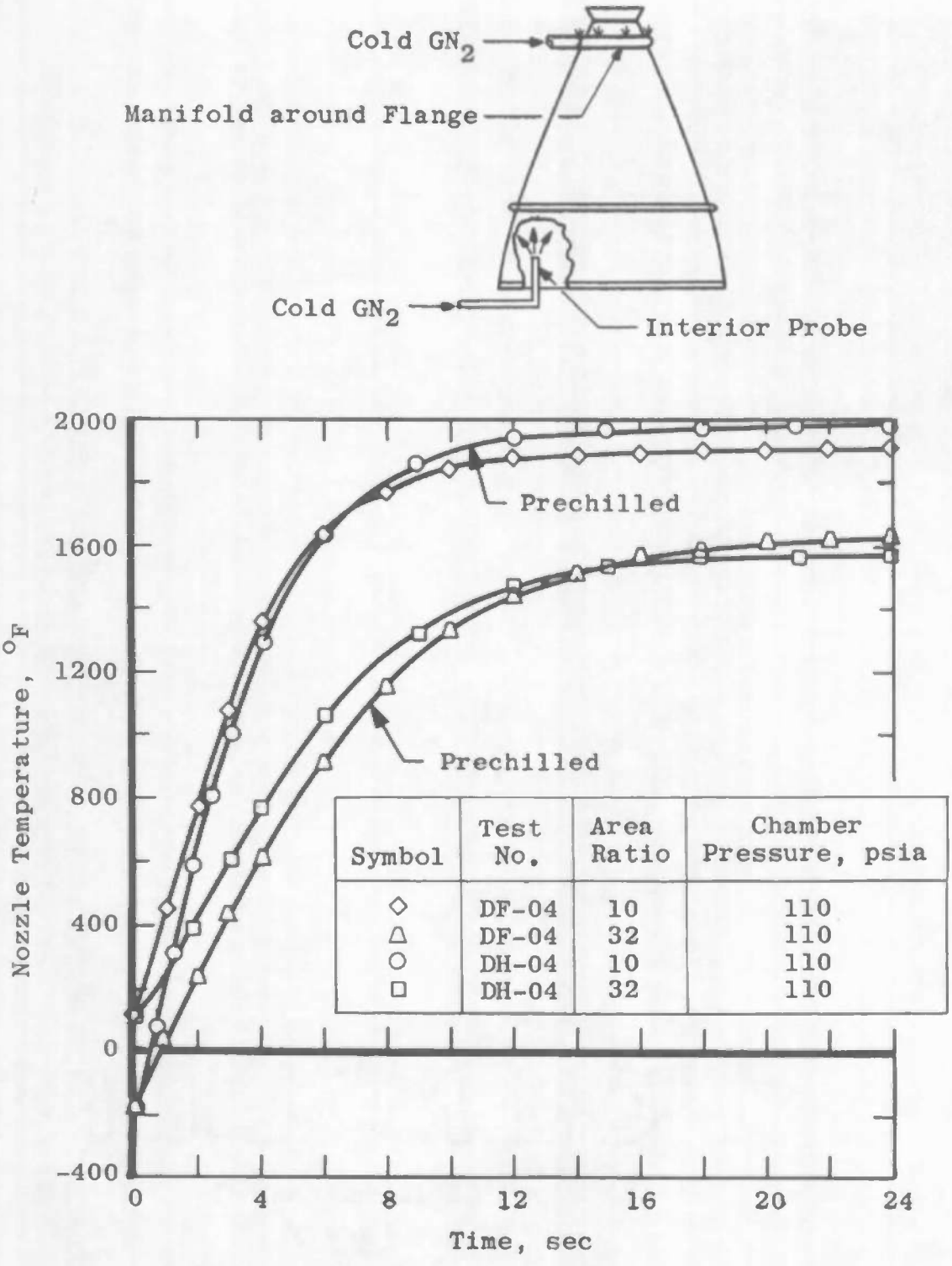

Fig. 32 Comparison of Nozzle Temperature with and without Initial Temperature Conditioning

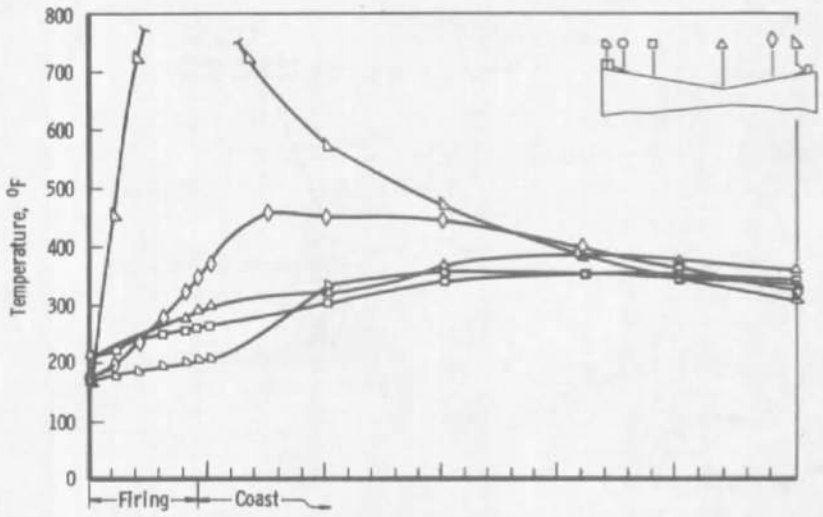

a. Test DD-06

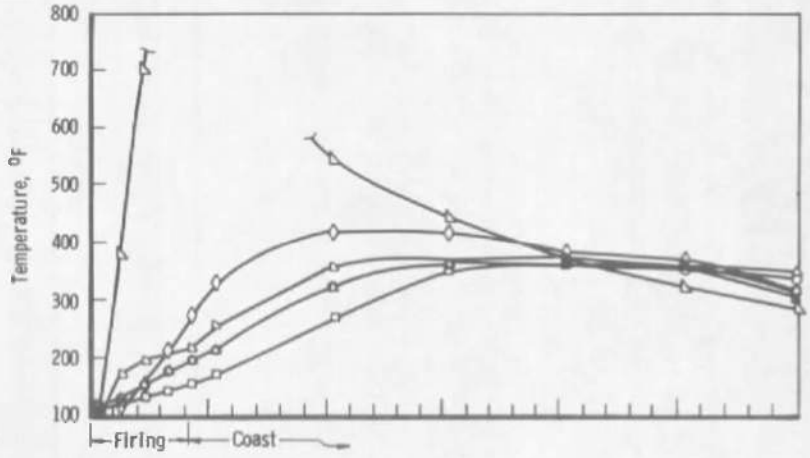

b. Test DE-04

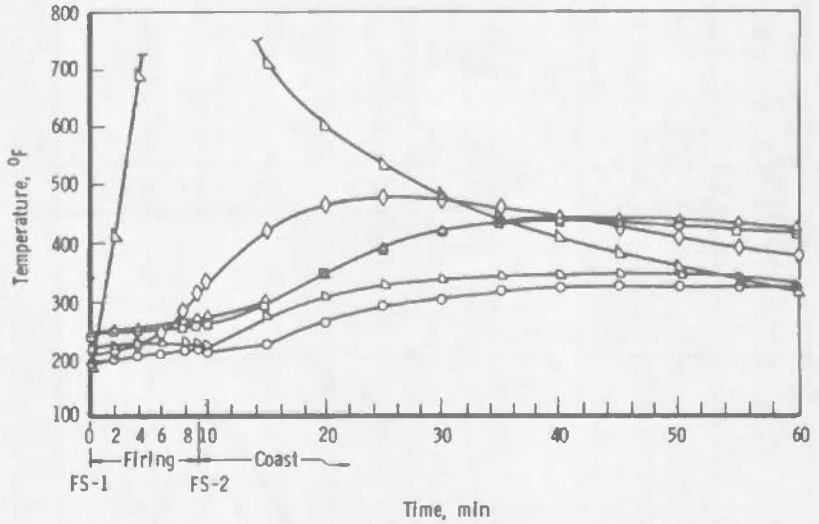

c. Test DG-06

Fig. 33 Combustion Chamber Outer Surface Temperatures for Three Long-Duration Tests

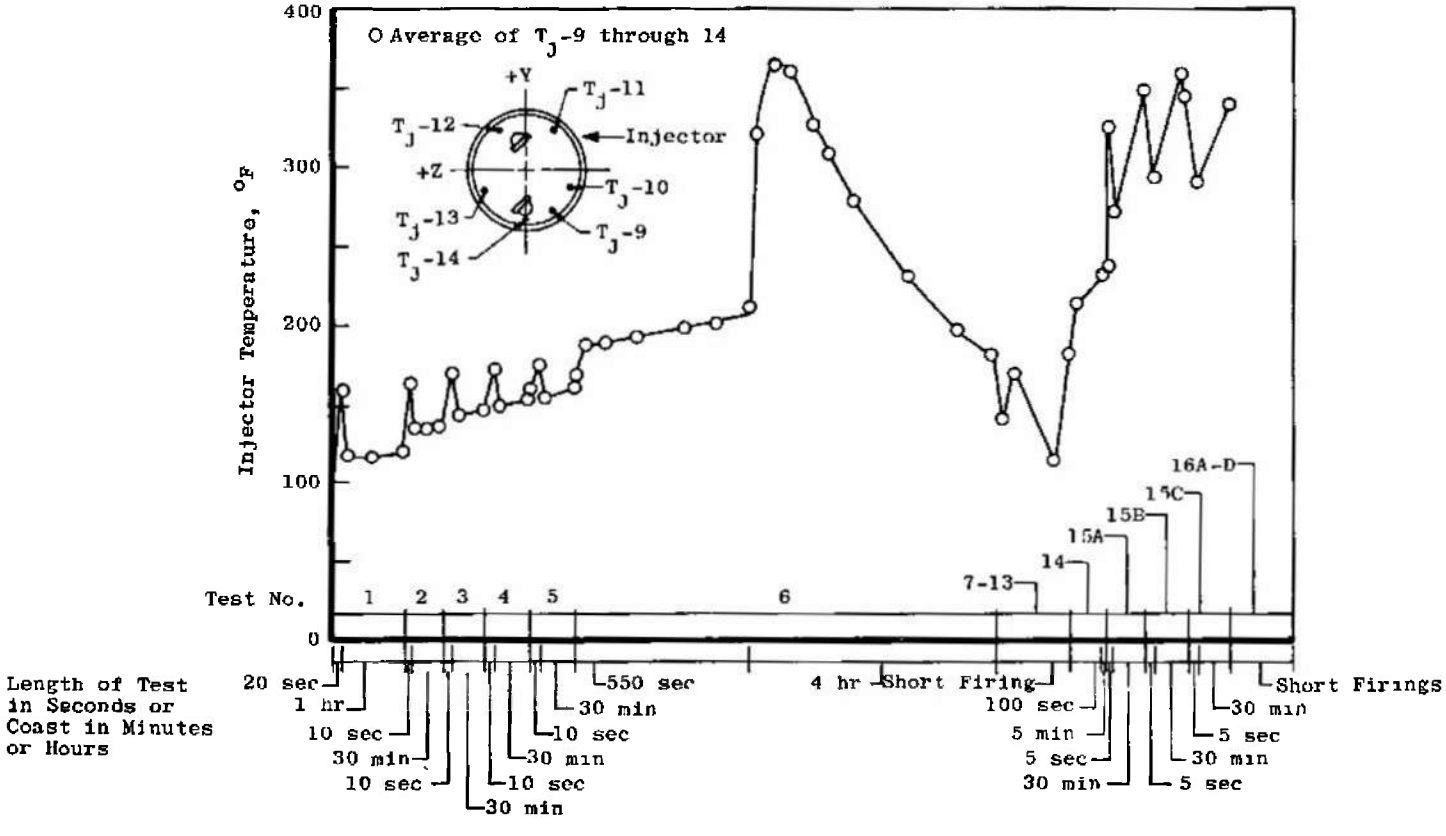

a. Test Series DD

Fig. 34 Injector Temperatures for Three Test Series

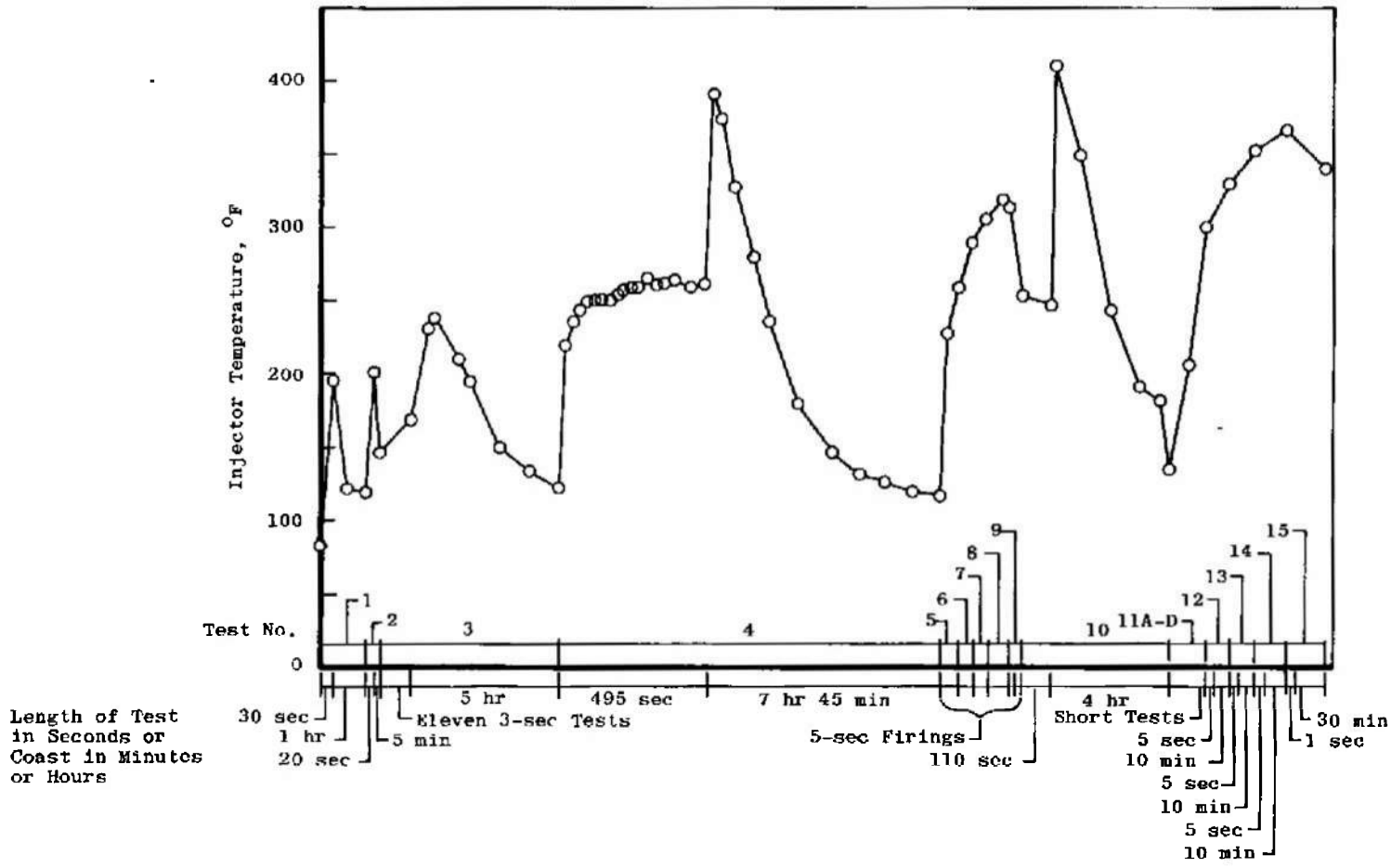

b. Test Series DE

Fig. 34 Continued

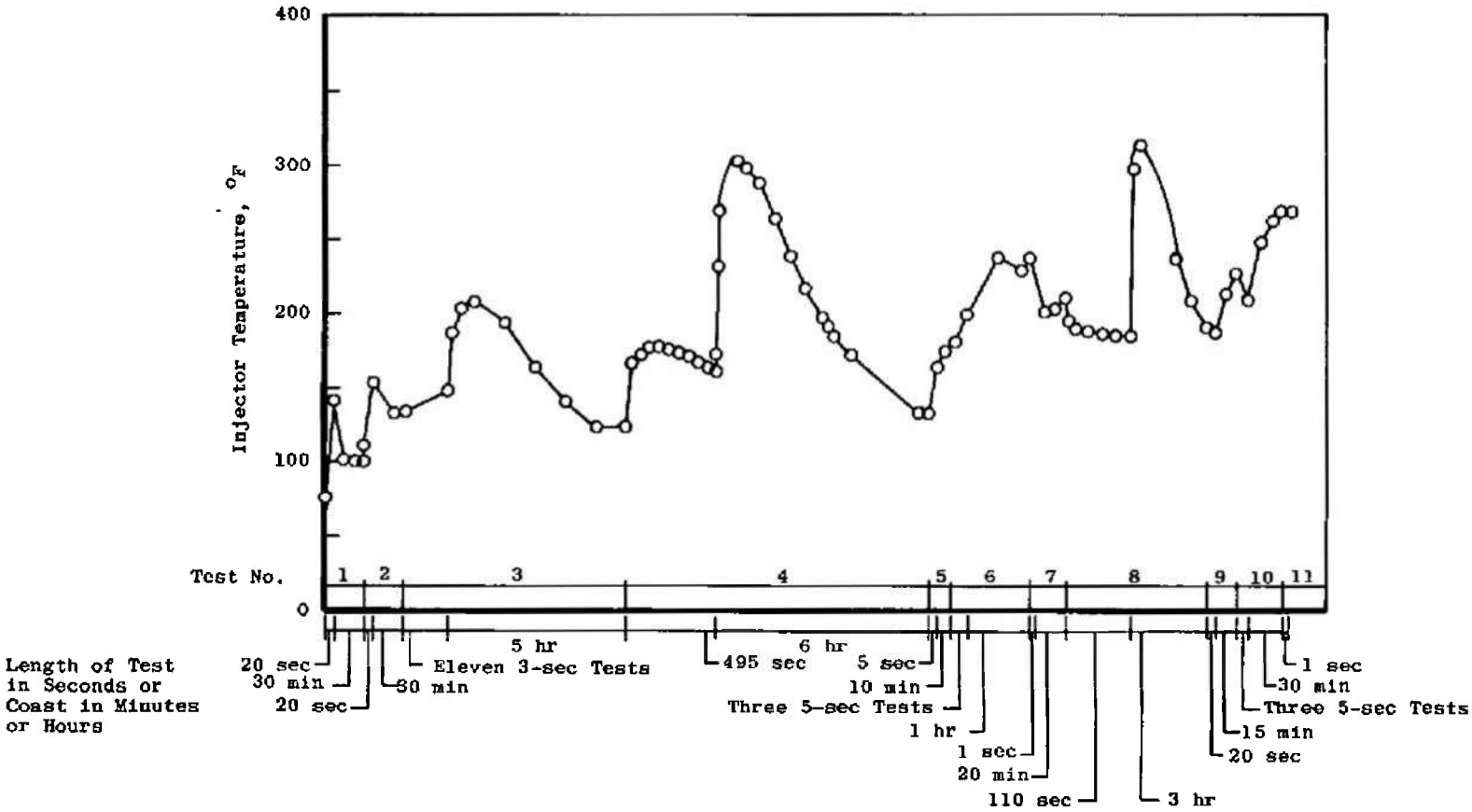

c. Test Series DH

Fig. 34 Concluded

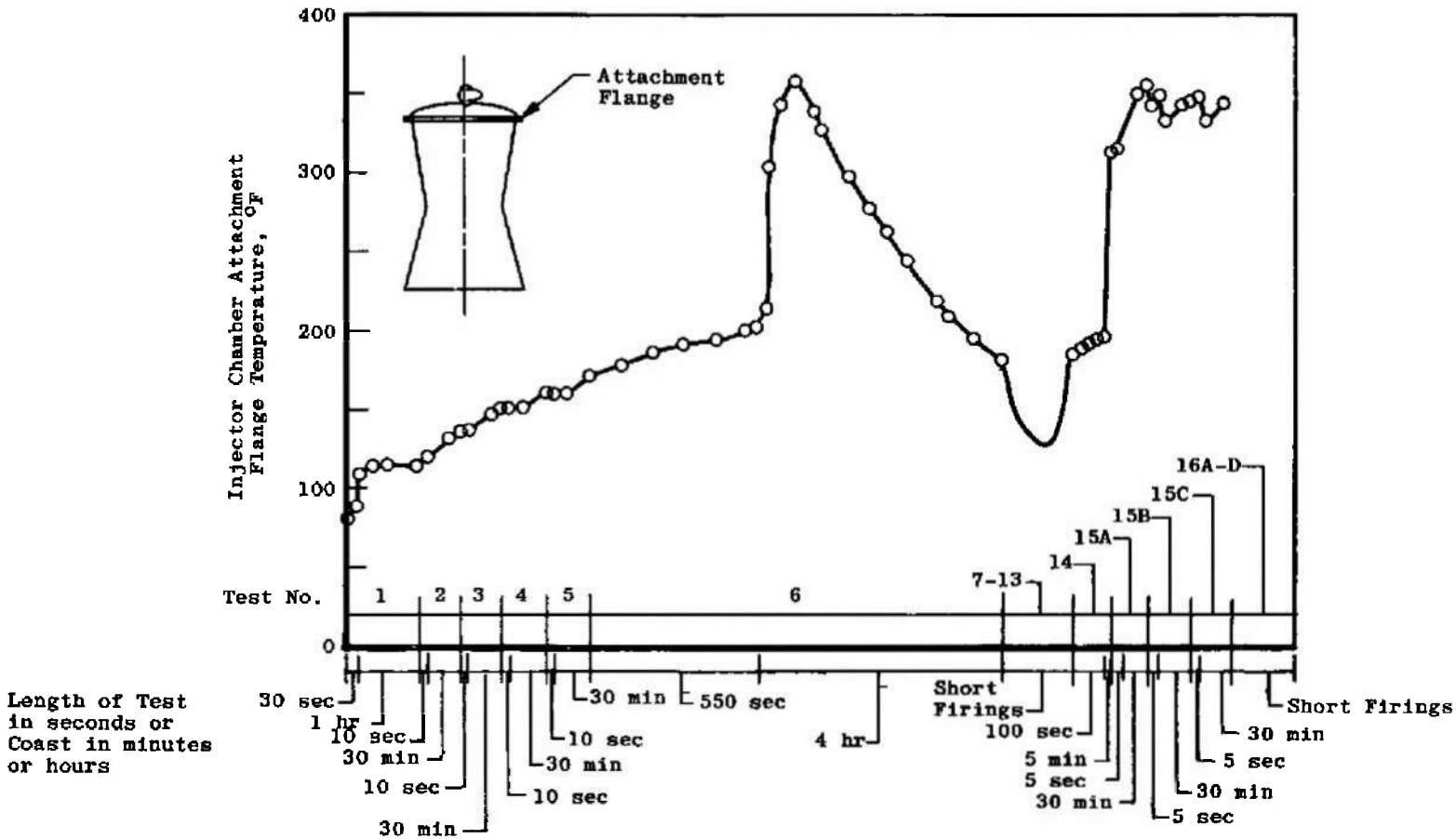

a. Test Series DD

Fig. 35 Injector/Chamber Attachment Flange Temperatures for Three Test Series

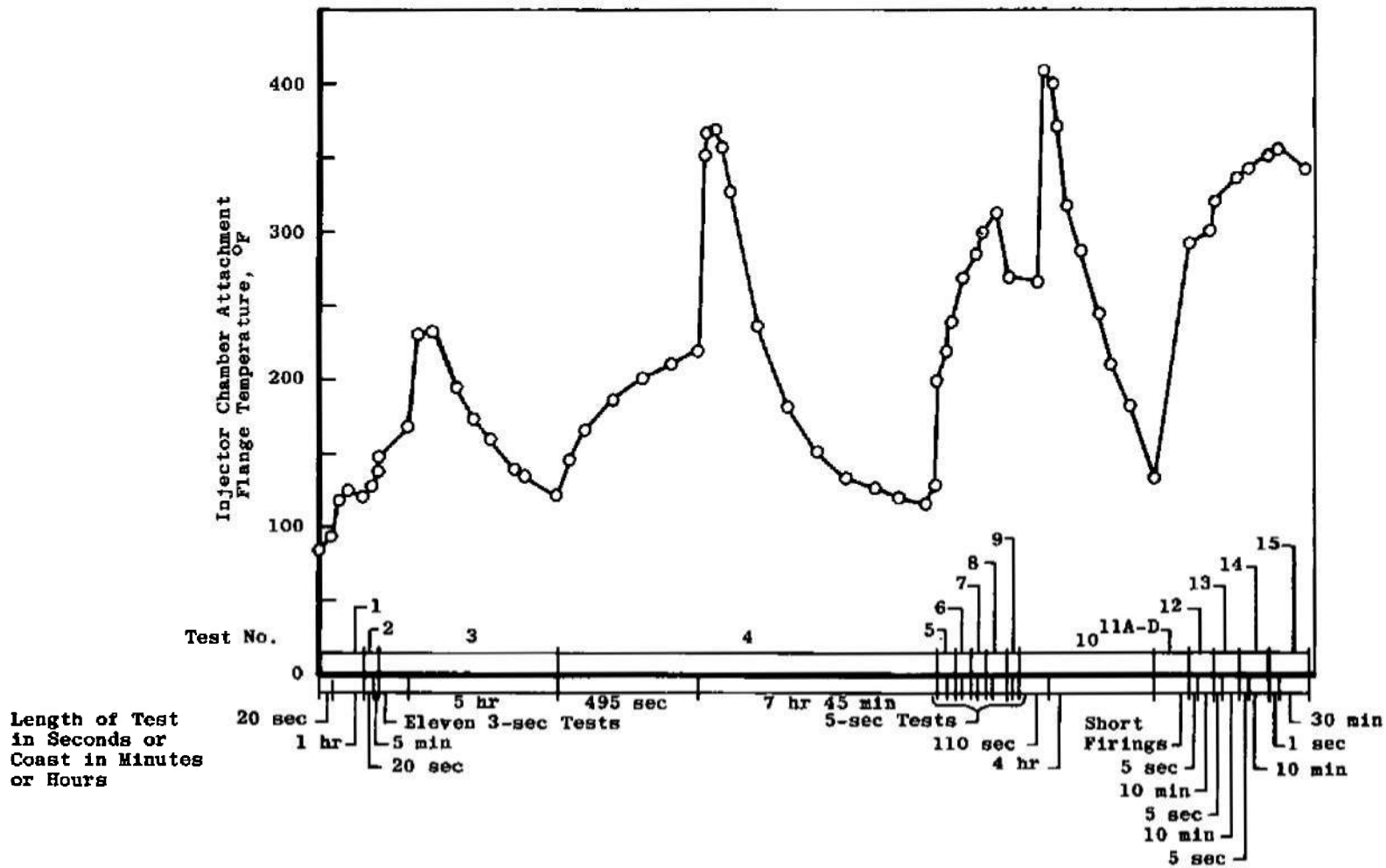

b. Test Series DE

Fig. 35 Continued

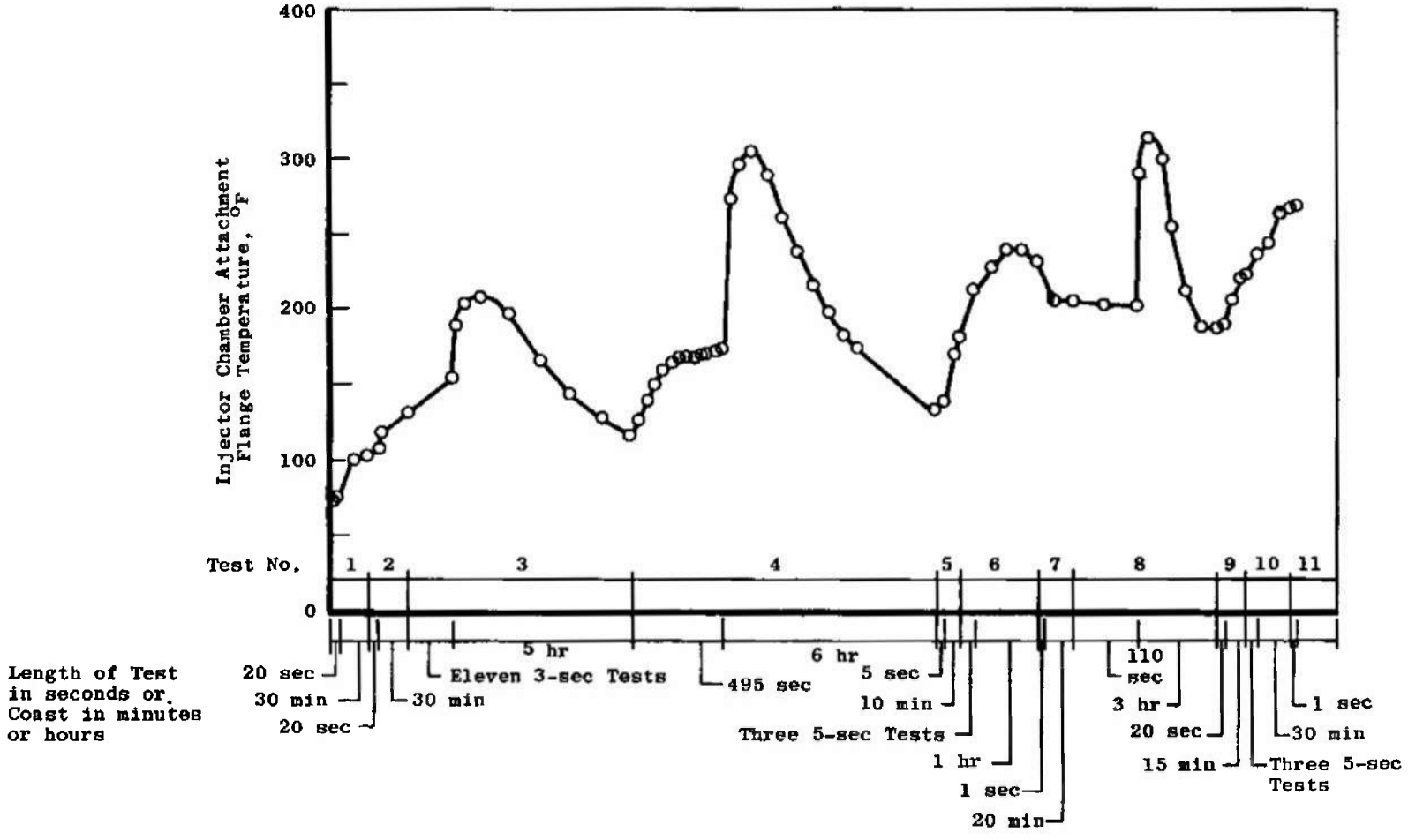

c. Test Series DH

Fig. 35 Concluded

TABLE I
GENERAL SUMMARY

Test No.	Date	Engine S/N	Firing Duration, sec	Coast Duration, min	TCV Bank	Test Objectives	Remarks
DD-01	8/4/68	21A	30.2	50	A-AB-B	Demonstrate Thrust Chamber Durability; Obtain Performance Data at Nominal Chamber Pressure and Mixture Ratio	
02			11.2	55	A		
03			10.9	30			
04			10.5	27			
05			10.8	40			
06			551.1	251			
07			0.37				
			4 Tests	60			
08			0.37	34			
09			0.57				
			4 Tests	1			
10			0.87	232			
11			0.97	1			
			0.96	1			
12			0.97				
			2 Tests	1	B		
13			0.96	32			
14			99.1	11			
15			6.2	30			
			5.6	30			
			5.5	30			
16			0.96				
			4 Tests	1			
17			0.96	--			
DE-01	8/12/68	21B	20.4	66	A-AB-B	Demonstrate Thrust Chamber Durability; Obtain Engine Performance at Nominal MR and High P_c	
02			20.6	5	A		
03			3.0				
			11 Tests	367			
04			496.1	457			
05			20.0	15			
06			5.7	10			
07			5.5	14			
08			5.1	34			
09			0.98	31	B		
10			110.4	376			
11			5.0				
			4 Tests	15			
12			5.6	12			
13			6.6	10			
14			5.7	10			
15			1.6	--			

TABLE I (Continued)

Test No.	Date	Engine S/N	Firing Duration, sec	Coast Duration, min	TCV Bank	Test Objectives	Remarks
DF-01	9/1/66	21C	21.1	260	A-AB-B	Demonstrate Thrust Chamber Durability at High P_c	
02			21.1	40	A		
03			3.0				
			11 Tests	340			
04			436.3	862			
05			15.1	35			Invalid NAA CSM Shutdown
06			10.6	12			
07			5.6	10			
08			6.3	31			
09	9/2/66		1.0	26	B		
10			110.4	171			
11			1.3	10			Invalid NAA CSM Shutdown
			20.7	16			
12			5.6	13			
13			5.6	10			
14			5.7	30			
15			1.0	--			
DG-01	9/22/66	21D	21.5	144	A-AB-B	Demonstrate Thrust Chamber Durability, Obtain Engine Performance at Various P_c and Nominal MR using Hot Propellants (110°F)	Invalid NAA CSM Shutdown
02			18.4	31	A		
03			9.1	60			
04			0.7	35			
05			11.2	55			
06			550.4	275			
07			0.39				
			5 Tests	27			
08			0.55				
			5 Tests	63			
09	9/23/66		0.97				
			5 Tests	95			
10			99.9	10	B		
11			5.6	30			
12			5.6	30			
13			5.7	30			
14			0.98				
			4 Tests	--			

TABLE I (Concluded)

Test No.	Date	Engine S/N	Firing Duration, sec	Coast Duration, min	TCV Bank	Test Objectives	Remarks
DH-01	10-14-66	21E	20.7	30	A-AB-B	Demonstrate Thrust Chamber Durability, Obtain Engine Performance at High P_c and Nominal MR, Stiff Links with Load Cells in Place to Determine Gimbal Actuator Loads; Side Load Measurements	Cooled Nozzle Extension and Nozzle Flange prior to Testing
02			20.6	35	A		
03			3.0				
			11 Tests	337			
04	10-15-66		496.4	360			
05			20.7	13			
06			5.5				
			6.2				
			5.5	84			
07			0.98	23	B		
08			109.9	143			
09			20.3	16			
10			5.7				
			5.8				
			6.0	30			
11			0.98	--			
DI-01	10/26/66	21F	30.4	85	A-AB-B	Demonstrate Thrust Chamber Durability; Engine Performance at Nominal MR and Various P_c using Hot Propellants (110°F)	
02			10.6	31	A		
03			10.8	29			
04			10.6	36			
05	10/27/66		10.8	73			
06			550.6	283			
07			0.39				
			5 Tests	36			
08			0.55				
			5 Tests	33			
09			0.98				
			1.0				
			0.98				
			0.98				
			0.98	52	B		
10			100.3	23			
11			5.4	40			
12			5.0	25			
13			6.1	31			
14			0.98				
			1.0				
			0.98	--			
			0.98				
			0.98				

TABLE II
SUMMARY OF ENGINE PERFORMANCE
a. Injector S/N 110

Test No.	Engine S/N	Time for 2-sec Average	Propellant Pressures, psia				Flow Rates, lb_m/sec			MR	T_o, °F	T_f, °F	P_c, psia	F_v, lbf	P_a, psia	$A_{t_{calc}}$, $in.^2$	I_{sp_v}, $\frac{lbf\text{-}sec}{lb_m}$	c*, ft/sec	C_{F_v}
			P_{ot}	POL-1, $P_{ot_{cs}}$	P_{ft}	PFL-1, $P_{ft_{cs}}$	$\dot{W}_o$	$\dot{W}_f$	$\dot{W}_t$										
DD-01	21A	7	170.6	169.5	161.0	155.7	42.90	22.50	65.40	1.907	70.0	80.4	97.6	20,407	0.084	121.64	312.04	5840	1.719
		9	170.6	169.4	160.9	155.6	42.90	22.50	65.40	1.907	70.9	80.5	97.6	20,392	0.080	121.64	311.81	5840	1.718
		15	171.0	169.1	160.9	155.4	43.69	22.70	66.39	1.925	70.9	80.5	99.1	20,683	0.076	121.48	311.54	5834	1.718
		25	171.0	168.3	161.0	155.5	42.37	22.40	64.77	1.892	70.9	80.6	97.0	20,184	0.073	121.28	311.64	5845	1.715
DD-02		7	151.0	150.7	184.8	175.7	36.98	26.35	63.33	1.403	71.2	80.5	96.8	19,859	0.081	120.15	313.57	5912	1.707
DD-02		8	151.0	150.7	184.7	175.6	37.03	26.35	63.38	1.405	71.2	80.6	96.9	19,885	0.077	120.20	313.42	5912	1.706
DD-03		7	156.4	153.6	182.1	172.7	37.97	25.81	63.79	1.471	71.5	80.7	97.3	20,014	0.115		313.77	5920	1.705
DD-03		9	156.0	153.7	182.1	172.7	37.97	25.78	63.75	1.473	71.5	80.7	97.3	20,056	0.091	120.53	314.59	5920	1.710
DD-04		7	164.0	160.9	171.0	162.7	40.34	23.90	64.24	1.688	71.8	80.8	97.4	20,105	0.079	121.03	314.23	5902	1.713
DD-04		9	164.3	160.9	171.1	162.7	40.44	23.94	64.38	1.690	71.8	80.8	97.4	20,204	0.076	121.22	313.84	5902	1.711
DD-05		7	165.9	162.9	162.4	156.0	41.33	22.79	64.12	1.813	72.1	80.9	96.5	20,065	0.103	121.18	312.91	5870	1.715
DD-05		9	165.8	162.9	162.3	155.9	41.28	22.79	64.07	1.811	72.1	80.9	96.6	20,087	0.088	121.03	313.51	5871	1.718
DD-06		7	158.5	153.5	172.1	164.5	38.54	24.54	63.07	1.571	67.1	81.0	96.0	19,818	0.074	120.83	314.22	5919	1.708
		9	158.5	153.5	172.1	164.4	38.43	24.50	62.93	1.568	67.1	81.0	96.0	19,814	0.072	120.62	314.86	5919	1.711
		21	158.8	153.2	172.1	164.2	38.43	24.50	62.93	1.568	67.2	81.0	96.0	19,792	0.067	120.64	314.51	5919	1.710
		31	158.5	153.0	172.1	164.0	38.48	24.47	62.95	1.573	67.2	81.1	95.9	19,778	0.067	120.74	314.19	5919	1.709
		301	158.6	156.4	172.4	166.1	38.97	24.64	63.61	1.582	68.4	80.8	97.4	19,870	0.080	120.18	314.07	5918	1.708
		547	156.7	151.5	172.8	163.5	37.59	24.64	62.23	1.526	70.2	80.8	95.1	19,582	0.080	120.43	314.66	5921	1.710
DD-14		7	151.6	157.0	168.0	168.7	38.83	24.53	63.35	1.583	74.4	84.0	96.6	19,923	0.117	120.62	314.47	5918	1.710
		9	151.6	157.1	168.0	166.8	38.78	24.59	63.37	1.577	74.4	84.0	96.7	19,897	0.099	120.61	315.57	5919	1.716
		11	151.6	157.0	168.0	166.8	38.78	24.56	63.34	1.579	74.4	84.0	96.6	19,969	0.084	120.58	315.29	5918	1.714
		21	151.6	156.8	168.0	166.7	38.72	24.56	63.28	1.577	74.4	84.0	96.5	19,910	0.071	120.64	314.75	5919	1.711
		31	151.5	156.6	167.9	166.5	38.72	24.59	63.31	1.575	74.4	84.0	96.5	19,925	0.070	120.73	314.70	5919	1.711
		97	151.9	155.7	167.9	165.9	38.46	24.52	62.98	1.568	74.5	84.1	96.2	19,888	0.079	120.96	315.77	5919	1.716

TABLE II (Continued)

a. Concluded

Test No.	Engine S/N	Time for 2-sec Average	Propellant Pressures, psia				Flow Rates, lb_m/sec			MR	T_o, °F	T_f, °F	P_c, psia	F_v, lbf	P_a, psia	$A_{t_{calc.}}$, in.^{2}	I_{sp_v}, $\frac{lbf\text{-}sec}{lb_m}$	c*, ft/sec	C_{F_v}
			P_{ot}	POL-1, $P_{ot_{ca}}$	P_{ft}	PFL-1, $P_{ft_{ca}}$	$\dot{W}_o$	$\dot{W}_f$	$\dot{W}_t$										
DE-01	21B	7	193.9	187.9	209.8	199.5	44.71	27.93	72.64	1.601	74.4	84.8	109.7	22,930	0.085	121.43	315.66	5900	1.721
		9	193.9	187.9	209.7	199.4	44.71	27.93	72.64	1.601	74.4	84.8	109.8	22,924	0.081	121.38	315.57	5900	1.721
		13	193.9	187.4	209.8	199.0	45.52	28.27	73.79	1.610	74.4	84.8	111.6	23,277	0.077	121.25	315.47	5899	1.721
		19	194.1	187.9	209.9	199.5	44.28	27.73	72.01	1.597	74.4	84.9	109.1	22,688	0.075	121.06	315.06	5901	1.718
DE-02		7	193.9	186.9	209.2	198.5	44.53	27.83	72.37	1.600	74.9	84.9	109.5	22,813	0.082	121.21	315.25	5900	1.719
		9	193.9	186.9	209.2	198.3	44.43	27.83	72.26	1.596	74.9	84.9	109.5	22,798	0.079	121.08	315.51	5901	1.720
		11	193.9	186.7	209.3	198.3	44.43	27.83	72.26	1.596	74.9	84.9	109.5	22,750	0.078	121.04	314.84	5901	1.717
		15	194.1	186.8	209.3	198.3	44.37	27.86	72.23	1.593	74.9	84.9	109.6	22,773	0.076	120.92	315.26	5901	1.719
DE-04		7	195.4	186.8	210.0	198.4	44.64	27.83	72.46	1.604	77.9	85.0	109.6	22,828	0.077	121.2	315.03	5900	1.718
		9	195.3	186.7	210.0	198.4	44.64	27.83	72.46	1.604	77.9	85.0	109.6	22,825	0.075	121.2	314.98	5900	1.718
		11	195.4	186.7	210.0	198.3	44.58	27.86	72.44	1.600	77.9	85.0	109.6	22,816	0.073	121.2	314.95	5900	1.717
		21	195.4	186.5	210.2	198.3	44.64	27.83	72.47	1.604	77.9	85.0	109.6	22,769	0.072	121.19	314.49	5900	1.715
		31	195.5	186.3	210.0	198.1	44.53	27.86	72.39	1.598	77.9	85.0	109.6	22,748	0.072	121.2	314.25	5900	1.714
		301	195.1	190.1	211.1	200.9	45.19	28.18	73.37	1.603	78.9	85.9	110.7	23,037	0.068	121.58	313.98	5900	1.712
		493	193.4	184.5	210.5	198.2	44.27	28.01	72.28	1.580	79.2	86.1	108.6	22,738	0.089	172.14	314.58	5902	1.715
DE-05		7	191.5	189.5	207.3	201.3	45.33	28.20	73.53	1.607	76.6	84.8	110.4	23,137	0.088	122.13	314.65	5899	1.716
		9	191.5	189.4	207.3	201.3	45.28	28.20	73.48	1.605	76.6	84.8	110.4	23,128	0.089	122.08	314.77	5900	1.717
		11	191.6	189.4	207.3	201.2	45.28	28.24	73.51	1.604	76.6	84.8	110.4	23,129	0.087	122.14	314.63	5900	1.716
		15	191.5	189.4	207.4	201.3	45.33	28.20	73.53	1.607	76.6	84.8	110.4	23,184	0.084	122.18	315.30	5899	1.720
DE-10		7	191.1	188.9	206.8	201.4	44.88	28.22	73.10	1.590	78.6	85.7	109.4	22,955	0.087	122.52	314.04	5901	1.712
		9	191.1	188.9	206.8	201.4	44.88	28.22	73.10	1.590	78.6	85.7	109.4	22,954	0.085	122.55	314.03	5901	1.712
		11	191.1	188.8	206.8	201.3	44.82	28.19	73.01	1.590	78.6	85.7	109.4	22,957	0.082	122.42	314.45	5901	1.714
		21	191.3	188.8	207.0	201.2	44.82	28.22	73.04	1.588	78.6	85.8	109.3	22,988	0.090	122.58	314.72	5901	1.716
		31	191.2	188.5	207.0	201.2	44.77	28.22	72.99	1.587	78.6	85.8	109.1	22,978	0.087	122.68	314.82	5902	1.716
		97	191.5	187.4	207.4	200.6	44.61	28.05	72.66	1.590	78.7	85.9	108.6	22,931	0.084	122.67	315.61	5901	1.721

TABLE II (Continued)

b. Injector S/N 93

Test No.	Engine S/N	Time for 2-sec Average	Propellant Pressures, psia				Flow Rates, lb_m/sec			MR	T_o, °F	T_f, °F	P_c, psia	F_v, lb_f	P_a, psia	A_{throat}, $in.^2$	I_{sp_v}, $\frac{lb_f\text{-sec}}{lb_m}$	c*, ft/sec	C_{F_v}
			P_{o_t}	POL-1, $P_{o_{tca}}$	P_{f_t}	PFL-1, $P_{f_{tca}}$	$\dot{W}_o$	$\dot{W}_f$	$\dot{W}_t$										
DF-01	21C	7	197.5	187.9	220.5	210.7	42.95	29.80	72.7	1.441	80.2	84.5	109.1	22,890	0.084	121.48	314.64	5861	1.727
		9	197.5	187.8	229.4	219.6	42.89	29.76	72.65	1.441	80.2	84.5	109.1	22,879	0.084	121.36	314.90	5861	1.729
		15	197.5	187.2	229.3	219.1	43.32	30.13	73.45	1.438	80.2	84.5	110.4	23,113	0.074	121.25	314.68	5861	1.728
		19	197.6	187.7	229.4	219.5	42.52	29.63	72.15	1.435	80.2	84.5	108.4	22,684	0.073	121.22	314.42	5861	1.726
DF-02		7	211.5	202.5	217.5	210.2	46.37	28.13	74.49	1.649	71.9	84.3	111.4	23,511	0.068	121.27	315.62	5832	1.741
		9	211.3	202.5	217.6	210.2	46.37	28.13	74.50	1.649	71.9	84.3	111.5	23,523	0.068	121.16	315.78	5832	1.742
		11	211.4	202.0	217.6	209.9	46.96	28.39	75.35	1.654	71.9	84.3	112.5	23,717	0.069	121.41	314.74	5831	1.737
		15	211.4	202.2	217.7	209.8	46.96	28.39	75.35	1.654	71.9	84.4	112.8	23,780	0.070	121.07	315.71	5831	1.736
DF-04		7	210.9	202.6	224.0	213.6	46.20	28.46	74.66	1.623	74.8	88.3	112.4	23,606	0.075	120.46	316.17	5837	1.743
		9	210.9	202.6	223.8	213.5	46.09	28.53	74.62	1.616	74.8	88.3	112.4	23,598	0.073	120.45	316.25	5836	1.743
		11	210.9	202.4	223.8	213.4	46.09	28.53	74.62	1.616	74.8	88.3	112.3	23,576	0.072	120.55	315.95	5838	1.741
		21	210.9	202.1	223.8	213.3	46.15	28.46	74.61	1.621	74.8	88.3	112.3	23,570	0.070	120.49	315.93	5837	1.736
		31	210.8	201.8	223.9	213.2	46.09	28.49	74.58	1.618	74.8	88.3	112.3	23,561	0.070	120.47	315.89	5838	1.735
		301	210.7	205.3	225.0	216.1	46.39	28.78	75.38	1.619	75.8	89.0	114.0	23,856	0.087	119.94	316.49	5838	1.739
		493	208.1	199.8	224.6	213.4	45.78	28.71	74.49	1.594	76.0	89.1	112.3	23,561	0.087	120.44	315.27	5842	1.737
DF-05		7	208.6	204.5	222.7	217.1	46.42	29.04	75.47	1.598	84.3	91.3	112.4	23,757	0.072	121.85	314.80	5841	1.734
		9	208.6	204.5	222.7	217.0	46.32	28.83	75.15	1.607	84.3	91.3	112.4	23,742	0.072	121.40	315.95	5840	1.743
		11	208.8	204.5	222.8	217.0	46.42	28.91	75.33	1.606	84.3	91.3	112.4	23,751	0.073	121.86	315.28	5840	1.740
DF-06		7	209.3	204.1	222.6	218.5	46.46	28.92	75.38	1.607	84.7	91.4	112.5	23,711	0.070	121.63	314.55	5840	1.733
DF-06		9	209.3	204.0	222.4	216.4	46.35	28.85	75.20	1.607	84.7	91.5	112.5	23,710	0.071	121.39	315.27	5840	1.739
DF-10		7	210.1	203.7	223.5	216.6	45.77	28.82	74.58	1.589	86.0	92.1	111.8	23,521	0.074	121.17	315.36	5843	1.737
		9	210.0	203.6	223.4	216.6	45.82	28.86	74.69	1.587	86.0	92.1	111.8	23,508	0.073	121.35	314.73	5843	1.733
		11	210.0	203.5	223.4	216.5	45.82	28.84	74.07	1.588	86.0	92.1	111.7	23,508	0.073	121.34	314.84	5843	1.736
		21	210.1	203.3	223.5	216.4	45.82	28.82	74.64	1.590	86.0	92.1	111.7	23,531	0.073	121.35	315.27	5842	1.738
		39	210.3	203.3	223.8	216.5	45.77	28.84	74.61	1.587	86.0	92.2	111.7	23,522	0.073	121.32	315.26	5843	1.738
		107	210.4	202.1	223.8	215.9	45.50	28.89	74.39	1.575	86.2	92.4	111.2	23,464	0.085	121.51	315.43	5845	1.739
DF-11		7	209.7	201.0	224.5	215.6	45.13	28.87	74.01	1.563	95.7	95.3	111.2	23,293	0.073	120.94	314.75	5846	1.732
		9	209.7	201.0	224.4	215.7	45.18	28.87	74.06	1.565	95.7	95.3	111.2	23,279	0.071	121.05	314.34	5846	1.730
		11	209.8	200.9	224.4	215.6	45.13	28.87	74.00	1.563	95.8	95.3	111.2	23,290	0.071	120.95	314.71	5846	1.732
		15	209.9	200.8	224.5	215.5	45.08	28.91	73.99	1.559	95.8	95.3	111.2	23,253	0.071	120.96	314.30	5847	1.730

TABLE II (Continued)

b. Concluded

Test No.	Engine S/N	Time for 2-sec Average	Propellant Pressures, psia				Flow Rates, lb_m/sec			MR	T_o, °F	T_f, °F	P_c, psia	F_v, lb_f	P_a, psia	$A_{t_{calc}}$, $in.^2$	I_{sp_v}, $\frac{lb_f\text{-sec}}{lb_m}$	c*, ft/sec	C_{F_v}
			P_{ot}	POL-1, $P_{ot_{ca}}$	P_{ft}	PFL-1, $P_{ft_{ca}}$	$\dot{W}_o$	$\dot{W}_f$	$\dot{W}_t$										
DG-01	21D	7	171.9	168.2	177.2	173.7	39.18	24.75	63.93	1.583	112.3	110.7	95.5	20,052	0.061	121.80	313.66	5855	1.724
		9	171.9	168.1	176.4	173.4	39.13	24.78	63.91	1.579	112.4	110.8	95.4	20,031	0.061	121.85	313.45	5855	1.722
		15	171.7	167.8	177.1	173.3	39.79	25.10	64.89	1.585	112.6	111.0	97.0	20,347	0.062	121.68	313.56	5854	1.723
		19	171.9	167.8	177.2	173.4	39.78	25.10	64.88	1.585	112.8	111.1	97.1	20,346	0.063	121.58	313.57	5854	1.723
DG-02		7	126.4	127.1	124.1	129.1	30.84	20.27	51.21	1.526	112.7	110.9	76.8	15,961	0.055	121.51	311.72	5863	1.711
DG-02		9	126.5	127.0	124.0	129.2	30.81	20.33	51.14	1.515	112.7	111.0	76.8	15,954	0.055	121.34	311.95	5864	1.712
DG-03		7	151.9	151.7	149.2	153.4	35.94	22.73	58.67	1.581	113.0	111.1	87.9	18,341	0.058	121.49	312.59	5855	1.718
DG-03		9	151.9	151.5	148.9	153.4	35.89	22.69	58.58	1.582	113.0	111.1	87.9	18,337	0.059	121.33	313.07	5855	1.720
DG-04		7	202.6	195.5	199.9	200.8	43.91	27.27	71.18	1.610	113.1	111.1	106.7	22,385	0.064	121.26	314.48	5850	1.730
DG-04		9	202.3	195.5	200.7	200.8	43.96	27.27	71.23	1.612	113.1	111.1	106.8	22,387	0.065	121.33	314.27	5850	1.728
DG-05		7	230.9	223.5	234.8	233.5	48.35	30.26	78.62	1.598	113.3	108.4	118.2	24,784	0.067	120.99	315.26	5852	1.733
DG-05		9	231.3	223.4	234.1	233.2	48.30	30.26	78.56	1.596	113.3	108.4	118.1	24,770	0.068	121.01	315.29	5853	1.733
DG-06		7	176.1	176.1	172.0	177.8	40.83	25.03	65.86	1.631	109.1	109.6	98.6	20,667	0.065	121.42	313.82	5847	1.727
		9	175.7	175.7	172.6	177.0	40.73	24.93	65.65	1.634	109.1	109.6	98.4	20,622	0.065	121.28	314.10	5846	1.729
		11	176.3	176.2	173.4	177.8	40.83	25.03	65.86	1.631	109.1	109.6	98.6	20,680	0.065	121.36	314.02	5847	1.728
		21	175.5	175.5	172.9	177.0	40.78	24.96	65.74	1.634	109.1	109.5	98.4	20,626	0.066	121.36	313.77	5846	1.727
		31	175.7	175.2	173.6	176.8	40.73	24.90	65.63	1.636	109.2	109.5	98.3	20,607	0.066	121.24	314.04	5846	1.728
		301	176.0	177.8	174.1	179.1	41.04	25.20	66.24	1.628	111.9	109.8	99.2	20,825	0.079	121.33	314.36	5847	1.730
		547	175.2	172.1	172.0	175.7	39.91	24.96	64.87	1.599	111.9	109.8	97.2	20,463	0.082	121.36	315.44	5852	1.734
DG-10		7	180.1	169.2	180.7	174.1	38.68	24.88	63.56	1.555	115.9	112.8	95.2	19,869	0.066	121.59	312.60	5859	1.717
		9	180.1	169.2	180.8	174.1	38.65	24.88	63.54	1.554	115.9	112.8	95.2	19,880	0.067	121.56	312.89	5859	1.718
		11	180.1	169.2	180.7	174.1	38.65	24.83	63.49	1.557	115.9	112.8	95.2	19,892	0.067	121.37	313.34	5859	1.721
		21	180.1	169.2	180.7	174.1	38.65	24.85	63.50	1.556	115.9	112.8	95.2	19,894	0.068	121.45	313.28	5859	1.720
		31	180.2	169.1	180.7	174.0	38.63	24.85	63.48	1.555	115.9	112.8	95.2	19,886	0.069	121.46	313.28	5859	1.720
		97	180.4	177.7	181.1	178.9	40.34	25.18	65.52	1.602	115.9	112.8	98.2	20,576	0.076	121.32	314.09	5852	1.727

TABLE II (Continued)

c. Injector S/N 105

Test No.	Engine S/N	Time for 2-sec Average	Propellant Pressures, psia				Flow Rates, lb_m/sec			MR	T_o, °F	T_f, °F	P_c, psia	F_v, lb_f	P_a, psia	At_{calc}, $in.^2$	I_{spv}, $\frac{lbf\text{-}sec}{lb_m}$	c*, ft/sec	CF_v
			P_{ot}	POL-1, $P_{ot_{ca}}$	P_{ft}	PFL-1, $P_{ft_{ca}}$	$\dot{W}_o$	$\dot{W}_f$	$\dot{W}_t$										
DH-01	21E	7	161.4	157.4	176.2	175.7	38.94	25.96	64.90	1.500	69.6	74.2	98.6	20,341	0.071	121.02	313.42	5918	1.704
		9	161.7	157.6	175.8	175.8	39.04	25.93	64.97	1.506	69.7	74.3	98.7	20,353	0.074	121.06	313.27	5917	1.704
		13	161.5	157.6	176.2	175.7	39.78	26.44	66.22	1.505	69.7	74.5	100.6	20,743	0.075	121.13	313.24	5917	1.703
		19	161.8	157.6	176.0	176.1	39.20	25.75	64.95	1.522	69.8	74.7	98.7	20,356	0.071	120.93	313.42	5915	1.705
DH-02		7	189.8	186.1	205.0	202.2	44.40	28.40	72.80	1.563	69.8	74.5	110.5	22,874	0.088	120.98	314.23	5909	1.711
		9	190.1	186.0	204.9	202.2	44.45	28.40	72.85	1.565	69.8	74.6	110.5	22,868	0.090	121.08	313.94	5909	1.709
		11	190.0	186.0	204.8	202.2	44.39	28.40	72.79	1.563	69.9	74.7	110.5	22,864	0.091	120.98	313.94	5909	1.710
		15	189.8	186.0	204.8	202.1	44.34	28.38	72.73	1.562	69.9	74.8	110.5	22,869	0.093	120.88	314.42	5909	1.712
DH-04		7	194.4	185.6	200.9	196.3	44.71	27.60	72.31	1.620	68.4	76.2	109.6	22,678	0.084	121.04	313.62	5900	1.710
		9	194.7	185.4	201.3	196.6	44.60	27.62	72.22	1.615	68.4	76.2	109.6	22,691	0.084	120.82	314.19	5900	1.713
		11	194.2	185.4	200.2	196.0	44.63	27.56	72.19	1.619	68.4	76.2	109.5	22,668	0.085	120.91	314.01	5900	1.712
		21	193.8	185.2	199.6	195.8	44.50	27.56	72.06	1.614	68.4	76.3	109.5	22,662	0.085	120.70	314.48	5901	1.715
		31	193.3	185.0	199.3	195.6	44.60	27.51	72.11	1.621	68.5	76.3	109.4	22,659	0.083	120.88	314.21	5900	1.714
		101	191.9	183.4	200.1	194.4	44.28	27.44	71.72	1.614	68.5	76.2	108.8	22,622	0.089	120.94	315.39	5901	1.720
DH-05		7	189.8	189.7	203.1	195.8	45.56	27.35	72.91	1.666	70.2	78.7	110.6	22,860	0.072	120.76	313.54	5892	1.712
		9	189.8	189.7	203.1	195.7	45.59	27.36	72.95	1.666	70.2	78.7	110.5	22,870	0.073	120.84	313.50	5892	1.712
		11	189.9	189.7	203.2	195.7	45.51	27.40	72.91	1.661	70.2	78.7	110.6	22,878	0.073	120.73	313.80	5893	1.713
		19	191.2	189.5	205.3	195.6	45.48	27.38	72.86	1.661	70.2	78.7	110.5	22,873	0.075	120.82	313.92	5892	1.714
DH-08		7	190.6	188.0	202.7	197.9	45.50	27.50	73.00	1.655	71.2	78.9	110.4	22,851	0.077	121.17	313.05	5894	1.709
		9	192.2	188.0	203.0	200.2	45.39	27.79	73.18	1.634	71.2	78.9	110.8	22,929	0.078	121.08	313.34	5893	1.709
		11	190.0	188.0	204.9	200.7	45.34	27.88	73.23	1.626	71.2	79.0	110.9	22,942	0.079	121.12	313.30	5899	1.709
		21	190.2	187.8	205.5	200.9	45.29	27.90	73.19	1.623	71.2	79.1	110.9	22,955	0.083	121.08	313.64	5900	1.711
		31	190.1	187.7	205.2	200.8	45.34	27.89	73.23	1.626	71.2	79.1	110.8	22,472	0.082	121.13	313.73	5899	1.711
		97	190.8	186.7	205.4	200.3	45.17	27.89	73.06	1.620	71.3	79.2	110.6	22,990	0.088	121.17	314.68	5900	1.716
DH-09		7	191.7	187.8	202.3	199.2	45.34	27.69	73.03	1.637	74.0	80.5	110.4	22,849	0.071	121.20	312.88	5900	1.707
		9	191.7	187.7	202.4	199.2	45.34	27.66	73.00	1.639	74.0	80.5	110.4	22,855	0.072	121.15	313.11	5897	1.708
		11	191.5	187.7	202.5	199.1	45.34	27.73	73.06	1.635	74.0	80.5	110.4	22,855	0.073	121.29	312.81	5897	1.707
		15	191.4	187.7	202.3	199.2	45.28	27.66	72.94	1.637	74.1	80.5	110.4	22,860	0.075	121.10	313.40	5897	1.710

TABLE II (Concluded)

c. Concluded

Test No.	Engine S/N	Time for 2-sec Average	Propellant Pressures, psia				Flow Rates, lb_m/sec			MR	T_o, °F	T_f, °F	P_c, psia	F_v, lbf	P_a, psia	At_{calc}, $in.^2$	I_{spv}, $\frac{lbf\text{-}sec}{lbm}$	c*, ft/sec	C_{Fv}
			P_{ot}	POL-1, $P_{ot_{ca}}$	P_{ft}	PFL-1, $P_{ft_{ca}}$	$\dot{W}_o$	$\dot{W}_f$	$\dot{W}_t$										
D1-01	21F	7	163.4	156.0	166.0	163.4	37.88	24.20	62.08	1.565	106.6	109.5	94.0	19,417	0.064	121.30	312.76	5904	1.704
		9	163.5	156.0	166.0	163.3	37.75	24.20	61.95	1.560	106.7	109.7	94.0	19,421	0.065	120.99	313.50	5805	1.708
		15	163.2	155.6	166.0	163.0	38.49	24.59	63.08	1.565	106.9	109.9	95.6	19,747	0.066	121.12	313.04	5904	1.706
		25	163.3	155.6	166.2	163.3	37.89	23.99	61.88	1.578	107.3	110.3	93.9	19,361	0.067	120.87	312.88	5802	1.706
D1-02		7	124.2	122.0	121.5	117.7	31.94	18.66	50.60	1.711	106.9	109.6	76.4	15,734	0.054	121.00	310.97	5878	1.702
D1-02		9	123.3	124.0	121.7	117.7	32.50	18.50	51.00	1.757	107.0	109.7	76.9	15,858	0.055	120.88	310.98	5867	1.705
D1-03		7	147.6	150.2	146.3	146.1	37.41	21.83	58.23	1.714	107.1	109.8	89.5	18,464	0.059	120.86	311.73	5877	1.707
D1-03		9	147.6	150.3	146.3	146.1	37.41	21.85	59.27	1.711	107.1	109.8	89.6	18,489	0.061	120.89	311.97	5878	1.708
D1-04		7	192.9	191.4	202.8	186.2	44.20	27.30	71.49	1.619	107.2	109.9	108.5	22,414	0.063	120.77	313.51	5896	1.711
D1-04		9	183.0	191.5	202.6	196.2	44.20	27.26	71.46	1.621	107.2	109.9	108.5	22,414	0.066	120.69	313.66	5895	1.712
D1-05		7	209.3	207.6	208.1	203.2	47.37	27.59	74.96	1.717	107.4	109.9	113.3	23,467	0.065	120.86	313.06	5877	1.714
D1-05		9	209.2	207.6	208.0	203.2	47.21	27.63	74.84	1.709	107.4	109.9	113.3	23,481	0.068	120.71	313.75	5878	1.717
D1-06		7	179.4	176.4	178.2	173.4	42.18	24.74	66.83	1.705	107.6	113.1	101.1	20,930	0.077	120.97	312.71	5878	1.711
		9	179.0	176.2	179.6	175.3	42.04	24.97	67.01	1.683	107.6	113.1	101.4	20,971	0.074	120.88	312.98	5884	1.712
		11	178.7	176.0	177.9	174.1	42.04	24.81	66.84	1.695	107.6	113.2	101.1	20,916	0.073	120.85	312.91	5881	1.712
		21	176.2	173.5	174.1	172.7	41.57	24.68	66.25	1.685	107.6	113.2	100.4	20,749	0.069	120.62	313.21	5883	1.713
		31	176.5	173.9	174.3	172.0	41.57	24.56	66.13	1.693	107.6	113.2	100.4	20,740	0.070	120.43	313.62	5882	1.716
		301	175.9	176.0	173.7	174.2	41.81	24.70	66.51	1.693	106.8	111.4	102.2	20,912	0.085	119.00	314.40	5882	1.720
		547	174.1	170.1	174.7	171.0	40.67	24.51	65.18	1.660	106.8	111.2	100.4	20,574	0.086	118.87	315.67	5888	1.725
D1-10		7	120.0	117.7	120.5	117.8	30.84	18.59	49.42	1.659	103.5	110.3	76.3	15,353	0.062	118.82	310.64	5889	1.697
		9	120.0	117.7	120.5	117.7	30.84	18.56	49.50	1.667	103.5	110.3	76.2	15,361	0.062	118.80	310.35	5887	1.696
		11	119.9	117.8	120.4	117.7	30.86	18.59	49.45	1.660	103.5	110.3	76.2	15,355	0.062	118.73	310.51	5888	1.697
		21	120.2	117.5	120.6	117.6	30.84	18.59	49.43	1.659	103.5	110.3	76.2	15,375	0.064	118.71	311.08	5889	1.700
		31	120.2	117.4	120.7	117.6	30.86	18.62	49.48	1.657	103.5	110.3	76.1	15,369	0.064	118.97	310.58	5889	1.700
		97	120.5	116.4	121.0	117.3	30.63	18.62	49.25	1.645	103.5	110.4	75.8	15,325	0.067	118.88	311.18	5891	1.700

TABLE III
SUMMARY OF TRANSIENT IMPULSE DATA – IGNITION

Test Number	Engine Serial Number	Thrust Chamber Valve Bank	Chamber Pressure, psia	Time from FS-1 to 90 percent of Steady-State Thrust, sec	Impulse from FS-1 to 90 percent of Steady-State Thrust, lb_f-sec
DD-01	21A	*	97	0.552	428
02		A		0.552	691
03				0.545	673
04				0.536	587
05				0.537	517
06				0.623	1,979
14		B		0.557	1,205
15A				0.515	660
15B				0.533	1,003
15C				0.536	1,089
DE-01	21B	**	110	0.543	572
02		A		0.541	700
03A				0.542	583
03B				0.531	538
03C				0.535	587
03D				0.531	503
03E				0.531	505
03F				0.535	559
03G				0.534	555
03H				0.531	565
03I				0.531	536
03J				0.536	569
03K				0.531	529
04				0.547	681
05				0.544	833
06				0.537	918
07				0.532	857
08				0.528	779
10		B		0.518	1,090
11A				0.540	1,135
11D		A		0.548	1,017
11E				0.528	691
11F				0.528	707
12				0.533	836
13				0.530	807
14				0.537	812

*First 10 sec, Valve Bank A; Valve Bank A and B 10 sec, Valve Bank B 10 sec
**First 10 sec, Valve Bank A, Valve Bank A and B 5 sec, Valve Bank B 10 sec

TABLE III (Continued)

Test Number	Engine Serial Number	Thrust Chamber Valve Bank	Chamber Pressure, psia	Time from FS-1 to 90 percent of Steady-State Thrust, sec	Impulse from FS-1 to 90 percent of Steady-State Thrust, lbf-sec
DF-01	21C	**	110	0.572	638
02		A		0.557	820
03A				0.536	460
03B				0.525	446
03C				0.523	475
03D				0.533	485
03E				0.529	444
03F				0.525	473
03G				0.530	442
03H				0.530	416
03I				0.529	398
03J				0.531	414
03K				0.533	456
04				0.550	591
05				0.604	602
06				0.544	753
07				0.536	726
08				0.535	653
10		B		0.518	785
11A				5.590	1,184
12				0.532	1,093
13				0.527	1,162
14				0.527	1,116
DG-01	21D	*	97	0.714	2,987
03		A	88	0.719	3,319
04			106	0.564	1,133
05			115	0.545	995
06			97	0.595	1,554
10		B		0.634	2,535
11				0.743	4,693
12				0.767	4,673
13				0.774	5,044

*Valve Bank A 10 sec, Valve Banks A and B 10 sec, Valve Bank B 10 sec
**Valve Bank A 10 sec, Valve Banks A and B 5 sec, Valve Bank B 5 sec

TABLE III (Concluded)

Test Number	Engine Serial Number	Thrust Chamber Valve Bank	Chamber Pressure, psia	Time from FS-1 to 90 percent of Steady-State Thrust, sec	Impulse from FS-1 to 90 percent of Steady-State Thrust, lb_f-sec
DH-01	21E	**	97	0.577	741
02		A	110	0.534	403
03A				0.529	398
03B				0.526	407
03C				0.532	430
03D				0.530	432
03E				0.530	428
03F				0.529	460
03G				0.526	416
03H				0.526	400
03I				0.528	392
03J				0.531	393
03K				0.531	387
04				0.582	1,285
05				0.546	711
06A				0.541	641
06B				0.536	644
06C				0.537	623
07				0.548	923
08				0.535	814
09				0.536	911
10A				0.490	829
10B				0.481	745
10C				0.480	680
11				0.489	855
DI-01	21F	*	97	0.792	4,365
02		A	77	---	---
03			88	1.135	10,329
04			106	0.545	706
05			115	0.536	729
06			97	0.713	3,611
10		B	77	---	---
11			97	0.818	5,311
12				0.831	5,348
13				0.816	5,018

*Valve Bank A 10 sec; Valve Bank A and B 10 sec; Valve Bank B 10 sec
**Valve Bank A 10 sec; Valve Bank A and B 5 sec; Valve Bank B 5 sec

TABLE IV
SUMMARY OF TRANSIENT IMPULSE DATA – SHUTDOWN

Test Number	Engine Serial Number	Thrust Chamber Valve Bank	Chamber Pressure, psia	Time from FS-2 to 1 percent of Steady-State Thrust, sec	Impulse from FS-2 to 1 percent of Steady-State Thrust, lb_f-sec
DD-01	21A	*	97	1.420	8,524
02		A		1.602	8,662
03				1.443	8,836
04				1.509	8,434
05				1.229	8,714
06				2.349	9,558
14		B		3.698	10,005
15A				1.739	8,450
15B				1.627	8,387
15C				1.692	8,428
DE-01	21B	**	110	2.665	9,773
02		A		2.684	10,148
03A				2.565	10,086
03B				1.364	9,680
03C				2.645	10,042
03D				1.378	9,734
03E				1.369	9,691
03F				2.665	10,069
03G				1.341	9,808
03H				1.833	9,860
03I				1.386	9,668
03J				2.000	9,938
03K				1.396	9,754
04				2.923	11,300
05				2.968	10,694
06				2.528	10,222
07				2.446	10,130
08		B		2.390	10,208
10		B		2.005	9,824
11A		A		2.249	9,479
11D				2.230	10,234
11E				2.187	10,388
11F				2.547	10,452
12				2.116	10,115
13				2.070	9,990
14				1.930	10,037

*Valve Bank A 10 sec, Valve Banks A and B 10 sec, Valve Bank B 10 sec
**Valve Bank A 10 sec, Valve Banks A and B 5 sec, Valve Bank B 5 sec

TABLE IV (Continued)

Test Number	Engine Serial Number	Thrust Chamber Valve Bank	Chamber Pressure, psia	Time from FS-2 to 1 percent of Steady-State Thrust, sec	Impulse from FS-2 to 1 percent of Steady-State Thrust, lbf-sec
DF-01	21C	**	110	2.235	10,305
02		A		2.644	10,531
03A				2.549	10,641
03B				2.709	10,738
03C				2.681	10,594
03D				2.463	10,665
03E				2.682	10,730
03F				2.664	10,729
03G				2.733	10,669
03H				2.664	10,734
03I				1.826	10,585
03J				2.642	10,874
03K				2.227	10,912
04				2.615	11,910
05				2.369	10,728
06				2.346	11,228
07				2.626	12,443
08				2.380	12,317
10		B		2.402	10,534
11A				1.957	8,511
12				3.363	12,665
13				4.728	13,852
14				7.342	14,428
DG-01	21D	*	97	3.607	10,594
02		A	77	2.417	8,777
03			88	2.176	9,346
04			106	2.195	11,574
05			115	2.567	12,599
06			97	3.399	11,652
11		B		2.677	9,615
12				1.679	9,200
13				1.720	9,365

*Valve Bank A 10 sec, Valve Bank A and B 10 sec, Valve Bank B 10 sec
**Valve Bank A 10 sec, Valve Bank A and B 5 sec, Valve Bank B 5 sec

TABLE IV (Concluded)

Test Number	Engine Serial Number	Thrust Chamber Valve Bank	Chamber Pressure, psia	Time from FS-2 to 1 percent of Steady-State Thrust, sec	Impulse from FS-2 to 1 percent of Steady-State Thrust, lbf-sec
DH-01	21E	**	97	3.148	10,302
02		A	110	2.934	11,433
03A				2.648	10,782
03B				2.669	11,158
03C				2.108	11,042
03D				2.140	11,136
03E				2.106	11,161
03F				2.137	11,050
03G				2.160	11,236
03H				2.199	11,216
03I				2.201	11,433
03J				2.258	11,468
03K				2.169	11,460
04				3.164	12,339
05				3.518	12,074
06A				2.412	11,714
06B				2.343	11,610
06C				2.308	11,610
08				3.289	11,780
09				3.258	11,887
10A				2.410	11,366
10B				2.608	11,361
10C				2.580	11,282
DI-01	21F	*	97	2.069	10,151
02		A	77	2.558	9,134
03			88	3.120	10,396
04			106	2.346	11,748
05			115	2.223	12,165
06			97	2.445	11,386
10		B	77	4.608	9,286
11			97	2.828	9,949
12				2.809	9,798
13				2.762	10,018

*Valve Bank A 10 sec, Valve Bank A and B 10 sec, Valve Bank B 10 sec
**Valve Bank A 10 sec, Valve Bank A and B 5 sec, Valve Bank B 5 sec

TABLE V
SUMMARY OF MINIMUM IMPULSE DATA

Test Number	Engine Serial Number	Thrust Chamber Valve Bank	Chamber Pressure Level, psia	Test Duration, sec	Impulse, lb_f-sec
DD-07A	21A	A	10	0.370	1,224
07B				0.370	1,165
07C				0.370	1,067
07D				0.370	1,013
08				0.370	986
09A			98	0.570	7,150
09B				0.570	7,214
09C				0.570	7,171
09D				0.565	7,233
10				0.570	7,470
11A				0.966	17,910
11B				0.961	17,925
12A		B		0.970	17,308
12B				0.968	17,752
13				0.963	17,657
16A			92	0.961	16,342
16B			96	0.960	17,507
16C				0.962	17,483
16D				0.960	17,622
17				0.960	17,597
DE-09	21B	B	109	0.975	19,353
DF-09	21C	B	112	0.975	22,561
15A		B	110	0.980	21,583
DG-07A	21D	A	15	0.385	1,858
07B			15	0.390	1,772
07C			12	0.385	1,594
07D			12	0.385	1,536
07E			12	0.385	1,528
08A			77	0.555	8,096
08B			84	0.555	8,498
08C			85	0.555	8,154
08D			82	0.555	7,893
08E			87	0.555	7,939

TABLE V (Concluded)

Test Number	Engine Serial Number	Thrust Chamber Valve Bank	Chamber Pressure Level, psia	Test Duration, sec	Impulse, lb_f-sec
DG-09A	21D	A	96	0.975	21,526
09B				0.975	21,542
09C				0.975	20,808
09D				0.975	21,267
09E				0.975	21,217
14A		B		0.980	18,044
14B				0.980	19,777
14C			97	0.975	19,938
14D			98	0.975	19,502
14E			98	0.980	19,308
DH-07	21E	A	110	0.979	21,045
11		A	110	0.980	21,027
DI-07A	21F	A	18	0.385	2,126
07B				0.390	1,970
07C				0.385	1,828
07D				0.385	1,783
07E				0.385	1,785
08A			80	0.555	7,460
08B				0.555	7,548
08C				0.555	6,955
08D				0.555	7,091
08E				0.555	7,376
09A			97	0.978	18,919
09B				1.008	18,753
09C				0.976	18,724
09D				0.978	18,828
09E		B		0.979	18,238
14A			97	0.978	17,566*
14B				1.000	17,716*
14C				0.978	17,943*
14D				0.978	17,801*
14E				0.978	18,242*

*Impulse Totalized to 1 percent Thrust Level

APPENDIX III
PROPELLANT FLOWMETER AND WEIGH SCALE CALIBRATIONS

GENERAL

An in-place flowmeter calibration system was installed in the J-3 test cell complex to duplicate the actual propellant conditions experienced by the flowmeter during a test (pressure, temperature, and flow rate). This facilitated an accurate measurement of propellant flow rates which the in-place technique uses to determine the flowmeter K-factor (lb_m-H_2O/cycle). With this K-factor, the propellant flow rates can be obtained during an engine firing.

In-Place Calibration Procedure

The flowmeter calibration system is presented schematically in Fig. III-1. Each flowmeter was in-place calibrated by recording its total output (signal counts) during a known time period while propellant flowed through the meter and accumulated in a weigh tank.

The following general procedure was used for all flowmeter calibrations. Propellant was flowed from the pressurized F-3 sump tank to the ground-level facility storage tank. After steady-state flow was established, the diverter valve was actuated to divert the flow through the flowmeter and into the weigh tank for approximately 60 sec and then diverted back to the facility storage tank. Flow was then terminated. The weigh scale net reading (discounting the effect of gas pressure on tank weight) represented the total weight of the measured propellant flowed through the flowmeter. Total flowmeter signal counts (recorded on magnetic tape) represented the flowmeter output between the signals (1 and 2, Fig. III-2) to the diverter valve. These totalized counts were then corrected for diverter valve transients using an oscillograph record of the diverter valve displacement. Figure III-2 indicates how these corrections were made. Thus a flowmeter constant with the units of lb_m-H_2O/cycle was determined using the corrected flowmeter counts, total propellant weight flowed, and propellant specific gravity.

Weigh Scale Calibration

During flowmeter calibrations, the accumulated propellant weight was obtained from a load cell installed in the linkage of a beam scale in the weigh scale system. The load cell was in-place calibrated by applying deadweights to the scale platform and obtaining a sensitivity factor for the load cell. Weights were applied in increments up to a

total of 3200 lb and removed incrementally to determine the linearity and repeatability of the system.

During flowmeter calibration, propellant was flowed into the weigh tank with the tank vents closed to prevent any loss of weight by propellant vaporization. Thus, it was necessary to establish the effect of gas pressures on the indicated tank weight. This was determined by maintaining various pressure levels (using GN_2) in the weigh tank while repeating deadweight loading and unloading sequences.

The deadweights used to calibrate the weigh scale were certified by the Engineering Support Facility at AEDC in accordance with NBS criteria. Weight corrections for local gravity and air buoyancy were also applied.

RESULTS

Oxidizer Flowmeter In-Place Calibrations

Five oxidizer flowmeter calibrations (Fig. III-3) were made during this testing using ARO 2-1/2 in. - 6 flowmeter S/N I-27561 (Fig. III-4). Each calibration consisted of approximately seven data points, except for the first calibration which was the certification consisting of nine data points. The average flowmeter constant for each calibration with the standard deviation (1σ) is listed below. These flowmeter constants were used to calculate the oxidizer flow rates for the test series as indicated below.

Test Series	Avg Propellant Temp, °F	K_{fm}, lb_m-H_2O/cycle	$\bar{K}$, lb_m-H_2O/cycle	1σ, percent
DD	78		0.07314	0.117
DE and DF	75	†		*0.105
DG	105		0.07343	0.199
DH	68		0.07343	0.050
DI	105		0.07381	0.052

*From equation of mean line.

† 2.66×10^{-6} (cps-400) + 0.07350

The 1σ deviation from the mean for all data was ±0.118 percent.

Fuel Flowmeter In-Place Calibration

Five fuel flowmeter calibrations (Fig. III-5) were conducted during this testing with ARO 2-1/2-4 flowmeter, S/N I-27559 (Fig. III-6). Each calibration consisted of approximately seven data points, except for the first certification calibration which consisted of 14 data points. The data from these calibrations are shown below. These flowmeter constants were used to calculate the fuel flow rates for the corresponding test series indicated in the tabulation below.

Test Series	Avg Propellant Temp, °F	Kfm, lb_m-H_2O/cycle	$\bar{K}$, lb_m-H_2O/cycle	1σ, percent
DD	82		0.07462	0.117
DE and DF	84		0.07465	0.157
DG	112		0.07454	0.107
DH	73	†		*0.024
DI	105		0.07472	0.078

*From equation of mean line.

† 2.58×10^{-6} (cps-450) + 0.07490

The 1σ deviation from the mean for all data was ±0.106 percent.

Overall System Accuracy

The overall accuracy of the in-place propellant calibration system was determined by considering the accuracy of the individual components in the system in conjunction with the precision of the flowmeter constants. The accuracy of the individual components and the overall system are listed below:

Component	Accuracy of Oxidizer (N_2O_4) System, 1σ, percent	Accuracy of Fuel (AZ-50) System, 1σ, percent
Deadweights	0.001	0.001
Weigh Scale and Load Cell Calibration	0.168	0.192
Flowmeter	0.118	0.106
Overall System	±0.205	±0.219

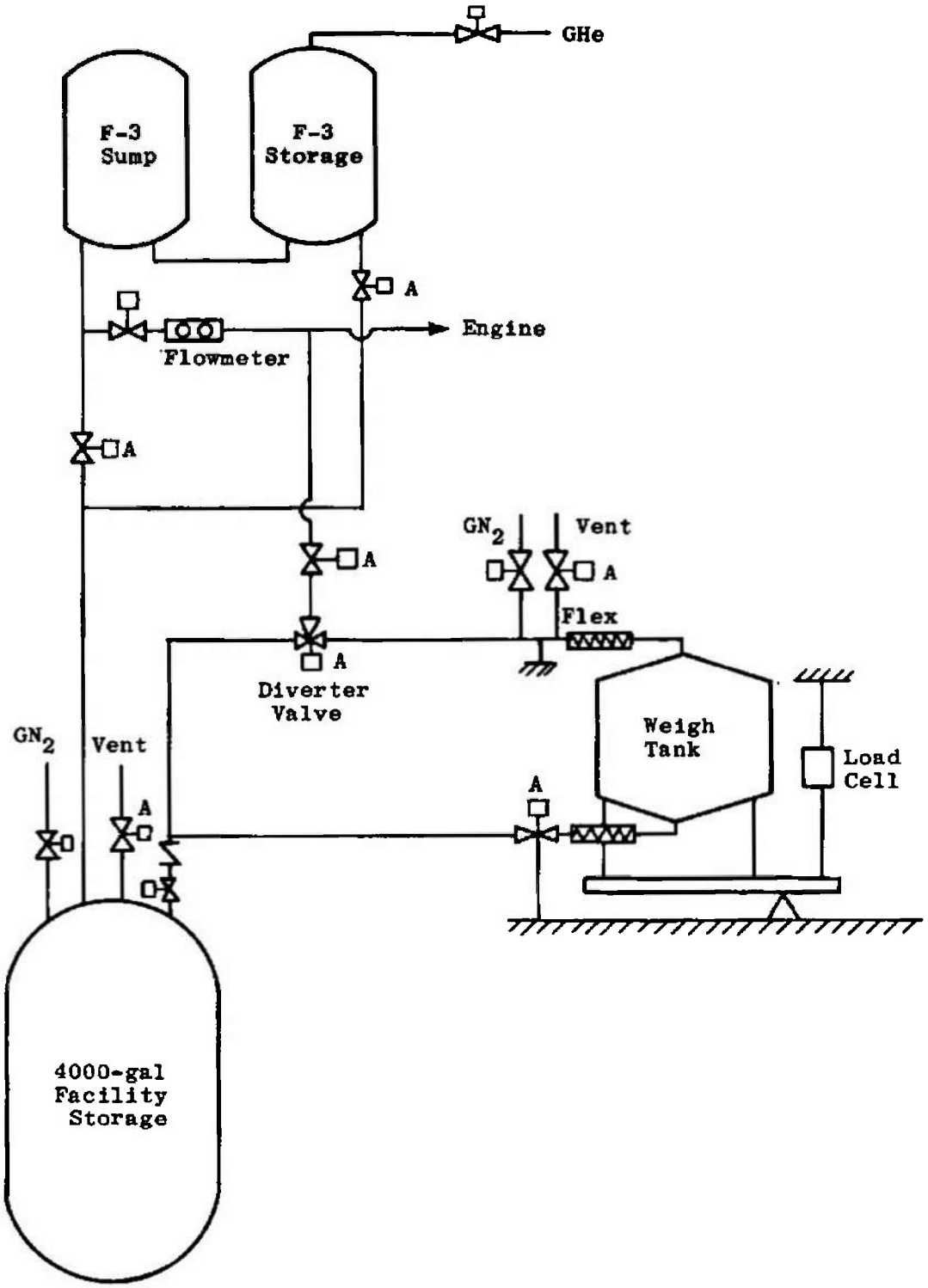

Fig. III-1 Schematic Diagram of J-3 In-Place Flowmeter Calibration System

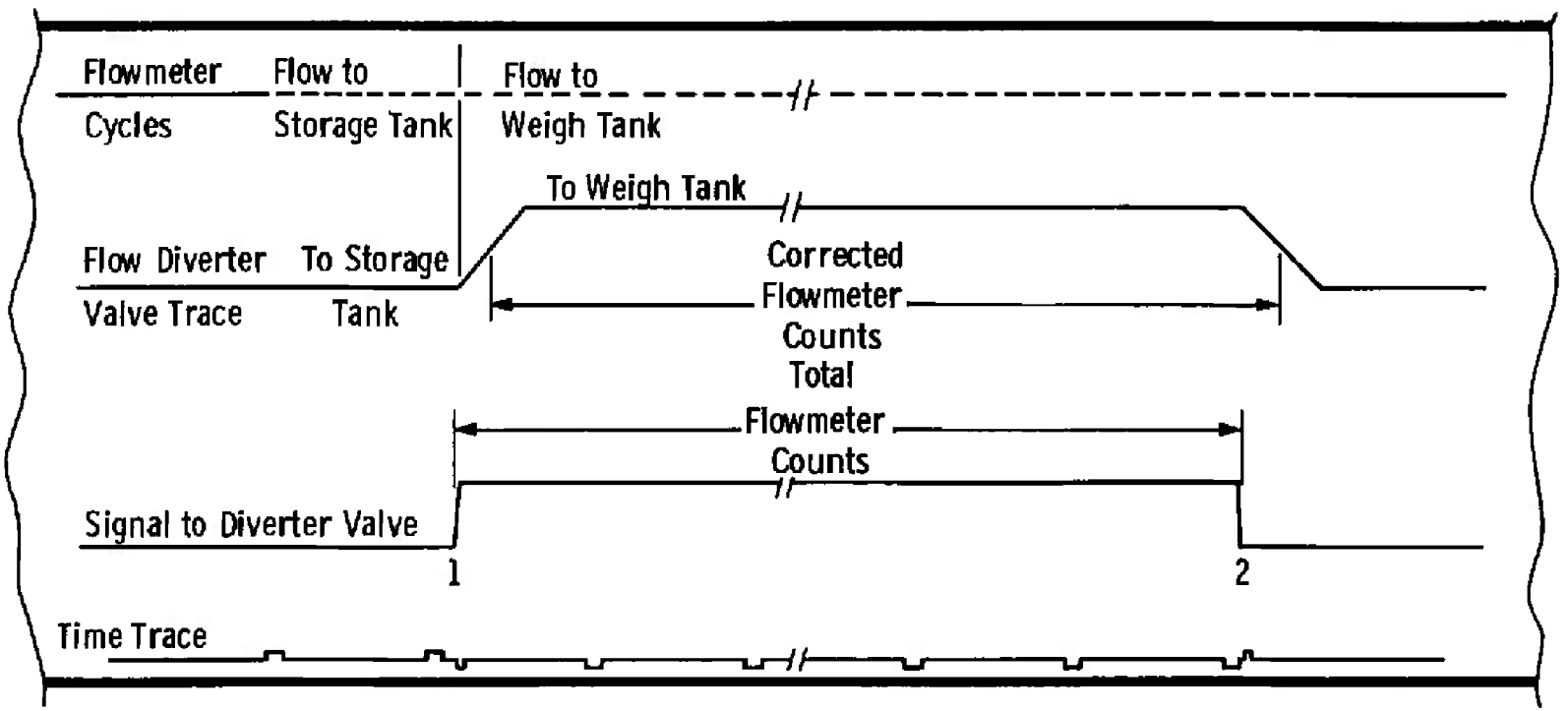

Fig. III-2 Typical Oscillograph Data for In-Place Flowmeter Calibration System

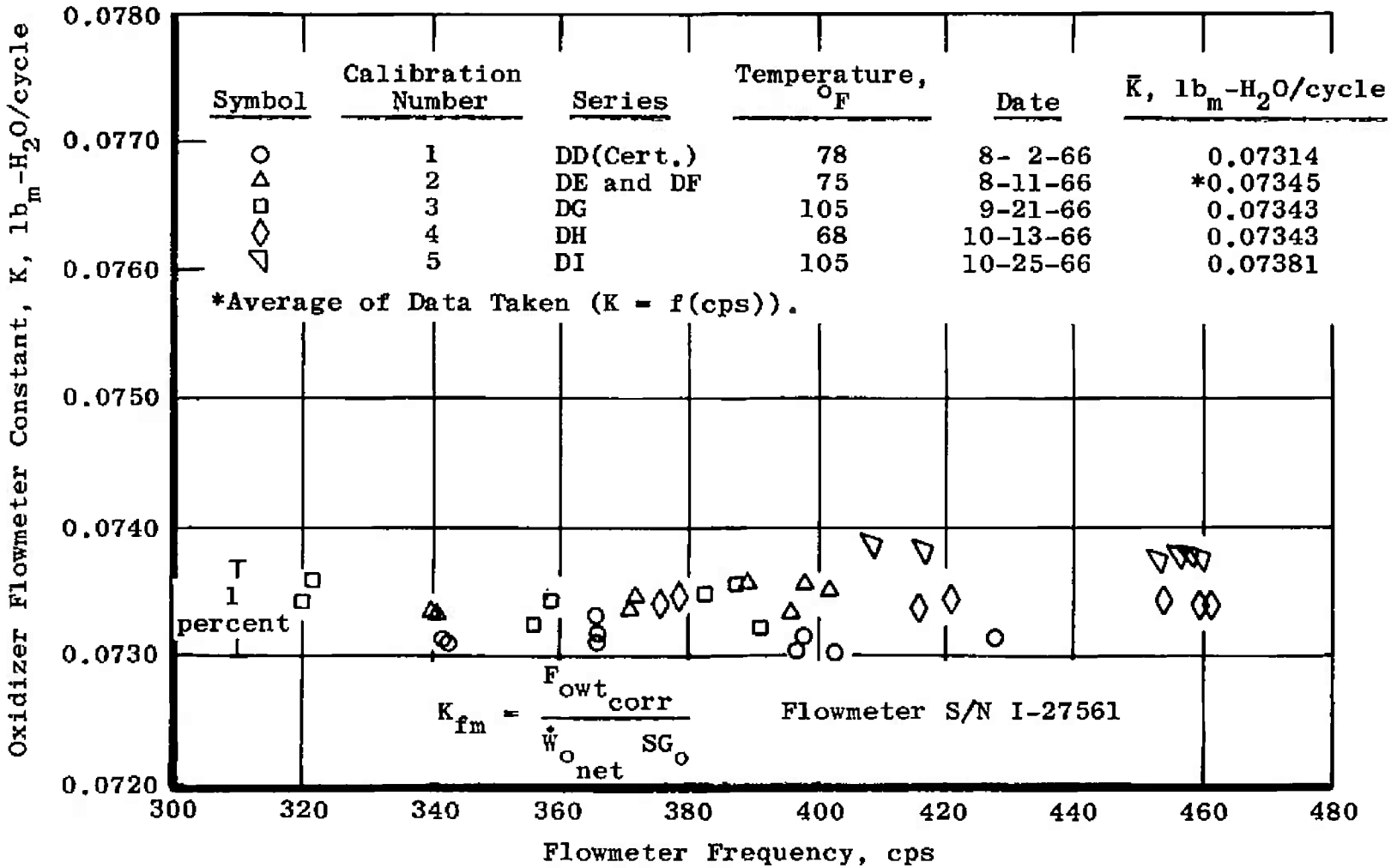

Fig. III-3 Oxidizer Flowmeter Calibrations

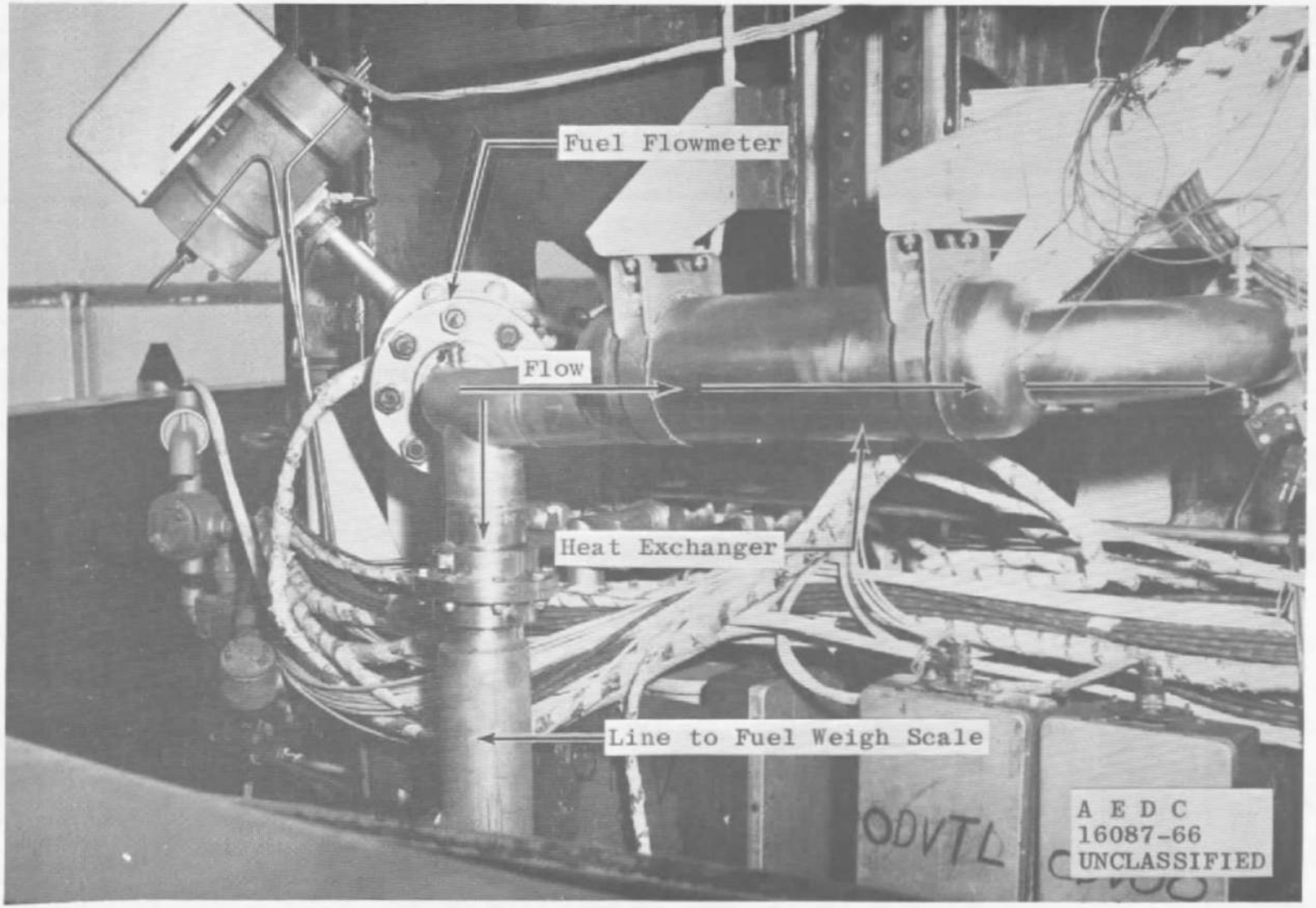

Fig. III-4 Fuel Propellant Line

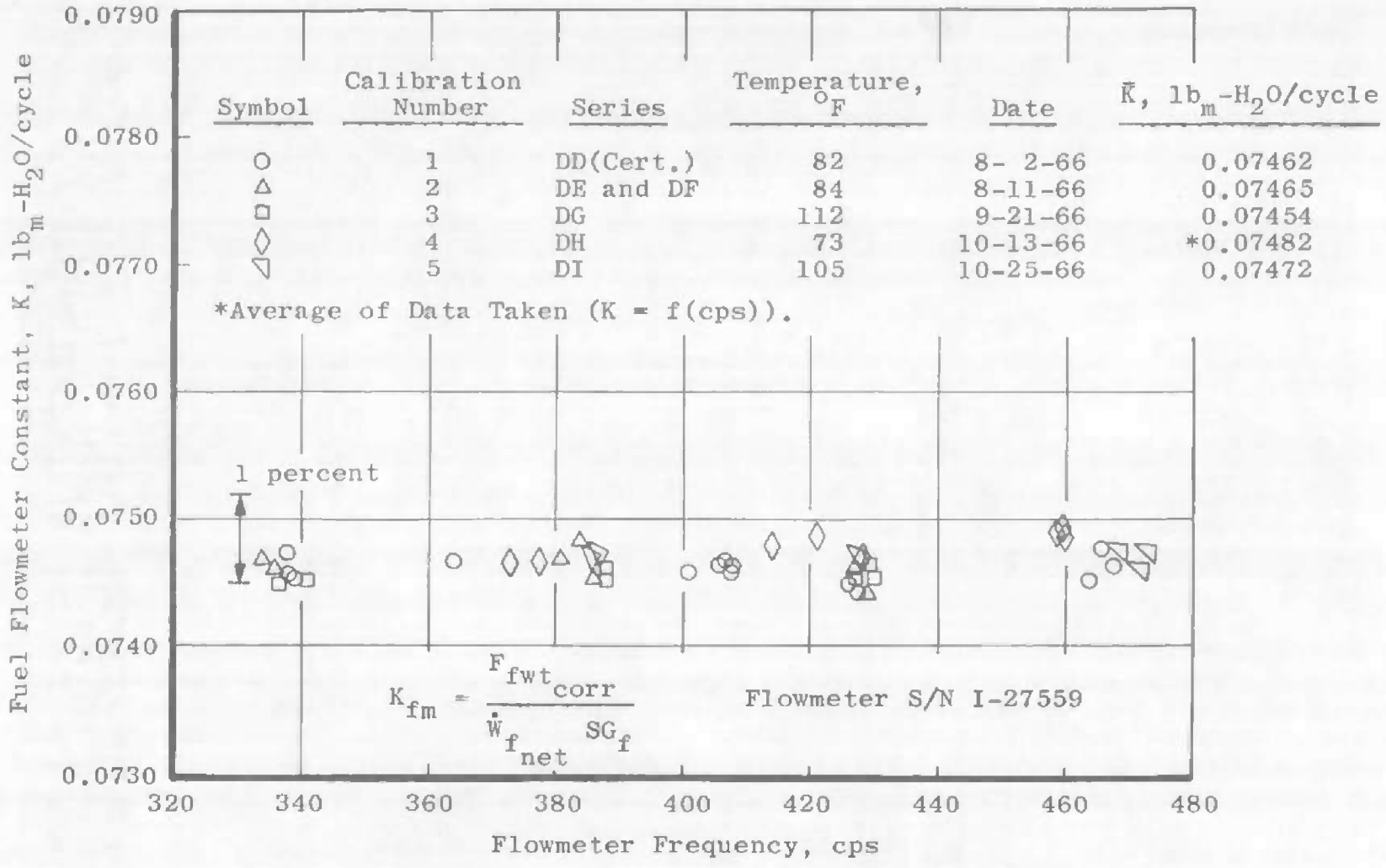

Fig. III-5 Fuel Flowmeter Calibrations

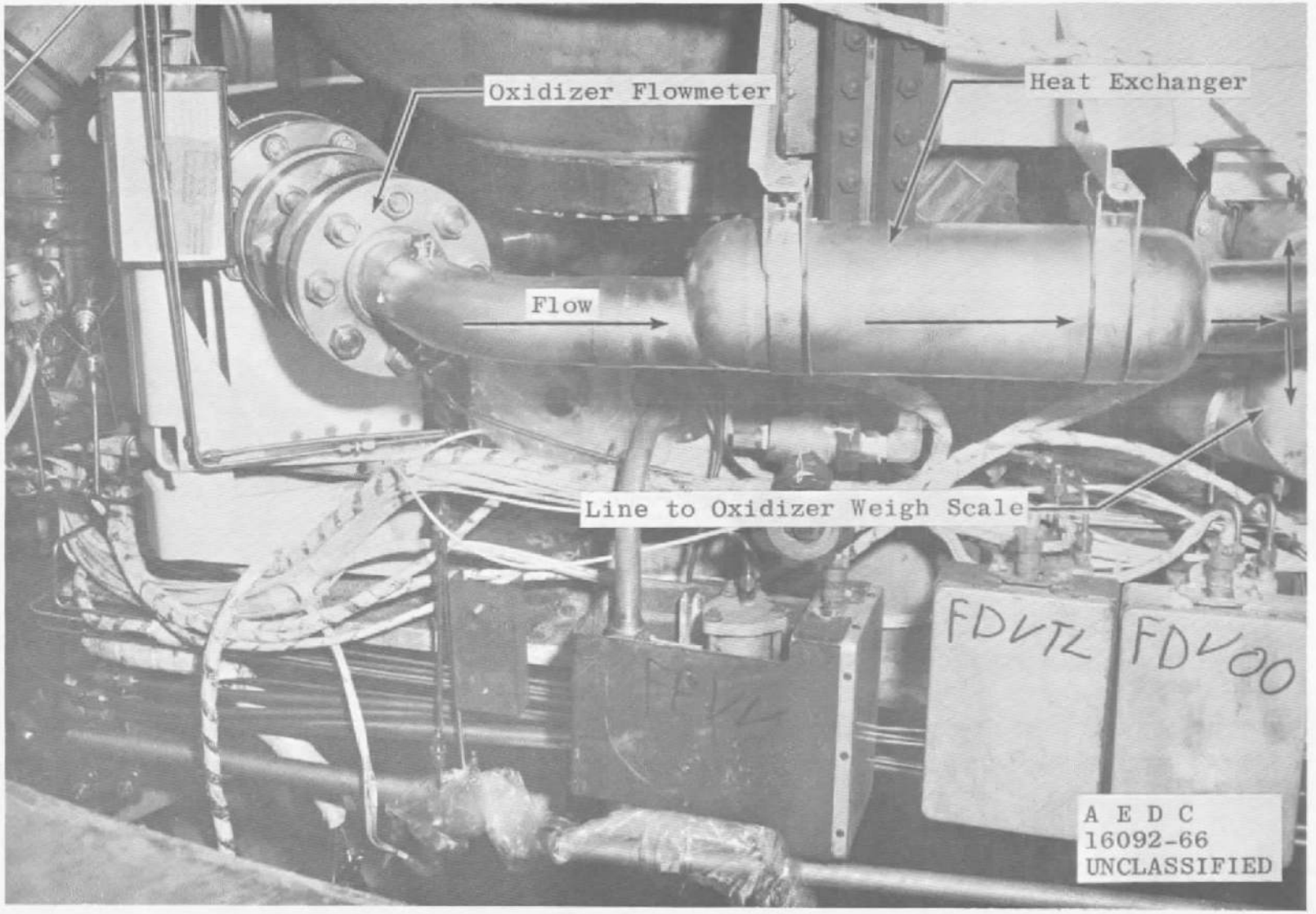

Fig. III-6 Oxidizer Propellant Line

APPENDIX IV
TEST SUMMARY

DD SERIES (DD-01 THROUGH DD-17)

Objectives of this series were to evaluate thrust chamber durability and obtain engine performance data at nominal chamber pressure and mixture ratio.

Propulsion system operation was normal during these tests. Stability recovery from the explosive pulse charge was satisfactory. This was the first test series at AEDC during which the A-1 design combustion chamber was used. Post-test condition of the chamber was fair except for one perforated blister in the ablative liner about midway between the injector and throat.

The engine was gimbaled during selected tests of this series.

DE SERIES (DE-01 THROUGH DE-15)

Test objectives were to demonstrate thrust chamber durability on the A-1 chamber design and obtain engine performance at nominal mixture ratio and 113 percent of nominal chamber pressure.

Stability recovery from the pulse charge was satisfactory. The combustion chamber sustained extensive losses of material in the forward few inches of the ablative lining; the remainder of the chamber endured quite well.

Engine gimbaling occurred during several tests of this series.

DF SERIES (DF-01 THROUGH DF-15)

Test objectives were to demonstrate thrust chamber durability on the A-1 chamber design and document engine performance at nominal mixture ratio and 113 percent of nominal chamber pressure.

Stability recovery from the pulse charge was satisfactory. The combustion chamber condition was excellent. Although this chamber is of the same design as the ones used on the two previous test periods, the resin-curing cycle was different on this chamber.

The engine was gimbaled during several tests of the period.

DG SERIES (DG-01 THROUGH DG-14)

Test objectives were to verify combustion chamber durability on the A-1 chamber design and engine performance at various chamber pressures and nominal mixture ratio. The test cell capsule and propellants were temperature conditioned to 110°F for this series.

Prior to this test period the bipropellant valve was noted to have small leakages through both the oxidizer and fuel passages. After DG-01 the fuel side of the valve still indicated at small leakage. Post-test condition of the ablative combustion chamber was excellent. The injector had several cracked welds at the juncture of the radial baffles and the central hub. This injector had been used on both DF and DG test periods, a total of about 1500 sec of firings.

Stability recovery from the pulse charge was satisfactory. Gimbaling occurred during several DG tests.

The NAA 360-deg flightweight heat shield was used for the first time at AEDC.

DH SERIES (DH-01 THROUGH DH-11)

Test objectives were thrust chamber (A-1) durability evaluation and engine performance at nominal mixture ratio and 113-percent nominal chamber pressure. A secondary objective was to cool the nozzle flange and nozzle extension to a low temperature (-100 to -300°F) prior to several firings to demonstrate nozzle extension survivance from thermal shock.

Prior to this series the downstream seals of the bipropellant valve were changed to stop the leakage noted during the DG series. Also, the linear potentiometers were installed for the first time at AEDC. Zinc chromate paste, RTV 757, and RTV 511 were placed individually around the nozzle extension attachment flange prior to this series for visual evaluation of the sealing efficiency of each during post-test inspection. Stiff links containing load cells were installed in place of gimbal actuators.

Post-test combustion chamber condition was excellent. The injector pitch bracket exhibited a small crack in the weld at the center attachment point to the injector. The nozzle extension endured the thermal shocks successfully.

Stability recovery from the pulse charge was satisfactory. Post-test inspection revealed that the pitch stiff link top attachment nut was stripped and backed off several turns.

DI SERIES (DI-01 THROUGH DI-14)

Test objectives were durability of the A-1 combustion chamber and engine performance evaluations at various chamber pressures and nominal mixture ratio with propellants and test cell walls temperature conditioned to 110°F. The engine was gimbaled during this series.

Combustion stability recovery from the pulse charge was satisfactory. Combustion chamber post-test condition was excellent. The crack in the injector pitch bracket weld (from the DH series) had not worsened.

GENERAL INFORMATION

The NAA flight combustion stability monitor was installed on all engines during this report period. However, because of the interactions between the test facility electrical systems, the data and operation of this unit were considered invalid.

UNCLASSIFIED
Security Classification

DOCUMENT CONTROL DATA - R&D
(Security classification of title, body of abstract and indexing annotation must be entered when the overall report is classified)

1 ORIGINATING ACTIVITY (Corporate author)	2a REPORT SECURITY CLASSIFICATION
Arnold Engineering Development Center ARO, Inc., Operating Contractor Arnold Air Force Station, Tennessee	UNCLASSIFIED
	2b GROUP N/A

3 REPORT TITLE
BLOCK II AJ10-137 APOLLO SERVICE MODULE ENGINE TESTING AT SIMULATED HIGH ALTITUDE (REPORT II, PHASE IV DEVELOPMENT)

4 DESCRIPTIVE NOTES *(Type of report and inclusive dates)*
N/A

5. AUTHOR(S) *(Last name, first name, initial)*
DeFord, J. F., McIlveen, M. W., and Berg, A. L., ARO, Inc.

6 REPORT DATE	7a TOTAL NO. OF PAGES	7b NO OF REFS
April 1967	116	12

8a CONTRACT OR GRANT NO.	9a. ORIGINATOR'S REPORT NUMBER(S)
AF 40(600)-1200 b. PROJECT NO. 9158 c. Program Area 921E d.	AEDC-TR-67-47 9b. OTHER REPORT NO(S) *(Any other numbers that may be assigned this report)* N/A

10. AVAILABILITY/LIMITATION NOTICES This document is subject to special export controls and each transmittal to foreign governments or foreign nationals may be made only with prior approval of National Aeronautics and Space Administration.

11. SUPPLEMENTARY NOTES	12. SPONSORING MILITARY ACTIVITY
Available in DDC.	National Aeronautics and Space Administration, Manned Spacecraft Center, Houston, Texas

13 ABSTRACT

Developmental testing was conducted on the Aerojet-General Corporation AJ10-137, Block II, Apollo Service Module Propulsion engine. The Block II engine was designed to improve performance and structural durability and was operated at nominal conditions of 97-psia chamber pressure and 1.6 mixture ratio with nitrogen tetroxide and Aerozine-50® propellants. Primary objectives of these tests were to determine engine ballistic performance and to verify durability of a new combustion chamber design. Performance and durability at off-design chamber pressures and mixture ratios were also documented. The test results presented indicate the trend in performance as a function of chamber pressure, propellant temperature, and mixture ratio. Erosion and blistering occurred in the ablative lining of the first two chambers tested. Altered construction of the last four chambers produced excellent durability. (~~AFR 310-2, Statement 2~~)

This document has been approved for public release and its distribution is unlimited. Per A.F. Letter Dated 27 June 1973

DD FORM 1 JAN 64 1473

UNCLASSIFIED
Security Classification

14 KEY WORDS	LINK A ROLE	LINK A WT	LINK B ROLE	LINK B WT	LINK C ROLE	LINK C WT
APOLLO Service module rocket engines liquid propellants ballistic performance engine durability static testing environmental testing	16-3					
1 Project Apollo 2. Rocket motors 3 " " 4 " " 5 Service Module Motors	AJ10-137 Development Performance					

INSTRUCTIONS

1. ORIGINATING ACTIVITY: Enter the name and address of the contractor, subcontractor, grantee, Department of Defense activity or other organization *(corporate author)* issuing the report.

2a. REPORT SECURITY CLASSIFICATION: Enter the overall security classification of the report. Indicate whether "Restricted Data" is included. Marking is to be in accordance with appropriate security regulations.

2b. GROUP: Automatic downgrading is specified in DoD Directive 5200.10 and Armed Forces Industrial Manual. Enter the group number. Also, when applicable, show that optional markings have been used for Group 3 and Group 4 as authorized.

3. REPORT TITLE: Enter the complete report title in all capital letters. Titles in all cases should be unclassified. If a meaningful title cannot be selected without classification, show title classification in all capitals in parenthesis immediately following the title.

4. DESCRIPTIVE NOTES: If appropriate, enter the type of report, e.g., interim, progress, summary, annual, or final. Give the inclusive dates when a specific reporting period is covered.

5. AUTHOR(S): Enter the name(s) of author(s) as shown on or in the report. Enter last name, first name, middle initial. If military, show rank and branch of service. The name of the principal author is an absolute minimum requirement.

6. REPORT DATE: Enter the date of the report as day, month, year; or month, year. If more than one date appears on the report, use date of publication.

7a. TOTAL NUMBER OF PAGES: The total page count should follow normal pagination procedures, i.e., enter the number of pages containing information.

7b. NUMBER OF REFERENCES: Enter the total number of references cited in the report.

8a. CONTRACT OR GRANT NUMBER: If appropriate, enter the applicable number of the contract or grant under which the report was written.

8b, 8c, & 8d. PROJECT NUMBER: Enter the appropriate military department identification, such as project number, subproject number, system numbers, task number, etc.

9a. ORIGINATOR'S REPORT NUMBER(S). Enter the official report number by which the document will be identified and controlled by the originating activity. This number must be unique to this report.

9b. OTHER REPORT NUMBER(S): If the report has been assigned any other report numbers *(either by the originator or by the sponsor)*, also enter this number(s).

10. AVAILABILITY/LIMITATION NOTICES: Enter any limitations on further dissemination of the report, other than those imposed by security classification, using standard statements such as:

(1) "Qualified requesters may obtain copies of this report from DDC."

(2) "Foreign announcement and dissemination of this report by DDC is not authorized."

(3) "U. S. Government agencies may obtain copies of this report directly from DDC. Other qualified DDC users shall request through _____."

(4) "U. S. military agencies may obtain copies of this report directly from DDC. Other qualified users shall request through _____."

(5) "All distribution of this report is controlled. Qualified DDC users shall request through _____."

If the report has been furnished to the Office of Technical Services, Department of Commerce, for sale to the public, indicate this fact and enter the price, if known.

11. SUPPLEMENTARY NOTES: Use for additional explanatory notes.

12. SPONSORING MILITARY ACTIVITY: Enter the name of the departmental project office or laboratory sponsoring *(paying for)* the research and development. Include address.

13 ABSTRACT: Enter an abstract giving a brief and factual summary of the document indicative of the report, even though it may also appear elsewhere in the body of the technical report. If additional space is required, a continuation sheet shall be attached.

It is highly desirable that the abstract of classified reports be unclassified. Each paragraph of the abstract shall end with an indication of the military security classification of the information in the paragraph, represented as *(TS)*, *(S)*, *(C)*, or *(U)*.

There is no limitation on the length of the abstract. However, the suggested length is from 150 to 225 words.

14. KEY WORDS: Key words are technically meaningful terms or short phrases that characterize a report and may be used as index entries for cataloging the report. Key words must be selected so that no security classification is required. Identifiers, such as equipment model designation, trade name, military project code name, geographic location, may be used as key words but will be followed by an indication of technical context. The assignment of links, rules, and weights is optional.